Granite: From genesis to emplacement

Michael Brown†
Laboratory for Crustal Petrology, Department of Geology, University of Maryland, College Park, Maryland 20742-4211, USA

INVITED REVIEW

ABSTRACT

At low temperatures (<750 °C at moderate to high crustal pressures), the production of sufficient melt to reach the melt connectivity transition (~7 vol%), enabling melt drainage, requires an influx of aqueous fluid along structurally controlled pathways or recycling of fluid via migration of melt and exsolution during crystallization. At higher temperatures, melting occurs by fluid-absent reactions, particularly hydrate-breakdown reactions involving micas and/or amphibole in the presence of quartz and feldspar. These reactions produce 20–70 vol%, melt according to protolith composition, at temperatures up to 1000 °C. Calculated phase diagrams for pelite are used to illustrate the mineralogical controls on melt production and the consequences of different clockwise pressure-temperature (*P-T*) paths on melt composition. Preservation of peritectic minerals in residual granulites requires that most of the melt produced was extracted, implying a flux of melt through the suprasolidus crust, although some may be trapped during transport, as recorded by composite migmatite-granite complexes. Peritectic minerals may be entrained during melt drainage, consistent with observations from leucosomes in migmatites, and dissolution of these minerals during ascent may be important in the evolution of some crustal magmas. Since siliceous melt wets grains, suprasolidus crust may become porous at only a few volume % melt, as evidenced by microstructures in residual migmatites in which quartz or feldspar pseudomorphs form after melt films and pockets. With increasing melt volume and decreasing effective pressure, assuming the residue is able to deform and compact, the source becomes permeable at the melt connectivity transition. At this threshold, a change from distributed shear-enhanced compaction to localized dilatant shear failure enables melt segregation. The result is a highly permeable vein network that allows transfer of melt to ascent conduits at the initiation of a melt-extraction event. Melt is drained from the anatectic zone via several extraction events, consistent with evidence for incremental construction of plutons from multiple batches of magma. Buoyancy-driven magma ascent occurs via dikes in fractures or via high-permeability zones controlled by tectonic fabrics; the way in which these features relate to compaction and the generation of porosity waves is discussed. Emplacement of laccoliths (horizontal tabular intrusions) and wedge-shaped plutons occurs around the ductile-to-brittle transition zone, whereas steep tabular sheeted and blobby plutons represent back freezing of melt in the ascent conduit or lateral expansion localized by instabilities in the magma–wall-rock system, respectively.

INTRODUCTION

The continental crust is not uniform (Rudnick and Gao, 2003); the upper crust is more silicic and is richer in SiO_2 and K_2O, whereas the lower crust is more mafic and is richer in Al_2O_3, FeO, MgO, and CaO. In addition, the upper crust is enriched in the light rare earth elements and has a large negative Eu anomaly compared to the lower crust. These differences are best explained by intracrustal differentiation due to anatexis of the lower crust and migration of the partial melt to the upper crust. This process leaves a lower crust with trace microstructural evidence of having melted and a more residual bulk chemical composition.

Geophysical surveys confirm that granites are concentrated in the upper continental crust (Vigneresse, 1995). This complements the view from petrological and geochemical studies of exhumed granulite terrains and xenoliths from volcanic conduits demonstrating that the primary source for the melt was residual paragneisses, orthogneisses, amphibolites, and granulites of the lower continental crust (Sawyer et al., 2011). Thus, reworking of the continental crust during orogenesis by extraction of melt from the lower portion and its emplacement in the upper portion is the principal process by which continents have become differentiated into a more mafic, minimally hydrated, and residual lower crust and a more felsic, more hydrated, and incompatible element–enriched upper crust (Brown and Rushmer, 2006).

This article is about the mechanism of crustal reworking and is concerned with granites produced predominantly by anatexis rather than by crystal fractionation of mantle-derived magma. It represents the latest in a series of reviews published during the past two decades (Atherton, 1993; Brown, 1994, 2007, 2010b; Petford et al., 2000; Sawyer et al., 2011), none of which is reviewed herein, but to which the interested reader is referred to follow the development of ideas during the past 20 yr. This article covers material similar to that in the book by Brown and Rushmer (2006), and it includes reference to papers in the *Virtual Special Issue* on crustal melting in the *Journal of Metamorphic Geology* (Brown, 2012).

AN HISTORICAL PERSPECTIVE

"Whereof what's past is prologue; what to come,
In yours and my discharge."
William Shakespeare, The Tempest
Act II, scene i, lines 253–254

"What's past is prologue" is engraved on the National Archives Building in Washington, D.C., and today the phrase is used liberally to mean that history influences, and sets the context for, the present. Thus, it is fitting in an article celebrating the 125th anniversary of the *Geological Society of America Bulletin* to review, briefly, landmark works published by the Geological Society of America relating to the genesis and emplacement of granite. This is followed by a summary of key ideas advanced during the past 50 yr, since they set the context for our present state of knowledge.

World War II led to a vast expansion in government support of science in the United States, which continued after the war with the establishment of the National Science Foundation in 1950. During the second half of the twentieth century, government support of science has

†E-mail: mbrown@umd.edu

GSA Bulletin; July/August 2013; v. 125; no. 7/8; p. 1079–1113; doi: 10.1130/B30877.1; 14 figures.

become the norm in the developed world, and this has driven a global proliferation of scientific journals since the 1960s. The combination of these factors makes any review of the modern literature daunting, and the summary presented here is highly selective.

Immediate Postwar Years (1945–1960)

In his 1947 address as retiring president of the Geological Society of America, Norman L. Bowen succinctly summarized the two alternate, diametrically opposed views relevant at that time about the origin of granite, as follows:

> "We can, indeed, for rough purposes, separate petrologists into the pontiffs and the soaks. Yet, among the pontiffs who bear the stigma of magma, there are none who do not believe that magmas contain volatile constituents of which the principal is water, that these may emanate from the magma and give rise to a liquor that pervades the invaded rocks, transforming them at times into igneous-looking rocks. The difference between the pontiff and the soak is that the latter must have his liquor in lavish quantities on nearly all occasions, but the former handles his liquor like a gentleman; he can take it or leave it according to the indications of the individual occasion, he can take it in moderation when it is so indicated, or again he can accept it in copious quantities and yet retain powers of sober contemplation of attendant circumstances.
>
> The difference of opinion just discussed is a wide difference, and there is little reason to believe that it will be resolved in the near future."
>
> —Bowen (1947)

Today, the difference of opinion has transferred to the field of isotope geochemistry, where it refers to the proportion of mantle versus crustal source material in granites (e.g., Kemp et al., 2009; Clemens et al., 2011; Clemens and Stevens, 2012).

A balanced account of the debate as it stood in 1948 was published in the landmark memoir *Origin of Granite* (Gilluly, 1948, Memoir 28). Memoir 28 was based on papers presented at the seminal conference meeting of the Geological Society of America held in Ottawa at the end of 1947, sandwiched between Read's well-known addresses to the Geological Society of London as president on "space" and "time" in plutonism (Read, 1948a, 1949). In a novel approach, the discussants exchanged papers before the full-day symposium to foster livelier debate from the floor and the podium. The resulting memoir reflects the debate of the time over the contrasting ideas about the formation of granite by the nebulous process of "granitization" or the simple process of crystallization from a melt. For Read, plutonism was "all these operations that give rise to the plutonic rocks, these as I define them comprising the vast transitional assemblage of the metamorphic, migmatitic and granitic rocks" (Read, 1948a, p. 156). At the other extreme from Read, Bowen (1948) was a firm believer in granite having formed by "the method of crystallization differentiation of (basalt) magma" (Bowen, 1948, p. 88).

A decade later, in another landmark memoir, *Origin of Granite in the Light of Experimental Studies in the System: $NaAlSi_3O_8$–$KAlSi_3O_8$–SiO_2–H_2O* (Tuttle and Bowen, 1958, Memoir 74), the magmatic origin of granite was demonstrated via experimental petrology, and in the following year, Buddington (1959) published his extensive review of granite emplacement. Following "the granite series" of Read (1948b), Buddington classified granites according to their level of emplacement in Earth's crust. On this basis, he referred to three types of granite: (1) epizonal granites—discordant plutons crystallized from magma with only minor evidence of granitization; (2) mesozonal granites—plutons that are in part discordant and in part concordant, and in which evidence of granitization is common but subordinate to emplacement of magma; and (3) catazonal granites—plutons that are predominantly concordant and for which granitization was argued to be a major factor associated with the emplacement of magma. Buddington argued for continuity between plutons of the epizone and the mesozone, but he was uncertain whether plutons of the mesozone extended down to roots in the catazone or were pinched off and isolated from it.

Progress during the Last 50 Years

Buddington's article in the *Geological Society of America Bulletin* marks a natural break. The 1960s represent the beginning of the modern era in petrological, geochemical, and structural studies of crustal melting and the formation of granite. However, in arguing for continuity among granites emplaced at different depths in the crust, Buddington's article planted the seed of a paradigm shift in interpreting crustal differentiation by melting as a self-organized critical system with feedback relations from source to sink (Brown, 2010a; Hobbs and Ord, 2010).

Crustal Melting: Experiments and Phase Equilibria Modeling

From experiments, we have a good understanding of phase relations in the granite system (Luth et al., 1964), how granite melt crystallizes (Maaløe and Wyllie, 1975; Scaillet et al., 1995), and how granite itself begins to melt (Johannes, 1984). In a landmark paper, in addition to field, petrologic, geochemical, and geochronological data, Presnall and Bateman (1973) used phase equilibria to argue that a major portion of the Sierra Nevada batholith must have been derived from the lower crust. Furthermore, these authors argued that conductive heat from the mantle and heat from radioactive decay in the crust were sufficient to cause melting in thicker crust, although they recognized the necessity for additional heat from subduction-related magmatism to melt thinner crust in the west. This article marks the beginning of the new debate about crustal versus mantle sources in granite petrogenesis.

Since the centennial article by Whitney (1988), which was concerned with the role and source of water in the evolution of granitic magmas, there have been major advances in our knowledge of crustal anatexis based on experimental studies of melting relations in a wide range of crustal protoliths and synthetic analogs. The range of rock types studied includes: pelites (Vielzeuf and Holloway, 1988; Le Breton and Thompson, 1988; Patiño Douce and Johnston, 1991; Carrington and Harley, 1995; Patiño Douce and Harris, 1998); other mica-bearing metasedimentary rock compositions (Conrad et al., 1988; Vielzeuf and Montel, 1994; Gardien et al., 1995; Montel and Vielzeuf, 1997; Stevens et al., 1997; Koester et al., 2002); amphibolites (Ellis and Thompson, 1986; Rushmer, 1991; Rapp et al., 1991; Wolf and Wyllie, 1994); and, combinations of different protoliths (Patiño Douce and Beard, 1995). In addition, there have been several theoretical analyses of crustal melting (Thompson and Algor, 1977; Thompson and Tracy, 1979; Thompson, 1982; Clemens and Vielzeuf, 1987; Connolly and Thompson, 1989; Vielzeuf and Schmidt, 2001).

This work has provided the foundation for studies using phase equilibria modeling (White et al., 2001, 2007, 2011; Johnson et al., 2008). Phase equilibria modeling has enabled inverse and forward modeling to better characterize the phase relations and chemography of crustal melting for a range of paragneiss and orthogneiss compositions in a chemical system that closely approaches nature (e.g., Johnson et al., 2008; Brown and Korhonen, 2009; Korhonen et al., 2010a, 2012). Because of this effort, we have a detailed understanding of the relationships between protolith fertility and melt production, and the consequences of melt drainage for the residue (White and Powell, 2002; White et al., 2004; Brown and Korhonen, 2009; Johnson et al., 2010, 2011).

Alphabet Granites

Chappell and White (1974) proposed that granites in the Lachlan fold belt of eastern Australia could be classified into one of two types, which they called I- and S-type granites. I-types, which were inferred to have formed from a metaigneous source, characteristically have amphibole and may have clinopyroxene and/or brown

biotite as additional ferromagnesian mineral(s), together with accessory titanite and magnetite. They are metaluminous to weakly peraluminous and relatively sodic, with a wide range of silica content (56–77 wt% SiO_2). S-types, which were inferred to have formed from a sedimentary source, characteristically have muscovite and red-brown (Ti-rich) biotite and commonly cordierite and/or garnet as the ferromagnesian mineral(s), together with accessory monazite and, generally, ilmenite as the oxide. They are strongly peraluminous and relatively potassic, with silica compositions restricted to higher values than the I-types (64–77 wt% SiO_2). In addition, White and Chappell (1977) clearly identified the fundamental relationship between high-grade metamorphism leading to crustal melting and the formation of granite magmas. Furthermore, in 1984 they recognized that the source for the I-types must have been relatively homogenous in comparison with the S-types (Chappell and White, 1984), which led to the view that the two types of granite came from source rocks of fundamentally different origin, namely sedimentray or supracrustal materials (S-types) and igneous or infracrustal, or underplated, materials (I-types). The classification was expanded to include M-type (from the mantle; White, 1979) and A-type (alkaline, relatively anhydrous, and anorogenic; Loiselle and Wones, 1979), and, finally, C-type (charnockitic granitoids; Kilpatrick and Ellis, 1992). Of these, only the A-type, which is relatively potassic, has high FeO/(FeO + MgO), and has elevated high field strength element concentrations, has achieved the same popularity as the I- and S-types.

The geochemistry of the A-type granites has been characterized by Collins et al. (1982) and Whalen et al. (1987), both of whom opted for derivation from relatively dry granulite residual from an earlier granite-producing event. The experiments of Clemens et al. (1986) and Skjerlie and Johnston (1992) supported this petrogenetic model, although other work has suggested a more fertile source and low pressures of melting (Creaser et al., 1991; Patiño Douce, 1997).

White and Chappell (1977; see also Chappell et al., 1987) proposed that the incorporation of "restite"—comprising mineral grains that were residual from the source and "clots" inferred to be pseudomorphs after such grains—with melt explained the observation that granites commonly have higher MgO + FeO than experimental liquids at an appropriate temperature. Furthermore, according to the "restite model," the principal control over the chemistry of granites is the degree of restite unmixing from the liquid, leading Chappell et al. (1987) to argue that granite suites with compositions controlled by restite unmixing image their sources. Criticism of the restite model centered on the identification of restite (Wall et al., 1987; Vernon, 2007), whereas objections to the restite unmixing hypothesis were based largely on chemical arguments about the inability of restite unmixing to replicate the chemical variability found in many granite suites (Wall et al., 1987).

Recently, the restite-unmixing hypothesis has been refined into the "peritectic assemblage entrainment" hypothesis of Clemens et al. (2011) and Clemens and Stevens (2012). The basic modifications to the restite model made by these authors are twofold. First, the entrained material excludes minerals in the source present in excess or not involved in the melting reaction, and, second, the peritectic mineral assemblage is identified by its chemical signature in the granite, but the entrained mineral grains are no longer present, having been dissolved during ascent. This avoids one of the principal objections to the "restite" model, as recently summarized by Vernon (2010), that all the crystals in granites appear to be magmatic and none appear to be pseudomorphs of residual crystals brought up from the source. Nevertheless, the S–I typology reflects the nature of the entrained material in both cases, and granites remain linked to their sources in this revised restite model (Clemens et al., 2011; Clemens and Stevens, 2012), even though they may not image their respective sources as earlier implied (Chappell et al., 1987; Clemens, 2003).

Finally, there is strong evidence from microgranular enclaves (Vernon, 1984, 1990, 2007; Vernon et al., 1988) and isotope geochemistry (McCulloch and Chappell, 1982; Collins, 1996; Keay et al., 1997; Healy et al., 2004; Kemp et al., 2007, 2009) for contamination and multicomponent sources for both I- and S-type granites. Therefore, it may be surprising to the reader that magma mixing has not been incorporated into either the restite unmixing or the peritectic assemblage entrainment hypothesis. The isotope evidence for source composition will be discussed later herein when considering mantle versus crustal inputs to granite magmatism.

Basalt as the Driver of Crustal Melting

It is commonly stated that mantle-derived magmas (basalts) provide the heat necessary for crustal melting, and this is certainly consistent with the requirement for a juvenile input to granite magma, as widely inferred from the isotope signature of many granites (e.g., Keay et al., 1997; Healy et al., 2004; Jahn et al., 2000; Kemp et al., 2007, 2009). This process has received strong support from numerical modeling (Huppert and Sparks, 1988; Bergantz, 1989; Fountain et al., 1989; Petford and Gallagher, 2001; Dufek and Bergantz, 2005). More recently, the model has evolved into a new paradigm for the genesis of intermediate and silicic magmas in "deep crustal hot zones" (Annen et al., 2006b), where, it is argued, hybridization of melts from mantle and crustal sources could explain the isotope data. This process may be particularly important in arcs (e.g., Petford, 1995), but it may be less applicable to melting and the generation of granites in zones of crustal thickening associated with collisional orogenesis, where mafic magma tends to be notably absent (e.g., Reichardt and Weinberg, 2012a, 2012b).

Rheology of Melt-Bearing Crust

In deformation experiments on melt-bearing rocks, the proportion of melt-bearing grain boundaries generally increases as the volume of melt increases, leading to bulk weakening. However, the deformation mechanisms that operate in nature and the locations of thresholds where deformation mechanisms change are only poorly understood. The effect of melt on deformation depends on the amount of melt and its distribution, as well as the grain size and strain rate (Dell'Angelo and Tullis, 1988). Furthermore, the deformation mechanism depends on whether melt can flow as fast as the imposed strain rate; otherwise, melt pressure will increase, leading to melt-enhanced embrittlement (Rutter and Neumann, 1995).

Arzi (1978) argued for a major change in mechanical behavior of melt-bearing rock at a "rheological critical melt percentage" around 20 ± 10 vol%, and van der Molen and Paterson (1979) proposed that granular framework–controlled flow behavior changed to suspension-like behavior at a "critical melt fraction" of 30–35 vol%. Notwithstanding, Rutter and Neumann (1995) found no evidence of such a change in behavior in their experiments, a disagreement they attributed to the different methods employed to change the melt volume at fixed temperature. In the earlier experiments, melt volume was controlled by increasing the water added to the charge, which decreased the viscosity dramatically for larger melt fractions. In contrast, in their experiments, Rutter and Neumann (1995) raised the temperature to increase the melt volume at fixed water content, which does not decrease the viscosity as dramatically. Overall, Rutter and Neumann (1995) argued that as melt volume increases so effective pressure decreases, and the behavior of the anatectic crust changes from distributed shear-enhanced compaction to localized dilatant shear failure. This increases permeability by formation of deformation bands into which melt is expressed.

Using an alternative approach based on percolation theory, Vigneresse et al. (1996) argued

for a minimum of 8 vol% melt to overcome the "liquid percolation threshold," above which melt pockets connect, but they also argued that melt volume must reach a "melt escape threshold" of 20–25 vol% to allow migration of melt with entrained solids over large distances. As discussed next, this first threshold is broadly consistent with results from deformation experiments. In a re-evaluation of the experimental data, Rosenberg and Handy (2005) argued for a change in mechanical behavior as an interconnected grain-boundary network of melt becomes established at ~7 vol%, which they called the "melt connectivity transition" (similar to the liquid percolation threshold of Vigneresse et al., 1996). They attributed continued weakening above the melt connectivity transition to melt flow within interconnected melt-rich domains, although continued weakening may be limited in nature by drainage of melt from the system at this threshold. Thus, the melt escape threshold of Vigneresse et al. (1996) is not realized in nature because melt is drained from the source at a much lower threshold, as suggested subsequently by Rabinowicz and Vigneresse (2004).

Melt Segregation, Ascent, and Emplacement

Inverse modeling of geochemical data from postcollisional granites generated during thermal relaxation of overthickened crust is consistent with drainage of melt in batches from crustal sources at depth (Deniel et al., 1987; Harris and Inger, 1992; Searle et al., 1997; Pressley and Brown, 1999; Clemens and Benn, 2010). The process by which melt may segregate from its residue and be extracted from the source in batches has been described and explained by Sawyer (1991, 1994, 1998, 2001), Brown (1994, 2010a), and Brown et al. (1995) based on examples from the field. These data support a model in which compaction drives melt into a network of veins that drains the source. The link with upper-crustal granites has been investigated by Brown and D'Lemos (1991), Pressley and Brown (1999), Solar and Brown (2001a), and Tomascak et al. (2005), and the consequences of melt loss for the preservation of peak mineral assemblages in residual granulites have been investigated by White and Powell (2002).

The mechanism of ascent of granite magma through the crust remains controversial. Transport through fractures (e.g., Clemens and Mawer, 1992; Brown, 2004; Weinberg and Regenauer-Lieb, 2010) or shear zones (e.g., Strong and Hanmer, 1981; D'Lemos et al., 1992; Hutton and Reavy, 1992; Brown, 1994; Rosenberg, 2004) or conduits controlled by strain (e.g., Brown and Solar, 1998a, 1998b, 1999; Weinberg, 1999) is the most commonly postulated mechanism. In addition, although discredited during the past 20 yr (e.g., Petford, 1996), the viability of diapirism under the right circumstances has been demonstrated by Burov et al. (2003) and Weinberg and Podladchikov (1994).

Similarly, the mechanism of emplacement of granite magma into the upper crust to form plutons remains controversial. Multiple papers identify the intimate relationship between deformation and emplacement, but with different means of accommodation argued for each case. Proposed mechanisms include: emplacement accommodated by local processes related to crustal-scale shear zones (e.g., Hutton, 1982, 1988a, 1988b; Grocott et al., 1994; Vigneresse, 1995; Weinberg et al., 2004, 2009); emplacement in a pull-apart structure along a shear zone (e.g., Guineberteau et al., 1987); emplacement into extensional shear zones (e.g., Hutton et al., 1990; Grocott et al., 1994); emplacement accommodated by multiple local material transfer processes (e.g., Paterson and Fowler, 1993; Paterson and Vernon, 1995); emplacement by dike wedging along a steep reverse-sense shear zone (e.g., Ingram and Hutton, 1994; Mahan et al., 2003); emplacement accommodated by raising the roof or depressing the floor of the pluton (e.g., Benn et al., 1997; Cruden, 1998; Brown and Solar, 1998b, 1999; Vigneresse et al., 1999; Clemens and Benn, 2010); and emplacement accommodated by stoping and assimilation, although the significance of this last process is debated (Glazner and Bartley, 2006, 2008; Saito et al., 2007; Clarke and Erdmann, 2008; Paterson et al., 2008; Yoshinobu and Barnes, 2008). The principal alternative mechanism of emplacement is diapirism (e.g., Ramsay, 1989; Paterson and Vernon, 1995; Miller and Paterson, 1999).

WHERE ARE WE NOW?

In the remainder of this anniversary article, the process of crustal melting, the types of melting, and the fertility of source materials are discussed first, including some of the geochemical consequences of melting along particular clockwise pressure (*P*)–temperature (*T*) paths. This is followed by a consideration of mechanisms of melt segregation and extraction, and mechanisms of ascent and emplacement. Finally, issues are identified for future research.

There is not sufficient space to be concerned with the way in which the crust gets hot enough to melt, and the interested reader is referred to Bea (2012) and Clark et al. (2011) for recent summaries of this topic. Instead, I assume that sufficient heat is generated in the orogenic crust by a combination of radioactive, mechanical (viscous dissipation or shear heating), and chemical (latent heat) processes, supplemented by heat advected with basalt influx from the mantle where there is evidence for this, and that this heat may be redistributed by conduction and advection via intracrustal melt migration.

MELTING THE CRUST

"Our main thesis is simple. Water is essential for the formation of granites, and granite, in turn, is essential for the formation of stable continents. The Earth is the only planet with granite and continents because it is the only planet with abundant water."

—Campbell and Taylor (1983)

Migmatites are complex rocks that are products of prograde melt-producing reactions, loss of most of this melt, and retrograde reactions involving melt left on grain boundaries. Evidence of this sequence of events is preserved in the mineralogy and microstructure of migmatites (at shallower levels) and granulites (at deeper levels) exhumed in orogens (e.g., Brown et al., 1999; Sawyer, 1999; Brown, 2001a, 2001b, 2002; Marchildon and Brown, 2001, 2002; Johnson et al., 2003a, 2004; Holness and Sawyer, 2008; White and Powell, 2002). Migmatite terranes commonly separate deeper-level, residual granulites that may preserve only minimal leucosome (quartzofeldspathic material related to melting but not necessarily preserving liquid compositions) from shallower-level granite terranes where the fugitive magma was emplaced in subsolidus crust. Thus, migmatite terranes are polygenetic in that they appear to represent levels in the crust where melting has occurred, from which melt has drained, in which melt has accumulated, and through which melt has transferred (e.g., Brown, 2001b, 2008). Leucosomes may have liquid compositions, they may consist of dominantly peritectic minerals, they may have cumulate compositions, or they may have crystallized from fractionated liquids (e.g., Brown, 2001b; Solar and Brown, 2001a).

Figure 1 is a calculated pressure *P-T* pseudosection (isochemical phase diagram) for an average amphibolites-facies pelite composition in the chemical system Na_2O–CaO–K_2O–FeO–MgO–Al_2O_3–SiO_2–H_2O–TiO_2–Fe_2O_3 (NCKFMASHTO; modified from Brown and Korhonen, 2009). Abbreviations used in this diagram are: Bt—biotite, Crd—cordierite, Grt—garnet, Kfs—K-feldpsar, Ky—kyanite, Liq—hydrous silicate melt, Mag—magnetite, Ms—muscovite, Opx—orthopyroxene, Pl—plagioclase, Qtz—quartz and Sil—sillimanite. This phase diagram may be used to investigate the process of melting for an undrained system (Brown and Korhonen, 2009). The effects of melt loss on the formation and preservation of suprasolidus

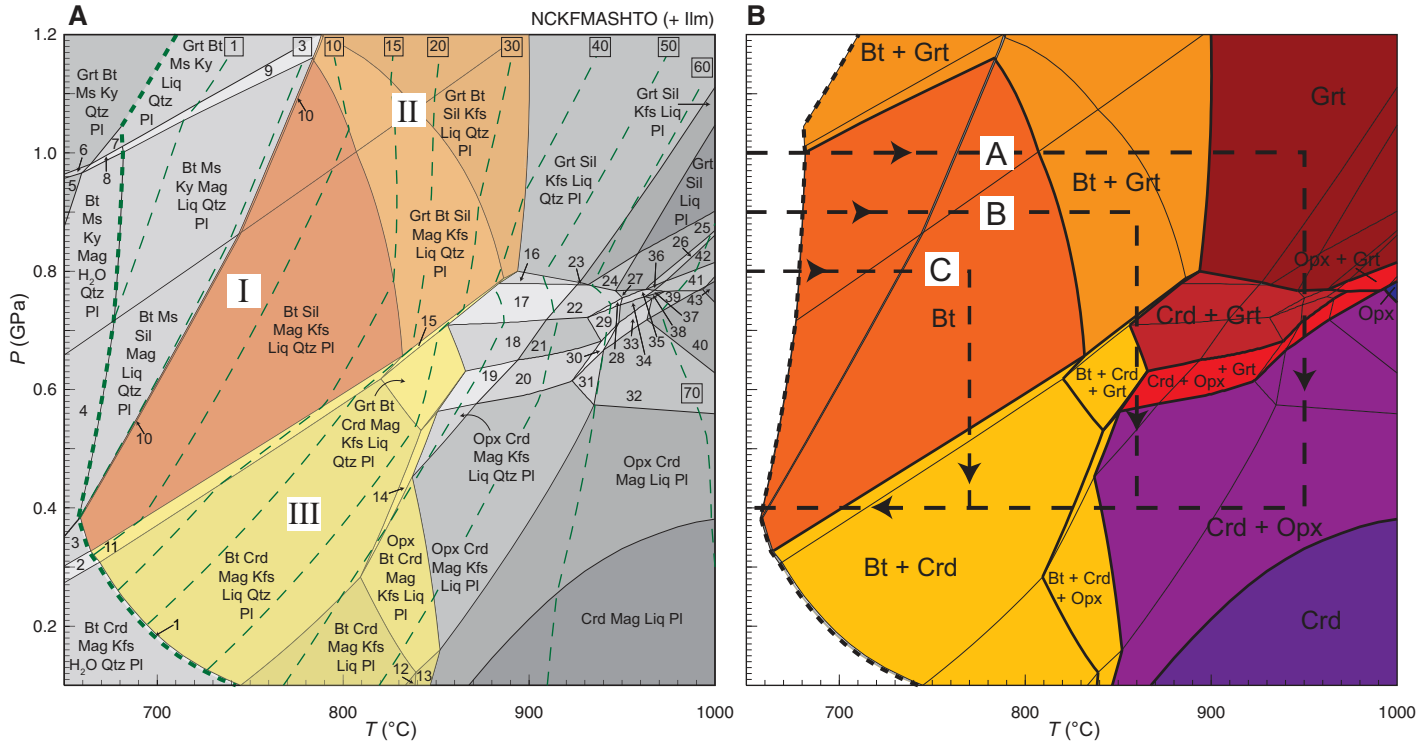

Figure 1. (A) Pressure (*P*)–temperature (*T*) pseudosection (isochemical phase diagram) calculated for an average amphibolites-facies pelite composition in the system Na_2O–CaO–K_2O–FeO–MgO–Al_2O_3–SiO_2–H_2O–TiO_2–Fe_2O_3 (NCKFMASHTO; modified from Brown and Korhonen, 2009). Abbreviations used in this diagram are: Bt—biotite, Crd—cordierite, Grt—garnet, Kfs—K-feldpsar, Ky—kyanite, Liq—hydrous silicate melt, Mag—magnetite, Ms—muscovite, Opx—orthopyroxene, Pl—plagioclase, Qtz—quartz and Sil—sillimanite. This diagram is drawn for a fixed composition, which means that processes such as melt loss cannot be considered in relation to this diagram but require calculation of a new pseudosection for the residual composition after an imposed melt drainage event. The heavy green dashed line represents the solidus. The three colored areas labeled I, II, and III are discussed further in the text. The pseudosection is contoured for melt mol% (light green dashed lines) for a rock saturated in H_2O at the solidus at 1.2 GPa; because the composition is fixed and melt loss is not considered, the amount of melt simply increases with increasing temperature, whereas in nature, melt drainage would be expected to occur. Due to the different amount of H_2O required to saturate the rock in aqueous fluid at different pressures along the solidus, the amount of fluid present along the low-*P* part of the solidus is an overestimation, and consequently the amount of melt produced at low pressures is overestimated. For clarity, the small multivariant phase assemblage fields are not labeled with the phase assemblage; these fields may be identified by reference to the caption to Figure 2 in Brown (2010b). (B) The same *P*-*T* pseudosection with the suprasolidus stability of the rock-forming ferromagnesian minerals emphasized. Below ~850–900 °C, biotite-bearing assemblages are stable (orange fields); at temperatures above the stability of biotite, at higher pressures, garnet-bearing assemblages are stable (red fields), whereas at lower pressures, cordierite-bearing assemblages are stable (purple fields). Three schematic clockwise *P*-*T* paths are shown, labeled A, B, and C; the petrological consequences of each of these evolutionary paths in *P*-*T* space are discussed in the text.

phase assemblages in peraluminous migmatites and residual granulites are discussed by White and Powell (2002) and are not reiterated here.

In the presence of aqueous fluid, common crustal protoliths, such as pelites and graywackes (Brown and Korhonen, 2009), and siliceous igneous rocks (Sawyer, 2010), begin to melt at temperatures of 650–700 °C at crustal pressures. However, the amount of pore fluid immediately below the solidus is small, and rocks in the granulite facies are essentially "dry" (Yardley and Valley, 1997), so that fluid-undersaturated conditions predominate during high-grade metamorphism, melts generally will be H_2O-undersaturated (Clemens, 2006), and the residue will eventually become (nominally) anhydrous (Xia et al., 2006). Thus, major melt production requires the breakdown of hydrate minerals in protoliths that also contain quartz and feldspar, for example, at temperatures above 750–800 °C for mica-bearing rocks and above 850–900 °C for amphibole-bearing rocks (Clemens, 2006). As melting continues to temperatures above the terminal stability of the hydrate phase involved, the melt becomes progressively drier by consuming solids to lower the H_2O content; this is mostly achieved by dissolving quartz and feldspar.

Fluid-present melting or fluid-absent hydrate-breakdown melting in migmatites and granulites may be distinguished based on the nature of the ferromagnesian minerals associated with leucosomes. Mica- and hornblende-bearing leucosomes without anhydrous minerals in mica- and hornblende-bearing hosts are more likely to be the product of fluid-present melting (Figs. 2A and 2B; for an example, see Milord et al., 2001), whereas leucosomes that carry nominally anhydrous (peritectic) minerals, such as garnet or pyroxene, are more likely to be a product of fluid-absent hydrate-breakdown melting (Figs. 2C and 2D; for an example, see White et al., 2004). Without additional aqueous fluid and at crustal temperatures up to 1000 °C, various crustal rocks, such as pelites, graywackes,

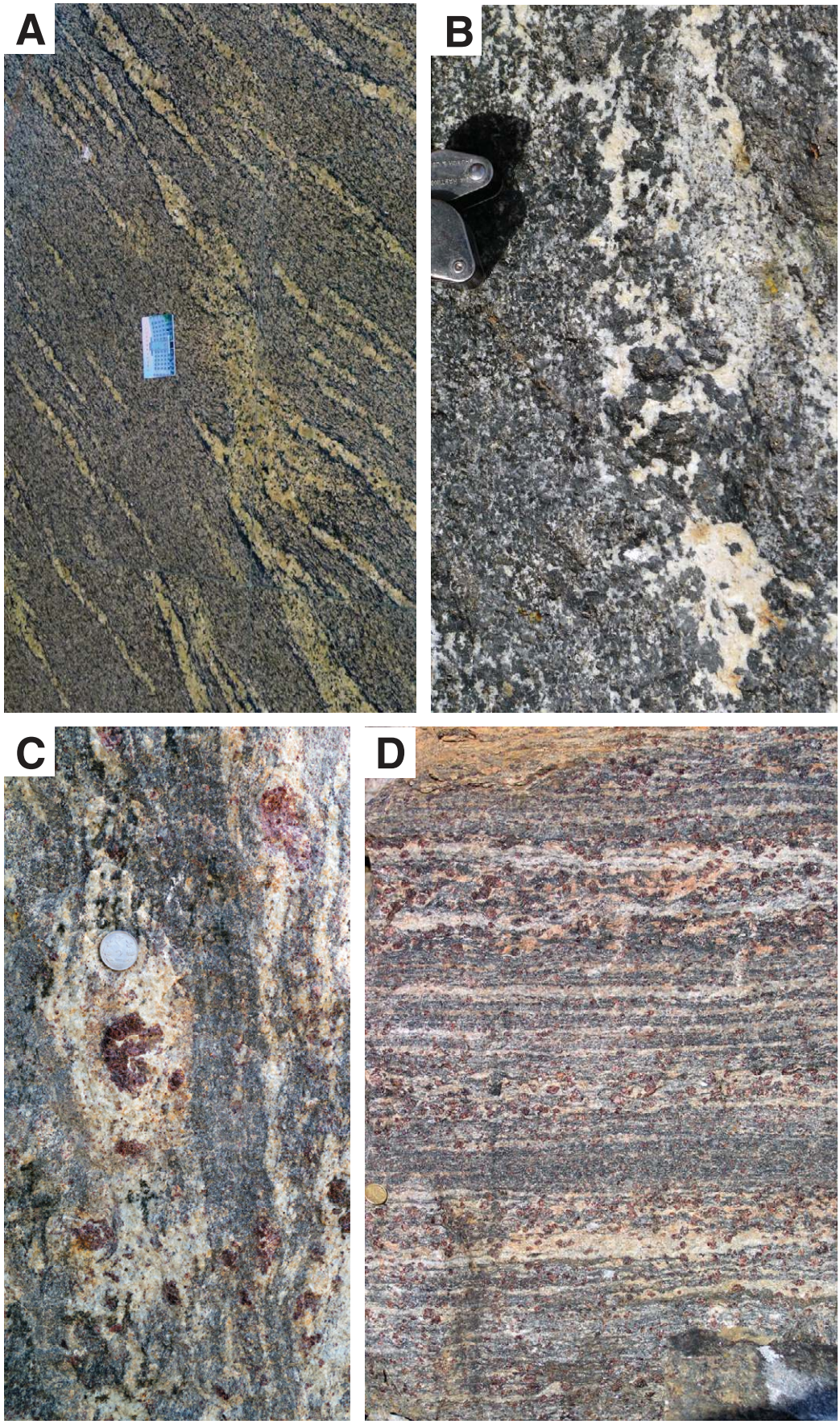

Figure 2. Mesoscale features associated with fluid-present (A and B) and fluid-absent hydrate-breakdown (C and D) melting. (A) Stromatic metatexite migmatite with biotite-rich melanosomes interpreted to have formed by fluid-present melting. Floor of the Guest Hotel foyer at the China University of Geosciences, Wuhan, China; door key card for scale. (B) Patch metatexite migmatite in amphibolite interpreted to have formed by fluid-present melting; note coarser hornblende crystals associated with the in situ leucosome. From Caishixi in the Taohuayu Geoheritage Scenic Area, Taishan, Shandong Province, China; hand lens for scale. (C) Stromatic metatexite migmatite (khondalite) with pristine peritectic garnet in the leucosomes indicating loss of melt prior to retrograde cooling and final crystallization; this is interpreted to have been a fluid-absent hydrate-breakdown melting event. From Kulappara in the Kerala khondalite belt, southern India; diameter of coin ~20 mm. (D) Mylonitized stromatic metatexite migmatite (high-pressure granulite) with pristine peritectic garnet associated with the leucosomes indicating loss of melt prior to retrograde cooling and final crystallization; this is interpreted to have been a fluid-absent hydrate-breakdown melting event. From the Lixão quarry in the Três Pontas–Varginha Nappe, southern Brasília belt, Brazil; diameter of coin ~20 mm.

granites, andesites, and some amphibolites, may yield 20–70 vol% of H_2O-undersaturated melt (Clemens, 2006) of which 80–95 vol% is extractable, with <<5 vol% remaining on grain boundaries in residual granulites (Sawyer, 2001). Whether this melt is homogeneous is another matter. Homogeneity will be determined by the rates of dissolution of minerals in contact with the melt, the rates of diffusive transport of their components through the melt, and whether residual minerals recrystallize (Acosta-Vigil et al., 2012b). These issues are fundamental for fluid-present melting at high degrees of reaction overstepping.

Fluid-Present Melting of the Crust

As discussed already, there is only a small amount of free aqueous fluid in the subsolidus crust as the solidus is approached with increasing temperature. Aqueous fluid may be introduced at convergent plate margins either above subducting oceanic plates in continental arc systems or during continental collision, for example associated with crustal-scale tectonic structures such as shear zones (Reichardt and Weinberg, 2012a, b). In addition, influx of aqueous fluid may occur locally, for example, associated with: (1) the inner zone of contact aureoles (Pattison and Harte, 1988; Symmes and Ferry, 1995; Johnson et al., 2003b; Droop and Brodie, 2012); (2) an influx of hydrous fluid at temperatures just above the solidus from metasedimentary rocks with a slightly higher solidus temperature that are still undergoing subsolidus muscovite breakdown (White et al., 2005); (3) zones of localized high-strain deformation (Johnson et al., 2001; Berger et al., 2008; Genier et al., 2008; Sawyer, 2010); and (4) extensional fracture systems (Ward et al., 2008).

Fluid-saturated melting is commonly postulated where there is a spatial association with igneous intrusions or tectonic structures and a mismatch between the observed volume of (apparently) locally derived leucosome and the calculated peak *P-T* conditions. In one example, Rubatto et al. (2009) postulated a series of related melting events driven by episodic influx of locally derived aqueous fluid at approximately constant temperature to explain the distribution of zircon overgrowths and ages from leucosomes in migmatites formed during a single Barrovian metamorphic cycle in the central Alps.

In orogens, relaxation of the yield stress developed in the brittle portion of the crust may result in a depth interval below the brittle-to-ductile transition zone characterized by an inverted pressure gradient (Petrini and Podladchikov, 2000; Stüwe et al., 1993; Stüwe and Sandiford, 1994). At depths where this inverted pressure gradient is less than the hydrostatic gradient of an interstitial fluid, an aqueous fluid that is subject to the confining pressure will migrate downward and stagnate where the rock pressure gradient equals the hydrostatic fluid gradient (Connolly and Podladchikov, 2004). This condition defines a depth of tectonically induced neutral buoyancy that also acts as a barrier to upward fluid flow. In combination with dynamic downward propagation of the brittle-to-ductile transition zone during the early stages of orogenic thickening, this phenomenon provides a mechanism to sweep upper-crustal aqueous fluids into the lower crust to promote melting as prograde heating evolves to peak temperatures.

The requirement for influx of aqueous fluid from an external source is obviated if the aqueous fluid that exsolved during magma ascent is recycled (Holk and Taylor, 2000). Evidence to support recycling of aqueous fluid comes from metamorphic core complexes of the Canadian Rockies, where there is a remarkable uniformity of mineral $\delta^{18}O$ values in the middle continental crust beneath detachment faults (Holk and Taylor, 2000). These zones of pervasive homogenization in $^{18}O/^{16}O$ are interpreted to result from exchange with magmatic or metamorphic aqueous fluid, and this same fluid appears to have promoted crustal melting. Holk and Taylor (2000) suggested that melting of pelites and graywackes began at *P-T* of ~0.8 GPa and ~750 °C in response to influx of aqueous fluid associated with thrusting and local muscovite breakdown. The resulting H_2O-rich magma ascended adiabatically through the crust, exsolving H_2O, which rose faster than the magma and exchanged oxygen with subsolidus rocks while catalyzing melting. Final crystallization of magma in plutons occurred at much shallower levels in the crust, where exsolution of H_2O enabled $^{18}O/^{16}O$ exchange with shallow subsolidus country rocks.

Fluid-present melting reactions may be congruent, for example, muscovite + biotite + plagioclase + quartz + $H_2O \rightarrow$ liquid, or incongruent, for example, biotite + plagioclase + quartz + $H_2O \rightarrow$ liquid + garnet + cordierite. In this case, given the different reactants and products involved, there will be concomitant differences in melt chemistry. The steep (at higher *P*) or negative (at lower *P*) slope of the solidus for fluid-present melting limits vertical migration of the melt because the melt crystallizes on decompression to the solidus (Fig. 1A). As temperature increases, if the available H_2O is consumed completely, then further melting must proceed by fluid-absent hydrate-breakdown reactions or by dissolution of quartz and feldspar.

Fluid-Absent Hydrate-Breakdown Melting

Fluid-absent hydrate-breakdown melting occurs over a range of temperatures after an initial insignificant H_2O-present melting step that yields minimal melt from the pore fluid present in the subsolidus protolith. In protoliths of appropriate mineralogy and at pressures above ~0.4 GPa (Fig. 1), melting continues with muscovite breakdown under upper-amphibolite-facies conditions and extends through the granulite facies with biotite breakdown (in peraluminous metasedimentary protoliths) and hornblende breakdown (in metaluminous graywackes and hydrated basaltic protoliths). Fluid-absent hydrate-breakdown melting is incongruent (i.e., solids >> solids + liquid), and nucleation of the solid products of the reaction may be difficult. As a result, once the melting reaction is overstepped, it is energetically favorable for initial diffusion-controlled melting to continue at sites where the solid products nucleated until melt connectivity is established, allowing melt to migrate. As shown in Figure 2C, leucosomes commonly provide evidence that melt generation and accumulation were concentrated around the peritectic product of the melting reaction (e.g., Waters, 1988; Jones and Brown, 1990; Powell and Downes, 1990; Brown, 2004). This process yields leucosomes with coarse-grained peritectic minerals in the center (Brown, 1994; Brown and Dallmeyer, 1996; White et al., 2004). Assuming equilibrium, the volume of melt produced will vary as a function of hydrate mineral content in the protolith and the *P-T* conditions achieved.

Information on fluid-absent hydrate-breakdown melting reactions for a variety of crustal protoliths has been obtained from melting experiments on natural rocks and synthetic mixtures (reviewed by Clemens 2006), and by evaluation of petrogenetic grids and thermodynamic modeling of phase equilibria (Spear et al., 1999; White et al., 2001, 2007; Johnson et al., 2008; Brown and Korhonen, 2009). Recent comparisons between the results of melting experiments on natural compositions and phase equilibria calculated by thermodynamic modeling for the same compositions yield good agreement, inspiring confidence in models for melting processes in the crust (Grant, 2009; White et al., 2011).

The composition of the glass in melting experiments on natural crustal rocks and synthetic compositions varies from granite to tonalite, depending on the composition of the starting material, the H_2O content, and the *P-T* conditions of melting (Clemens, 2006). When these glass compositions are compared with melt inclusions in peritectic minerals in migmatites

and granulites or with the full range of compositions in naturally occurring suites of granite sensu lato, it is clear that a significant portion of the natural compositions cannot be matched with the experimental glass compositions (e.g., Stevens et al., 2007; Cesare et al., 2011; Bartoli et al., 2013). One explanation for this discrepancy is that natural melts selectively entrain peritectic minerals from the source (Stevens et al., 2007; Clemens et al., 2011; Clemens and Stevens, 2012), and that these entrained mineral grains are dissolved or achieve equilibrium during ascent through a process of dissolution-reprecipitation cycling in the melt (Villaros et al., 2009a; Taylor and Stevens, 2010).

This model receives support from the observation in a stromatic migmatite from southern Brittany of garnet within the leucosomes, as imaged using high-resolution computed X-ray tomography, interpreted to be entrained peritectic residue trapped during transport (Brown et al., 1999). Many similar examples have now been reported (Fig. 3; e.g., Taylor and Stevens, 2010; Lavaure and Sawyer, 2011), including entrainment of accessory minerals, particularly zircon, from the source (Watson, 1996). Support is also provided by rare enclaves of strongly melt-depleted residue in granite, such as that described by Solar and Brown (2001a), and rare meter-sized pods consisting of 50–70 vol% garnet (with sillimanite, biotite, plagioclase, and quartz), such as those described by Dorais et al. (2009). In the latter example, from the Cardigan pluton in New Hampshire, whole-rock chemistry suggests that the garnetites either are restites or represent melt-depleted xenoliths; similar neodymium and strontium isotope composition of garnetite and granite, and detailed mineral chemistry reported by Dorais and Tubrett (2012) support an interpretation as restite. Dorais et al. (2009) calculated a magma-ascent rate of >1000 km/yr and proposed that fast ascent inhibited restite dissolution in the Cardigan pluton; they suggested that slower rates of ascent might account for the paucity of restite preserved in most peraluminous granites.

Accessory Minerals

Accessory minerals in granites, especially zircon, monazite, and apatite, have an importance that far outweighs their modal abundance. Both zircon and monazite potentially may be used to determine the age of crystallization of melt retained in the source and of granite emplaced in the upper crust. In addition, in many granites, inherited grains, particularly forming cores in magmatically-precipitated zircon, preserve information about the source. Accessory minerals represent a significant reservoir for a number of petrogenetically important trace elements. These elements include zirconium, yttrium, the heavy rare earth elements, hafnium, and uranium in zircon, and phosphorus, thorium, and the light rare earth elements in monazite. As a result, the dissolution, entrainment, and crystallization of accessory minerals exert a strong control on the trace-element chemistry of granites (Watt and Harley, 1993; Bea, 1996; Watson, 1996; Watt et al., 1996; Bea and Montero, 1999; Brown et al., 1999). Furthermore, zircon and monazite may be used to estimate the temperature of crystallization of the granite host (e.g., Watson and Harrison, 1983; Montel, 1993), and the difference between hosts that are rich or poor in inherited zircon has led to a division into "cold" and "hot" granites, respectively (Miller et al., 2003).

The trace element and isotope composition of many granite bodies has been interpreted to record disequilibrium with respect to refractory accessory minerals in the source (Watt and Harley, 1993; Ayres and Harris, 1997; Jung, 2005; Zeng et al., 2005a, 2005b; Perini et al., 2009; Villaros et al., 2009b; Acosta-Vigil et al., 2012a; McLeod et al., 2012). This feature is sometimes incorrectly inferred to record "disequilibrium melting." However, lower-than-expected concentrations of trace elements and isotope disequilibrium may occur for several reasons.

These reasons include kinetic effects inhibiting dissolution during melting (Watt and Harley, 1993; Watson, 1996; Watt et al., 1996), non-Henrian behavior during melt-solid partitioning (Bea, 1996), and the sequestration of grains as inclusions in major rock-forming minerals (Bea, 1996; but for a contrary view, see Watson et al., 1989). In general, accessory mineral solubility is a function of temperature and melt composition (Harrison and Watson, 1983, 1984; Rapp and Watson, 1986; Montel, 1993). For example, zircon solubility increases strongly with increasing temperature but decreases with increasing silica and aluminum saturation index (Watson and Harrison, 1983; Bea et al., 2006).

During crustal melting, it is the major elements that determine the thermodynamically stable phase assemblages during melting, and

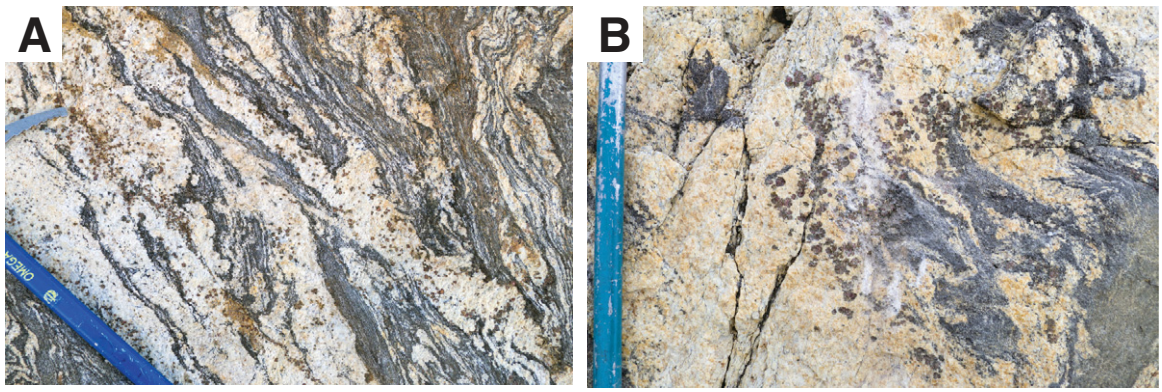

Figure 3. Examples of peritectic assemblage entrainment consequent upon biotite-breakdown melting and melt migration. (A) Leucosomes in stromatic metatexite migmatite link continuously with thin garnet-bearing, high-aspect-ratio tabular granites. The peritectic garnet decreases in the mode with distance away from the migmatite melanosomes, suggesting limited peritectic assemblage entrainment. From the eastern side of Mount Avers in the central part of the Fosdick migmatite-granite complex, Marie Byrd Land, West Antarctica; handle of ice axe for scale. (B) Local concentrations of peritectic garnet are developed in granite against an enclave of stromatic metatexite migmatite. From the eastern side of Mount Avers in the central part of the Fosdick migmatite-granite complex, Marie Byrd Land, West Antarctica; handle of ice axe for scale.

for these elements, the melt and residue are generally in equilibrium at the time scale of interest. In contrast, factors other than thermodynamic equilibrium control the trace-element distributions between the melt and accessory minerals in the residue, so that the melt extracted may be undersaturated with respect to trace-element concentrations and out of isotope equilibrium.

Suprasolidus Phase Equilibria, *P-T* Paths, and the Consequences for Melt Chemistry

Melting may occur by increasing temperature or decreasing pressure at an appropriate temperature above the solidus. With reference to Figure 1A, with increasing temperature, significant melting of metapelite, as modeled in the NCKFMASHTO system, begins with the breakdown of muscovite and biotite at P above ~0.4 GPa across a narrow trivariant phase assemblage field where muscovite is eliminated and K-feldspar appears (field 10 at the low-temperature edge of area I in Fig. 1A). This muscovite-out reaction is followed by a broad quadrivariant phase assemblage field across which melt volume increases by dissolution of quartz and feldspars up to the high-temperature boundary of area I (at a maximum T of 830 °C at 0.66 GPa in Fig. 1A).

With increasing T at $P > 0.66$ GPa, garnet appears across the boundary between areas I and II and progressively increases at the expense of biotite, which is eliminated after an interval of 60–120 °C at the high-temperature boundary of area II (Fig. 1A). At this stage, at ~900 °C, <30 to >40 mol% melt has been generated from this particular protolith composition. With increasing T at $P < 0.62$ GPa, biotite breaks down to cordierite via a narrow trivariant phase assemblage field where sillimanite is eliminated (field 11 at the high-pressure edge of area III in Fig. 1A). Cordierite increases at the expense of biotite across a broad temperature interval of up to 120 °C, after which orthopyroxene appears with cordierite up to the high-temperature boundary of area III (Fig. 1A). At this stage, at ~850 °C, <40 to >50 mol% melt has been generated from this particular protolith composition, but this will be an overestimate because the amount of water in the system was set at 1.2 GPa (Fig. 1A, caption). At $T > 820$ °C at intermediate pressures ($0.62 < P < 0.66$ GPa), both garnet and cordierite appear at the expense of biotite (Fig. 1A).

The composition of all solid-solution phases, including melt, changes as *P-T* evolves, and the topology of the phase diagram will change as the bulk composition changes with melt loss (Yakymchuk et al., 2011). Figure 1B emphasizes the suprasolidus stability of the ferromagnesian silicate minerals for the pseudosection shown in Figure 1A. Using this phase diagram, several aspects of the melting process and the consequences for melt trace-element chemistry may be investigated in relation to different *P-T* paths and the stability of the ferromagnesian silicate minerals.

In the pseudosection, biotite is stable at all pressures at temperatures up to 850–900 °C (Fig. 1B). Since biotite may include accessory minerals such as zircon, monazite, xenotime, and apatite, the stability of biotite may exert a strong control on the trace-element chemistry of the melt, as well as the degree of zircon inheritance. Garnet is stable at moderate to high pressures and temperatures (Fig. 1B), and the development of garnet as a peritectic product of biotite-breakdown melting exerts a strong control on the rare earth element chemistry of both melt and residue. At moderate to low pressure at high temperature, cordierite and orthopyroxene are the stable phases (Fig. 1B). In summary, Figure 1B shows: (1) the suprasolidus stability of biotite before the appearance of garnet, the stability of biotite with garnet, and the stability of garnet beyond the stability of biotite at higher pressures; and (2) the suprasolidus stability of biotite before the appearance of cordierite, the stability of biotite with cordierite, and the stability of cordierite and orthopyroxene beyond the stability of biotite at lower pressures.

The reader is reminded that Figure 1 is a model system designed to illustrate suprasolidus phase equilibria for an average amphibolites-facies pelite. The activity-composition (a-x) models for the phases considered under suprasolidus conditions do not incorporate manganese (White et al., 2007). Accordingly, manganese is not included in the model system used to calculate Figure 1 (Brown and Korhonen, 2009). This omission causes garnet to appear at a higher temperature in the model system than in nature. Similarly, fluorine will stabilize biotite to higher temperatures in real systems.

The utility of the modeling approach is illustrated by reference to three schematic clockwise *P-T* paths appropriate to collisional orogenesis. The consequences of counterclockwise *P-T* paths may be assessed by reference to White and Powell (2002), White et al. (2004), and Clarke et al. (2007). The three clockwise paths cross different phase assemblage fields with different ferromagnesian mineral stabilities that have direct impact on the chemistry of the melt, particularly for the trace-element concentrations and isotope signature, as discussed more fully in the following.

Melting begins at the solidus. For path A in Figure 1B, during the prograde evolution a pulse of melting occurs around 750 °C due to muscovite breakdown, which has consequences for rubidium and strontium concentrations, and strontium isotope chemistry (discussed in the following). Further along the prograde segment of the *P-T* evolution, biotite reacts out completely around 900 °C—creating the potential for dissolution and/or entrainment of any sequestered accessory minerals—with garnet as the peritectic product. This process has consequences for the trace element and isotope chemistry of the melt, since various accessory minerals are the main hosts for zirconium, uranium, thorium, and the rare earth elements (Bea, 1996; discussed further later herein), although heat production may be largely unaffected (Bea and Montero, 1999; Bea, 2012), and garnet preferentially sequesters the heavy rare earth elements. Melting continues during initial decompression at 950 °C, at which point (around 0.75 GPa) close to 70 mol% melt has been produced (Fig. 1A), assuming an unrealistic situation in which no melt is lost from the system.

The prograde segment of path B in Figure 1B crosses the "garnet-in" line but does not reach the "biotite-out" line, creating the potential for dissolution and/or entrainment of some but not all of the sequestered accessory mineral grains. Thus, some zircon and monazite are predicted to remain sequestered within biotite in the residue, with implications for the trace-element chemistry of the melt. At peak temperature of 860 °C, slightly over 20 mol% melt is produced. Additional melting is predicted to occur during high-temperature decompression, but multiple cycles of melt buildup and melt loss during the prograde evolution will limit melt production during decompression (Yakymchuk et al., 2011). During decompression, garnet will be replaced by cordierite and orthopyroxene, unless melt is drained from the system; then reaction of garnet to cordierite and orthopyroxene is limited by the reduced melt available for reaction. Without melt loss, retrograde cooling at 0.4 GPa should result in a final subsolidus assemblage of Bt + Ms + Sil + Mag + H_2O + Qtz + Pl (+Ilm), although the free H_2O at this low pressure is a direct consequence of the amount of H_2O in the system having been set at the solidus at 1.2 GPa (Fig. 1A, caption).

Along path C in Figure 1B, the "garnet-in" line is not crossed on the prograde segment, and biotite remains stable, which may restrict the availability of sequestered accessory mineral grains to dissolve and/or become entrained in the melt, with implications for the chemistry of melt and residue. Garnet is not produced, so the melt is not depleted in the heavy rare earth elements. Along the decompression segment at 770 °C, path C crosses the low-variance Bt + Sil Crd + Mag + Kfs + Qtz + Pl + Liq (+Ilm) field (field 11 on Fig. 1A) involving biotite-

breakdown melting, eliminating sillimanite and producing cordierite, which yields an additional ~15 mol% melt (Johnson and Brown, 2004).

Along the prograde and decompression segments of all three of the model *P-T* paths, H_2O is partitioned into the hydrous silicate melt. In a closed system, cooling potentially will lead to retrogression by reaction between melt and residue (Brown, 2002; White and Powell, 2002). However, the common occurrence of pristine or only weakly retrogressed peritectic minerals in residual migmatites and granulites requires that most melt was drained from the lower crust (Waters, 1988; Powell and Downes, 1990; White and Powell, 2002). This conclusion is consistent with the presence of granites in the upper crust (Brown, 2001b, 2005, 2008; Guernina and Sawyer, 2003) and geochemical evidence, including isotope data, that links granites with lower-crustal sources (Pressley and Brown, 1999; Solar and Brown, 2001a; Johnson et al., 2003c; Tomascak et al., 2005; Hinchey and Carr, 2006). The consequences of open system processes on the dissolution and growth behavior of zircon and monazite with respect to evolving pressure, temperature and silicate mineral assemblages in high-grade, melt-bearing source rocks have been considered briefly by Kelsey et al. (2008).

More about Melt Composition

Melt extraction is expected to occur soon after the melt connectivity transition is reached at ~7 vol% melt (Rosenberg and Handy, 2005; approximately equivalent to 7 mol% melt in Fig. 1A). Thus, multiple cycles of melt buildup and drainage are predicted along the suprasolidus prograde *P-T* evolution (Handy et al., 2001; Brown, 2007, 2010a; Hobbs and Ord, 2010), and the melt volumes predicted for closed-system behavior will not be retained at depth in the orogenic crust. As a result of melt extraction, the bulk composition of the source is likely to have been changed multiple times during the evolution to peak temperature, even allowing for melt flux through the system (Brown, 2004, 2006, 2007). Since the composition of solid solution phases changes with changes in the intensive variables, successive batches of magma will have different major-element compositions (Yakymchuk et al., 2011).

As melt migrates relative to the solid residue during segregation and extraction, so the major- and trace-element composition of the liquid may evolve by interaction with the matrix to determine the chemical signature of the extracted melt (Jackson et al., 2003, 2005; Getsinger et al., 2009). For example, incompatible elements will preferentially enter the melt to be transported upward, whereas compatible elements will be retained in the residue to be transported downward by compaction as the melt is extracted. Thus, the transport of melt relative to the solid matrix of mineral grains is a basic driver in generating temporal and spatial diversity in the major- and trace-element compositions of granite magmas.

Various accessory minerals (principally zircon, rutile, monazite, and apatite) are the main hosts for zirconium, uranium, thorium, and the rare earth elements (Watt and Harley, 1993; Bea, 1996; Bea and Montero, 1999; Kelly at al., 2005; Zeng et al., 2005a, 2005b, 2005c; Kelsey et al., 2008; Kelsey and Powell, 2011). Notwithstanding, it is not clear that breakdown of these minerals under suprasolidus conditions necessarily will lead to saturation of the melt in the liberated elements, since many rock-forming minerals in the granulite facies may become enriched in these elements (Reid, 1990; Fraser et al., 1997; Villaseca et al., 2003, 2007). For example, during prograde fluid-absent hydrate-breakdown melting, as phosphates dissolve, the highly compatible yttrium and heavy rare earth elements are partitioned into peritectic garnet (Pyle et al., 2001), but the light rare earth element and europium budget is controlled by the stability of feldspar (Villaseca et al., 2007). As much as one-third of the zirconium content of residual pelites may be sequestered in rutile and garnet, and although breakdown of garnet to cordierite by reaction with melt during decompression releases zirconium, this simply forms new zircons as inclusions in cordierite (Fraser et al., 1997; Degeling et al., 2001), with possible implications for depletion of zirconium in the melt. For a different protolith composition, Reichardt and Weinberg (2012a) have shown that, during fluid-present melting of calc-alkaline plutonic rocks, the formation of heavy rare earth element–enriched hornblende and its retention in the residue may generate magmas with high (chondrite-normalized) lanthanum to ytterbium and high strontium to yttrium ratios similar to adakites.

In fluid-absent hydrate-breakdown melting, low melt fractions may be isolated along the hydrate grain boundaries. In this case, there is the potential to liberate trace elements concentrated in accessory minerals located along hydrate grain boundaries or possibly from those grains located close to the edges of the hydrate. In contrast, in fluid-present melting, low melt fractions form predominantly at quartz-feldspar grain junctions, which may limit the opportunity for equilibration with trace elements in accessory minerals associated with hydrate grain boundaries or sequestered in hydrate minerals. Synanatectic deformation is also critical (Walte et al., 2005). For example, granular flow (diffusion accommodated grain-boundary sliding) allows melt migration along grain boundaries, which enables better interaction between accessory mineral grains and the interstitial melt, whereas diffusion creep by dissolution-precipitation favors equilibration of grain surface compositions with the interstitial melt. Deformation also favors rapid melt extraction, which may inhibit equilibration between melt and residue (Watt et al., 1996).

The flux of trace element(s) into the melt during dissolution of accessory minerals is a function of radial diffusion-controlled dissolution rate and surface area, which are correlated with grain size, and the degree of undersaturation of the melt with respect to the element(s) concerned (Watson, 1996). Monazite and zircon populations commonly have different average grain size, and the range of grain sizes may vary from protolith to protolith within a source terrane (Nemchin and Bodorkos, 2000). These attributes may lead to relative differences in light rare earth element and zirconium concentrations among small volumes of melt produced in different parts of the source, subject to the caveats discussed previously.

Rock-forming and accessory mineral behavior during melting is important in relation to the isotope composition of the melt. The isotope composition of a melt depends on the minerals being consumed during melting and the time elapsed since the last isotope equilibration event. For example, the initial lead (Pb) isotope composition of a melt is sensitive to the age(s) and abundance of zircon in the source and the amount of radiogenic lead that is incorporated into the melt through dissolution of zircon (Hogan and Sinha, 1991). Similarly, the samarium and neodymium content, the samarium to neodymium ratio, and the neodymium isotope composition of a melt depend on the amount of apatite and monazite dissolved in the melt and the degree of samarium to neodymium fractionation and neodymium isotope disequilibrium (Ayres and Harris, 1997; Zeng et al., 2005a, 2005b).

In contrast, the micas, amphiboles, and feldspars control the rubidium and strontium content, the rubidium to strontium ratio, and the strontium isotope composition of a melt. Although apatite also incorporates strontium, the strontium isotope composition of any melt will be dominated by feldspar, which is much more abundant in any source rock. Muscovite and biotite have very high rubidium to strontium ratios (generally >50), whereas plagioclase and hornblende have very low rubidium to strontium ratios (generally <1), so that fractionation during nonmodal melting will yield liquids with distinct isotope signatures (Harris and Inger, 1992; Zeng et al., 2005a, 2005b, 2005c; Farina

and Stevens, 2011). Since the hydrate involved in fluid-absent crustal melting and the stoichiometry of the melting reaction change with increasing temperature, as discussed earlier, lower-temperature melts and higher-temperature melts are likely to have distinctive chemistries and isotopic compositions. In addition, strontium isotope disequilibrium may occur if melt extraction is sufficiently fast to prevent trace-element and isotope equilibrium between melt and residual minerals (Hammouda et al., 1996; McLeod et al., 2012). Spatial and temporal heterogeneity in the initial isotopic composition of granites may be inherited from the source. The heterogeneity is preserved in granites because of the incremental construction of plutons from multiple batches of magma and the lack of pluton-wide homogenization (Deniel et al., 1987; Hogan and Sinha, 1991; Pressley and Brown, 1999; Tomascak et al., 2005; Farina and Stevens, 2011; McLeod et al., 2012).

During crustal melting, various factors affect the dissolution of accessory minerals such as zircon, monazite, and apatite, and consequently control the concentration of the various essential structural constituents derived from these minerals in the melt. These factors include: the microstructural location of the accessory minerals (along grain boundaries or sequestered as inclusions) and the stability of the major rock-forming minerals that host inclusions (Watson et al., 1989; Bea et al., 2006); the kinetics of dissolution (Bea, 1996; Watson, 1996); the extent of anatexis (Rubatto et al., 2001); the chemistry of the melt (Watson and Harrison, 1983); and the *P-T* path (Roberts and Finger, 1997). Some of these and other factors affect the precipitation of these accessory minerals during crystallization and consequently the saturation of the melt in the various essential structural constituents of these minerals. These factors include: the bulk rock chemical composition (Kelsey et al., 2008); the entrainment of residual grains (Watson, 1996); the *P-T* path (Roberts and Finger, 1997); the chemistry of the melt (Watson and Harrison, 1983); and fractionation at all scales due to decreasing saturation levels of the essential structural constituents in accessory minerals with falling temperature or the formation of diffusion-controlled compositional gradients in the melt adjacent to crystallizing minerals (Wark and Miller, 1993).

As a result, the use of zirconium and the light rare earth element concentrations of granites to determine magma temperatures based on zircon and monazite solubility (Miller et al., 2003; Chappell et al., 2004) may be flawed in some circumstances. For example, low-zirconium granites may reflect sources that follow a *P-T* evolution similar to path C (or possibly path B) in Figure 1B. In this case, zircon may remain sequestered or partially sequestered in biotite. Even a high-temperature *P-T* evolution similar to path A (or possibly path B) may reduce the zirconium available to the melt if a proportion of the zirconium is partitioned into the peritectic minerals. Thus, rather than being true low-temperature melts, as might be inferred from their zirconium concentrations, low concentrations of zirconium may be a function of sequestration of zircon (Bea, 1996) or of high-temperature element partitioning in the source (Villaseca et al., 2007).

Mantle versus Crust as Sources

Recently, it has become popular to argue that granites emplaced in continental margin arc systems were crystallized from hybrid magmas with both mantle and crustal inputs in the source (Keay et al., 1997; Gray and Kemp, 2009), particularly I-type granites. If this interpretation is shown to be correct, then I-type granites may provide a link between the process of formation of crust in arcs and the generation and differentiation of ancient continental crust (Davidson et al., 2005; Dufek and Bergantz, 2005; Hawkesworth and Kemp, 2006; Kemp et al., 2007, 2009; Lackey et al., 2008).

Kemp et al. (2007) used hafnium and oxygen isotope compositions obtained from zoned zircon crystals to investigate the petrogenesis of the classic hornblende-bearing (I-type) granites of eastern Australia. The hafnium and oxygen isotope compositions correlate with each other over the full range, from compositions characteristic of the mantle to those characteristic of metasedimentary protoliths (cf. Keay et al., 1997). Kemp et al. (2007) argued that this covariation demonstrates that the granites were formed by reworking of metasedimentary protoliths by mantle-derived melts and not by melting of lower-crustal igneous protoliths as previously proposed (Chappell et al., 2004, and references therein).

This perspective receives support from experiments concerning the relative contributions of crust and mantle to granite magmas (Patiño Douce, 1999). With the exception of peraluminous granites, Patiño Douce (1999) concluded that all other granite magmatism is associated with crustal growth rather than just recycling.

In contrast, Clemens et al. (2011) maintain that I-type granites are of purely crustal origin, but they are derived from arc volcanic and sedimentary rocks of intermediate composition that pass on the isotope signature of a mixed mantle and crustal source. These authors propose that the distinctive chemistry of the I-types is due to peritectic assemblage entrainment, specifically, differential entrainment of peritectic clinopyroxene, plagioclase, and ilmenite/titanomagnetite, and entrainment of residual apatite and zircon. Although rare in I-types, where pyroxenes occur, they have the textural and chemical characteristics of magmatically precipitated minerals (Vernon, 2010). Small crystals of peritectic origin entrained in melt from the source are inferred to be dissolved and/or recrystallized during ascent and crystallization.

At convergent plate margins, the proportion of supracrustal to juvenile material may vary through time, as shown by Lackey et al. (2008) for the central Sierra Nevada batholith and by Kemp et al. (2009) for the Australian Tasmanides. In a wide-ranging study of granites from the Australian Tasmanides, Kemp et al. (2009) showed that the S-type, I-type, and A-type granites define striking secular trends in ε_{Nd}-ε_{Hf}-$\delta^{18}O$. These trends correlate with cycles from shortening to extension related to slab advance and retreat that control the proportion of source inputs. Each cycle begins with S-type granites derived by melting of a thickened turbidite-filled backarc basin as slab advance changes to retreat, leading to input of basaltic melt that provides both heat and fluids for anatexis of the turbidites. Subsequently, I-type granites are generated during ongoing slab retreat and lithospheric extension by the increase in input of juvenile basalt. These I-type granites have ^{18}O-enriched zircons that show evidence of extensive sediment incorporation into a juvenile basaltic melt (Kemp et al., 2007, 2009). The juvenile component within the granites increased from the Cambrian to the Triassic, consistent with a decreased input of sedimentary detritus from the craton as the arc-backarc system migrated oceanward with time. A-type granites in the Tasmanides are closely associated with mafic intrusives that have similar geochemical and isotopic characteristics to the granites (Turner et al., 1992; Kemp et al., 2005). Contradicting the original interpretation of a lower-crustal origin from residual granulite, these data point to an origin by differentiation from alkaline basaltic melt, with trends to lower zircon ε_{Hf} and sparse inherited zircon cores reflecting variable but volumetrically minor incorporation of crust (Kemp et al., 2005, 2009).

In a contrary perspective, Villaros et al. (2012) have shown that the time-evolved ε_{Hf} arrays for inherited zircon cores from the Pan-African S-type granites of the Cape granite suite overlap closely with the ε_{Hf} range displayed by the magmatic zircon rims at the time of crystallization of the granites. Thus, in contrast to the earlier studies discussed already, which have interpreted similar arrays to reflect mixing between crustal- and mantle-derived magmas,

Villaros et al. (2012) argued that these arrays may be wholly inherited from the source, reflecting mixing among various crustal materials of different ages with original hafnium isotope compositions. This interpretation supports the original view of S-type granites, i.e., that they inherit their chemical characteristics from the source. If this interpretation is correct, it provides strong support for the hypothesis that peritectic assemblage entrainment is the primary mechanism by which granite magmas acquire compositions more mafic than the range defined by the compositions of crustal melts (Clemens and Stevens, 2012).

An additional example of polyphase crustal reworking largely without any juvenile input is provided by the Fosdick migmatite-granite complex of West Antarctica, which preserves evidence of two crustal differentiation events along a segment of the former active margin of Gondwana, one in the Devonian–Carboniferous and another in the Cretaceous (Korhonen et al., 2010a, 2010b, 2012). The Hf-O isotope composition of zircons from Devonian–Carboniferous granites is explained by mixing of material from two crustal sources consistent with the high-grade metamorphosed equivalents of a Lower Paleozoic turbidite sequence and a Devonian calc-alkaline plutonic suite without input from a more juvenile source (Yakymchuk et al., 2013b). In contrast, the Hf-O isotope composition of zircons from Cretaceous granites requires a contribution from a more juvenile source in addition to contributions from the high-grade metamorphosed equivalents of the turbidite sequence and the Devonian calc-alkaline plutonic suite (Yakymchuk et al., 2013b). The Fosdick complex granites contrast with coeval granites in other localities along and across the former active margin of Gondwana, including the Tasmanides of Australia and the Western Province of New Zealand, where the wider range of more radiogenic ε_{Hf} values of zircon suggests that juvenile material played a larger role in granite genesis. This suggests arc-parallel and arc-normal variations in the proportion of crustal reworking versus crustal growth along the former active margin of Gondwana (Yakymchuk et al., 2013b).

CURRENT VIEWS ON MELT SEGREGATION AND EXTRACTION

In several studies, the size-frequency distributions and spacing of plutons show power-law distributions; these distributions have been used to argue that magmatic systems are self-organized from the bottom up (Bons and Elburg, 2001; Cruden and McCaffrey, 2001; Cruden, 2006; Koukouvelas et al., 2006). This view is consistent with multiple studies of relict anatectic systems (Brown and Solar, 1998a; Brown, 2005, 2010a; Hall and Kisters, 2012; Yakymchuk et al., 2012) and results from modeling (Petford and Koenders, 1998; Bons and van Milligen, 2001; Ablay et al., 2008; Hobbs and Ord, 2010) that suggest melt extraction may be a self-organized critical phenomenon.

The formation of upper-crustal plutons requires that melt be generated and separated from solid residue within lower-crustal sources and then become focused into high-permeability ascent conduits to feed the roots of plutons. This mass transfer involves a multitude of physical and chemical processes that operate at several different length and time scales linked by feedback relations between melting and deformation (Brown, 2010a). However, the rheology of crust composed of two distinct but interacting phases, a stiffer solid matrix that hosts a weaker liquid, is complex. Evaluating this rheology is made difficult by the dramatic change in strength that occurs as melting progresses, the dependence of strength on grain-scale distribution of the melt, and the melt pressure, which will be at or close to lithostatic. As a result, actively melting crust is a highly dynamic nonlinear system with history- and time-dependent behavior, characterized by changes in deformation mechanism and redistribution of melt by two-phase flow (Vigneresse, 2004; Rosenberg and Handy, 2005; Walte et al., 2005; Rutter and Mecklenburgh, 2006; Závada et al., 2007; Schulmann et al., 2008).

If this interpretation of anatectic systems is accepted, then effect is fed back to cause, which may be negative, tending to stabilize the system, or positive, leading to instability. This nonlinear behavior leads to unpredictability, which is expressed in anatectic systems by melt-extraction events. Random fluctuations drive the self-organization of anatectic systems, allowing them to explore new structures while attempting to find the preferred structure (the "attractor"). Over time, these fluctuations permit the anatectic system to approach a point at which the properties change suddenly (the critical point) and to maintain itself at that point (e.g., where the matrix in a dynamic system goes from nonpercolating [disconnected] to percolating [connected] or vice versa). This property is called self-organized criticality. If it is assumed that an anatectic system can mutate, then the system may change toward a more static or a more changeable configuration. If the configuration is too static, a more changeable configuration will be selected, and vice versa, until a particular dynamic structure that is optimal for the system is achieved. Thus, anatectic systems adapt to converge on the optimal structure for melt extraction (Brown, 2010a; Hobbs and Ord, 2010).

Inferences from Residual Migmatites and Granulites

Pseudomorphs of melt-filled pores in migmatites (Holness and Sawyer, 2008) are consistent with pervasive melt flow at the grain scale. Similar to texturally equilibrated rocks, melt is inferred to flow along three-grain edges, where the geometry of the conductive channels is controlled by the wetting relations between solid and liquid phases (Laporte et al., 1997), or along individual grain boundaries if these dilate under tectonic stresses (Schulmann et al., 2008).

At outcrop scale, leucosome distribution records the interplay between deformation and mesoscale migration of melt, and it provides information about the minimum permeability of the anatectic zone (Tanner, 1999; Sawyer, 2001; Marchildon and Brown, 2002, 2003; Guernina and Sawyer, 2003; Brown, 2004, 2010a). Although not ubiquitous at all leucosome intersections, for reasons related to the origin of the leucosomes (peritectic vs. cumulate vs. liquid) and the mechanism of crystallization (cooling vs. diffusive loss of H_2O), petrographic continuity (similar modal mineralogy, grain size, and microstructure) between concordant and discordant leucosomes, as shown in Figure 4, is a common occurrence that has been reported in multiple studies (Maaløe, 1992; Brown, 1994, 2004, 2006; Oliver and Barr, 1997; Marchildon and Brown, 2001, 2002, 2003; Sawyer, 2001; Guernina and Sawyer, 2003; Weinberg and Mark, 2008; Hall and Kisters, 2012). Based on this robust observation, networks of leucosome-filled deformation bands in migmatites are inferred to be evidence of the former active melt flow networks in the suprasolidus crust (Jones and Brown, 1990; Allibone and Norris, 1992; Brown, 1994, 2001a, 2001b, 2004, 2005, 2006, 2010a; Collins and Sawyer, 1996; Oliver and Barr, 1997; Sawyer, 1998, 2001; Brown et al., 1999; Sawyer et al., 1999; Daczko et al., 2001; Guernina and Sawyer, 2003; Marchildon and Brown, 2003; White et al., 2004; Weinberg and Mark, 2008; Hall and Kisters, 2012; Yakymchuk et al., 2012).

In the Karakoram shear zone, Weinberg and Mark (2008) have shown that melt migrated from grain boundaries to layer-parallel leucosomes in stromatic metatexite migmatite, and then to the axial surfaces of developing folds, where intersecting leucosomes formed pipe-like "backbone" structures for faster flow parallel to the fold hinge lines. Synchronous folding and melt migration led to layer disaggregation, transposition, and the formation of diatexite migmatites, demonstrating that melt migration was an integral part of the accommodation of strain (Weinberg and Mark, 2008, their fig. 15).

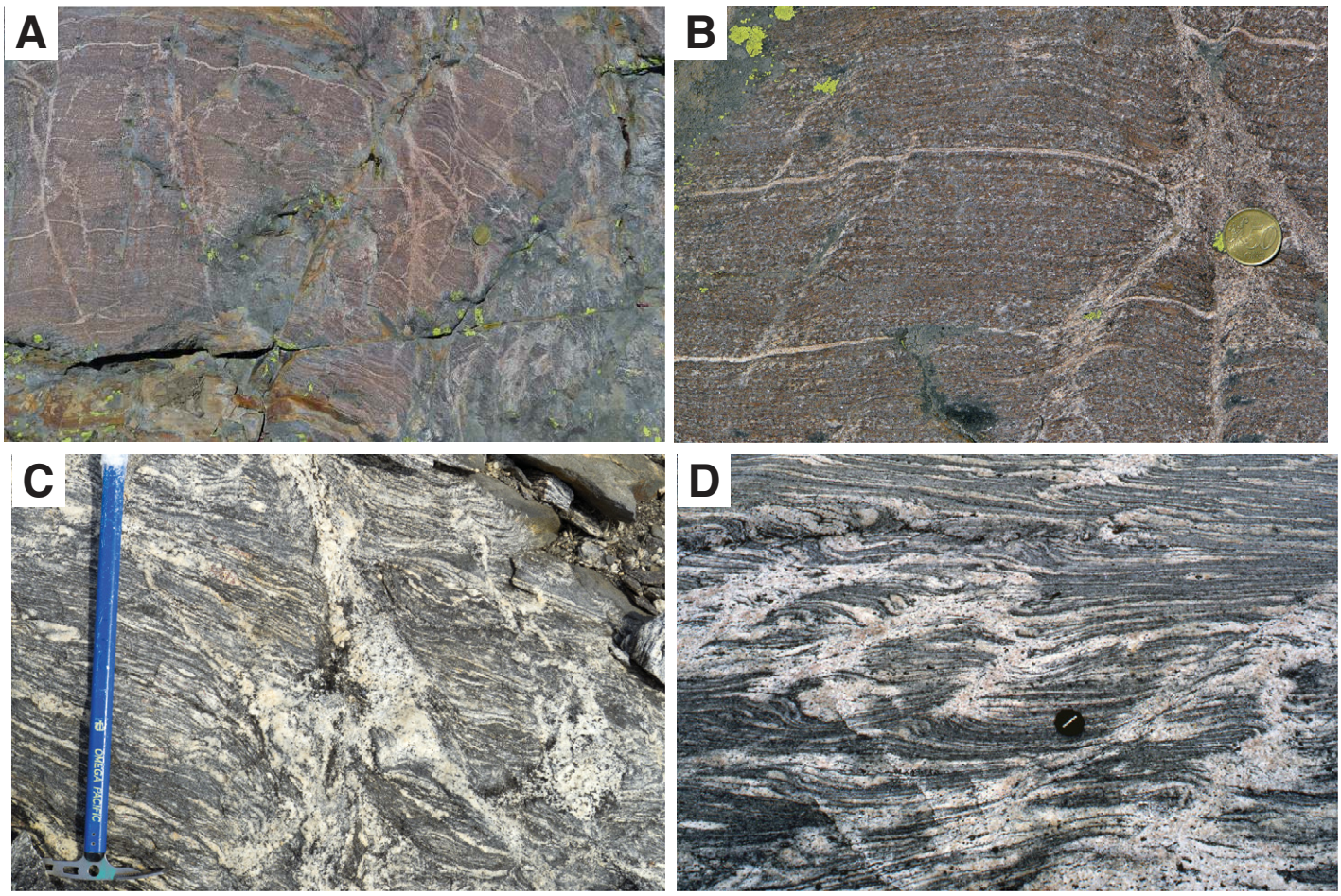

Figure 4. Features associated with inferred former melt-bearing structures in metatexite migmatites that are consistent with melt flow down deformation-induced gradients in hydraulic potential from foliation-parallel leucosome stomata to dilation and shear bands. The dilation and shear bands represent faster-flow melt-extraction pathways formed by the change from distributed shear-enhanced compaction to localized dilatant shear failure, which enhances permeability if the porosity is low, enabling focused melt flow. (A) Net structured metatexite migmatite with thin layer-parallel leucosome stromata (equivalent to compaction bands) and transverse leucosome veins in dilation and shear bands. From a kilometric raft of migmatite within the Hoyos granodiorite, central Gredos, Avila batholith, central Spain; diameter of coin is ~15 mm. (B) Close-up of the same outcrop as that in A, showing details of the linkage between leucosome in the stromata and leucosome in the shear bands; diameter of coin is ~15 mm. (C) Example of petrographic continuity (similar microstructure, mineralogy and mode) between leucosome in stromatic metatexite migmatite and leucosome concentrated in shear bands. From 1070 m peak in the western part of the Fosdick migmatite-granite complex, Marie Byrd Land, West Antarctica; pencil for scale. (D) Example of leucosome in shear band network that is in petrographic continuity (with similar microstructure, mineralogy and mode) with leucosome in the foliation-parallel stomata, inferred to record a former melt reservoir. From the Tolstik Peninsula, Karelia, Russia; diameter of lens cap is 55 mm.

Similarly, leucosomes in migmatites exposed on Kangaroo Island, South Australia (Weinberg et al., 2013), suggest migration of melt toward the hinge zones of antiformal folds. At these sites, funnel-shaped networks of leucosome form a root zone that links up toward a central axial-planar channel, forming the main melt-extraction pathways during folding.

Leucosomes that lie in orientations parallel to fold axial surfaces form perpendicular to the axis of maximum shortening and, by inference, in the plane perpendicular to the local maximum principal stress. The implication is that melt pressure was able to overcome the maximum principal stress plus the tensile strength of the host parallel to it. This may occur during folding if the differential stress is small and a fabric is developed in the plane perpendicular to the maximum principal stress (Wickham, 1987; Lucas and St. Onge, 1995; Brown and Solar, 1998a; Vernon and Paterson, 2001).

As discussed earlier herein, the preferential occurrence of peritectic minerals in leucosomes (Figs. 2C and 3A), in spite of a homogeneous distribution of reactant minerals in the protolith, supports an inference that melting was localized at these sites (Powell and Downes, 1990; Brown, 2004; White et al., 2004). The preservation of the peritectic minerals with only minimal retrogression supports an inference of melt loss. Leucosomes occur in networks of deformation bands, indicating that strain was localized by the concentration of melt around the peritectic minerals and that melt drained via the leucosome networks. In addition, melt loss is inferred if bulk chemistry reveals a depleted composition for residual source rocks in comparison with the expected protolith composition (e.g., Solar and Brown, 2001a; Korhonen et al., 2010a,

2010b), and it is also implied by the formation of collapse structures (Bons et al., 2008). Nevertheless, net melt loss estimated qualitatively based on this type of evidence is a minimum, since residual migmatites and granulites preserve an integrated record of melt flux through the anatectic zone (Brown, 2004; Olsen et al., 2004; Slagstad et al., 2005; Korhonen et al., 2010a, 2010b).

One consequence of melt flux is that leucosomes are rarely primary liquid compositions; commonly, they are of two types. In the first type, the compositions exhibit strong positive europium anomalies and low zirconium concentrations, features that are expected of leucosomes formed during the early stage of segregation and extraction. Leucosomes of this type represent either early crystallization of feldspars and quartz (Sawyer, 1987; Solar and Brown, 2001a, 2001b; Johnson et al., 2003c, 2012; Korhonen et al., 2010b) or prograde growth and accumulation of peritectic feldspar (together with a ferromagnesian peritectic mineral, such as garnet, and possibly residual quartz) as the result of chemical potential gradients present during melting (White et al., 2004). In the second type, the compositions show strong negative europium anomalies and high zirconium, features that are expected of leucosomes formed from percolating fractionated melt trapped during cooling of the terrane (Sawyer, 1987, 1998; Solar and Brown, 2001a, 2001b; Hinchey and Carr, 2006; Korhonen et al., 2010b; White and Powell, 2010).

The contrast between cumulate and fractionated leucosome compositions is generated as melt migrates because it encounters host rock that is cooler than the liquidus for the melt composition, which causes crystallization of liquidus minerals (likely feldspar and quartz) on the channel walls. Thus, there is a continuous process of crystallization and liquid fractionation during extraction until the evolved melt crosses the anatectic front, after which, if the evolved liquid is of sufficient volume, it ascends to an upper-crustal pluton.

Additional complexity in leucosome compositions arises where hybridization of melts from different protoliths occurs in the source or a leucosome network is reused multiple times. For example, Reichardt et al. (2010) described leucosomes that root in different protoliths, merging with each other and homogenizing as they link up to form a hierarchy of channels, feeding into stocks, plutons, and ultimately into the Karakoram batholith. This interpretation is supported by the hybrid isotope signature of leucosomes, which is intermediate between the protolith signatures, and their similarity to intrusive granites. Thus, the leucosomes represent part of a complex melt flow network indicative of large-scale interconnectivity. The hybrid isotope signature is interpreted to result from local equilibration by microscale interaction between new melt batches and previously crystallized magmatic rocks as melt migrated via grain boundaries along an S-C fabric related to syn-anatectic deformation rather than any mixing among melt batches (Hasalová et al., 2011).

The features of leucosomes described here are strong evidence that residual source rocks were both zones of melt generation and zones of melt transfer (Brown, 2004, 2006, 2007; Olsen et al., 2004; Korhonen et al., 2010a, 2010b).

Formation of Melt Flow Networks

Under equilibrium conditions in isotropic crust, melting begins at multiphase grain junctions that include quartz and feldspar, and commonly a hydrate mineral. However, Earth's crust is anisotropic and in a state of stress, with variations in bulk composition and grain size that influence sites where melting begins and where melt accumulates. Fluid-absent hydrate-breakdown melting commonly begins at sites of lower pressure, once the initial thermal overstep is close to that required to overcome the activation energy for a particular melting reaction (Brown and Solar, 1998a).

The source becomes permeable at the melt connectivity transition, and melt extraction may occur if the solid residue is able to deform and compact (Rabinowicz and Vigneresse, 2004; Rutter and Mecklenburgh, 2006). With increasing melt volume, the effective mean stress decreases, and the behavior of the anatectic crust may change from distributed shear-enhanced compaction, which reduces permeability, to localized dilatant shear failure, which enhances permeability if the porosity is low (Rutter, 1997; Rutter and Mecklenburgh, 2006). Thus, focused melt flow requires dilatant shear failure at low melt fractions, consistent with the melt connectivity transition of Rosenberg and Handy (2005) and the concept of a melt segregation window as proposed by Rabinowicz and Vigneresse (2004).

Fabric-parallel compaction bands may form in anisotropic rocks as pockets of melt become overpressured and fail by loss of cohesion at grain boundaries and injection of melt along these boundaries, or by a cavitation-driven dilation process, or by propagation of ductile fractures. Formation of compaction bands during early, distributed shear-enhanced compaction implies a flow law that permits localization in the strain-hardening regime (Sheldon et al., 2006). As the melt fraction reaches the melt connectivity transition, the change to localized dilatant shear failure enables melt to move from compaction bands into shear bands (oblique to fabric) and dilation bands (generally fabric-normal) as determined by gradients in hydraulic potential (van der Molen, 1985; Maaløe, 1992; Brown et al., 1995; Brown and Rushmer, 1997; Sawyer, 2001; Guernina and Sawyer, 2003). This process leads to the formation of outcrop-scale melt-filled deformation band networks, as evidenced by leucosome networks in residual crust (Figs. 3A and 4).

Thus, a continuous link for melt flow from pores to vein networks may be created, producing a system that cycles between melt accumulation and melt loss, where this process is modulated by the rate of melt production and the deformation-induced pressure gradients driving the melt flow from grain boundaries to vein networks. The way in which these vein networks connect to ascent conduits where melt ascent is driven by buoyancy remains enigmatic, although theoretical and phenomenological models have been proposed (Clemens and Mawer, 1992; Petford and Koenders, 1998; Brown and Solar, 1999; Weinberg, 1999; Bons et al., 2001, 2004; Leitch and Weinberg, 2002; Brown, 2004; Ablay et al., 2008; Hobbs and Ord, 2010).

Focusing Melt for Extraction

Fertile crustal rocks have the potential to yield a variable amount of melt at the metamorphic peak, according to the compositional balance, and so source volumes may vary from about ten times to only two times the volume of a pluton, according to the crustal temperature achieved (Brown, 2001a, 2001b). Ultimately, melt drains from the source via a limited number of discrete tabular or cylindrical conduits to feed upper-crustal plutons (Vigneresse, 1988; Brown and Solar, 1998b; Vigneresse et al., 1999; Cruden, 2006).

The common association of middle-crustal migmatites with outcrop-scale bodies of granite suggests that regional-scale migmatite-granite complexes preserve an integrated record of melt generation, melt loss, melt passage, and melt entrapment. As such, they represent the upper levels of the anatectic zone through which fugitive magma was transferred from deeper in the source to accumulate in plutons in the shallower crust (e.g., Brown and Solar, 1999; Brown, 2004, 2005; Olsen et al., 2004; Slagstad et al., 2005; Korhonen et al., 2010a, 2010b; Morfin et al., 2013). In the source, a critical point may be reached at some combination of melt fraction and distribution that enables formation of conduits of a size that allows melt to be extracted episodically. For this to occur, it is likely that the melt volume

will be above the melt connectivity transition at ~7 vol% melt and that a melt-bearing network of deformation bands will have been formed (Brown, 2004, 2010a).

The anatectic front—equivalent to the solidus and representing the upper surface of the melt-bearing source, a dynamic feature during orogenesis (Brown and Solar, 1999)—is recorded in orogenic crust by the first appearance of leucosome, corresponding to the fluid-present solidus. The height from the anatectic front to the level of emplacement varies according to the tectonic setting, the degree of orogenic thickening, and the amount of subsequent extension or collapse. Along an active continental margin, the distance separating the granite source from the site of melt accumulation is rarely going to be more than 30 km and commonly will be less, and the thickness of the source is likely to be <20 km; this is shown schematically in Figure 5A. In Figure 5B, melt has been drained from the source, and a pluton has been emplaced at the level of the ductile-to-brittle transition zone. The rates of melt production (not shown in Fig. 5B), extraction (Q_{Ex}), ascent (Q_{As}), and emplacement (Q_{Em}) are assumed to be balanced at the crustal scale by various feedback relations (Cruden, 1998; Brown, 2004, 2010a; Hobbs and Ord, 2010).

The spacing of plutons in formerly active continental margins and collisional orogens (Bons and Elburg, 2001; Cruden, 2006) strongly suggests that ascent is spatially focused, and the spacing of plutons likely reflects the footprint of the source being drained beneath them (Fig. 6). Since there are only a small number of feeders to an individual pluton, and the footprint of the source that is drained for any single pluton is unlikely to be smaller than the lateral extent of the granite, as illustrated schematically in Figure 6, the principal unresolved issue in melt extraction is focusing the melt flow to the ascent conduit(s).

There are several ways by which focused flow of melt to ascent conduits may be achieved. Where lower-crustal fabrics are shallow, and, therefore, the anisotropy of permeability is shallow, melt flow down hydraulic potential gradients to ascent conduits or major shear zones is commonly postulated (e.g., Brown, 2005, 2006; Rosenberg, 2004), and may be driven by gravitational potential due to differences in topographic relief (Hobbs and Ord, 2010). The effect of applied differential stress is limited by the flow strength of melt-bearing crust (Rutter and Mecklenburgh, 2006). Nonetheless, if the hydraulic potential gradient is maximized, such as at low melt fractions in crust with contrasting lithologies that create an extrinsic anisotropy of permeability to channel flow along particular layers with strong intrinsic anisotropy of permeability, then lateral melt flow driven by deformation may be kilometric (Hobbs and Ord, 2010, their table 2). In circumstances where the tectonic fabrics are steep, fabric anisotropies are expected to control extraction of melt, with the form of the magma-ascent conduits mimicking the apparent finite strain (Fig. 7; Brown and Solar, 1998a, 1998b, 1999; Weinberg et al., 2009; Marcotte et al., 2005).

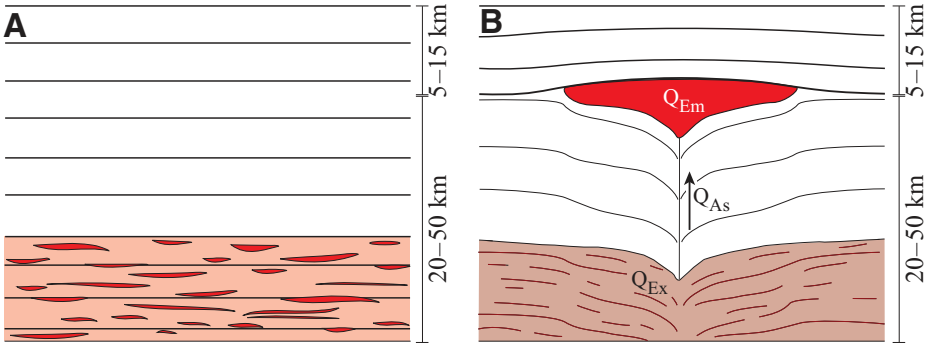

Figure 5. Schematic diagram to illustrate melt extraction, ascent, and emplacement along an active continental margin (based on a model in Cruden, 1998). (A) Segregated melt in the suprasolidus source, shown schematically in red, is located in fabric-parallel stromata and thin sills prior to formation of dikes to allow ascent. (B) After melt ascent, a pluton has formed at the level of the ductile-to-brittle transition zone, with space being made by a combination of lifting of the roof and depression of the floor, accommodated by volume loss in the source due to efflux of the melt. The rates of melt production (not shown on diagram), extraction (Q_{Ex}), ascent (Q_{As}), and emplacement (Q_{Em}) are assumed to be balanced at the crustal scale. The depths shown on the right-hand side of the figures are intended as a general indication of the likely range along an active continental margin. As a consequence of melt extraction, the source is less fertile and more residual.

Since the solidus surface is a dynamic feature in three dimensions during orogenic deformation (Brown and Solar, 1999), the anatectic zone expands upward as the solidus surface is displaced to shallower crustal levels during the prograde metamorphic evolution, but it contracts downward during the retrograde stage. Given regional-scale variations in strain along the length of an orogen, it is likely that the solidus surface in three dimensions is uneven and undulating, with antiformal culminations and synformal troughs. Under these circumstances, the solidus surface may act as a melt-impermeable boundary, or permeability barrier, at the base of the subsolidus crust, analogous to models for melt extraction at mid-ocean ridges (Sparks and Parmentier, 1991; Gregg et al., 2012). Although such a permeability barrier must inevitably be associated with a crystallization front at the solidus, the uneven and undulating nature of the front may allow melt to migrate upslope, driven by buoyancy, to points of melt extraction that form at antiformal culminations in the solidus surface. Melt accumulates at these points of melt extraction until the volume is sufficient to allow it to ascend by buoyancy to the level of pluton emplacement. The size and spacing of plutons will be determined by the location of these melt-extraction points (Fig. 6; Brown and Solar, 1999).

Lower-crustal melting driven by heat supply is a continuous process. In contrast, melt extraction is a discontinuous process that is cyclic (e.g., Brown and Solar, 1998a; Handy et al., 2001; Rabinowicz and Vigneresse, 2004). The switch from a continuous to a discontinuous process is fundamental and has been discussed before (Brown and Solar, 1998a; Handy et al., 2001); it is a consequence of the nonlinear feedback relations during melting (Brown, 2010a; Hobbs and Ord, 2010).

CURRENT VIEWS ON MAGMA ASCENT AND EMPLACEMENT

Leucosome networks and mesoscale pods of diatexite, migmatite, and granite within residual host rocks provide evidence of the storage system for melt accumulation prior to extraction. The storage networks and locally ponded melt feed the ascent conduits that transport magma to shallower levels in the crust (Brown, 1994; Sawyer, 1998; Brown, 2004, 2006, 2007, 2010a; Reichardt and Weinberg, 2012a).

In general, plutons are constructed incrementally (e.g., Deniel et al., 1987; Brown and Solar, 1999; Pressley and Brown, 1999; Miller, 2008; Clemens and Benn, 2010), consistent with

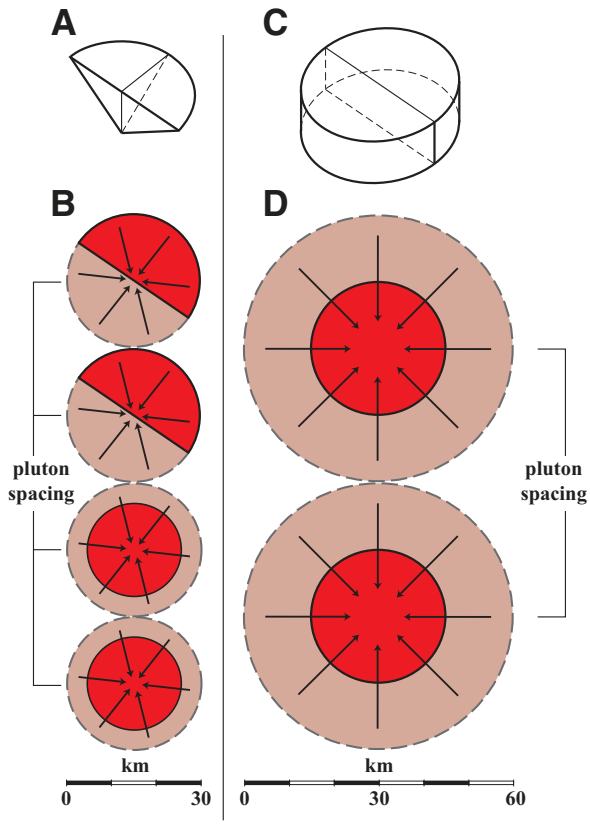

Figure 6. Pluton-source relations in orogens and the spacing of plutons (based on a model in Brown, 2001a). (A) Perspective view of horizontal semicircular half-cone–shaped pluton of diameter ~30 km and half-height ~5 km. (B) Plan view of two horizontal semicircular half-cone–shaped plutons of diameter ~30 km (upper pair; red ornament) and two horizontal circular cone-shaped plutons of diameter ~21 km (lower pair; red ornament) in relation to the footprint for a source of sufficient volume to fill the pluton (for a source ~30 km diameter, based on an assumed thickness of 15 km and 20 vol% melting with 20 vol% fractional crystallization of the melt during transport through the source; dashed line). One implication of this model for the assumptions made is that plutons will be spaced at least 30 km apart (center to center) whether they are semicircular half-cone–shaped or circular cone-shaped plutons. (C) Perspective view of a horizontal tabular intrusion of diameter ~30 km and thickness ~10 km, which is four times greater in volume than the plutons discussed in B. (D) Plan view of two horizontal tabular intrusions of diameter ~30 km (red ornament) in relation to the footprint for a source of sufficient volume to fill the intrusion (for a source ~60 km diameter, based on an assumed thickness of 15 km and 20 vol% melting with 20 vol% fractional crystallization of the melt during transport through the source; dashed line). One implication of this model for the assumptions made is that intrusions will be spaced at least 60 km apart (center to center). A more sophisticated discussion of pluton-source shape and volume relations, and melt extraction and source accommodation mechanisms, is given in Cruden and McCaffrey (2001) and Cruden (2006).

expectations for cyclic melt extraction from the source. Growth of plutons by addition of discrete magma batches is confirmed by high-precision zircon geochronology coupled with the identification of isotopically distinct units despite the cryptic internal structure of many plutons (Deniel et al., 1987; Hogan and Sinha, 1991; Brown and Pressley, 1999; Pressley and Brown, 1999; Coleman et al., 2004; Matzel et al., 2005, 2006; Schaltegger et al., 2009; Miller et al., 2007; Miller, 2008; Clemens and Benn, 2010; Acosta-Vigil et al., 2012a). This view of pluton construction is supported by detailed structural studies of granite, particularly where anisotropy of magnetic susceptibility has been used to map cryptic fabrics and to identify discrete emplacement lobes in plutons (Stevenson et al., 2007).

Sheeted granites provide evidence of the feedback relations among episodic melt extraction, common ascent conduits for successive pulses of magma, and local pluton inflation as melt flow stalls (Brown et al., 1981; Brown and Solar, 1998b, 1999; Brown and McClelland, 2000; Mahan et al., 2003; Bartley et al., 2008). In particular, Bartley et al. (2008) proposed that upper-crustal plutons may be constructed by a crack-seal mechanism, involving incremental growth by diking, with emplacement either between earlier sheets of granite and wall rocks (antitaxial growth) or within earlier sheets of granite (syntaxial growth). The problem with this hypothesis, as the authors admit, is that compelling evidence of pluton construction by multiple diking is absent in the interior of many plutons. Indeed, where cryptic contacts have been established, the form of the individual pulses commonly appears not to be dike-like. This is not surprising. The cryptic nature of internal contacts in granites suggests that successive melt batches were emplaced into mushy magma that was not fully crystallized; such mushy zones are natural traps for ascending batches of magma. Thus, entrapment is likely to have obscured evidence of the ascent process.

Laccoliths (horizontal tabular intrusions) and wedge-shaped plutons (also called lopoliths) typically have large aspect ratios, with horizontal dimension ~12–6 times the vertical dimension as thickness increases from 50 m to 5 km (McCaffrey and Petford, 1997; McCaffrey and Cruden, 2002). The volume of magma emplaced in the upper crust may vary by tectonic setting. In one study from an area of 1.5×10^5 km^2 in the Lachlan fold belt of eastern Australia—an accretionary orogenic belt that developed above a retreating trench at a continental margin—Bons and Elburg (2001) estimated that ~10^3 plutons with a volume greater than 1 km^3 were emplaced during Silurian–Devonian orogenic events. This yields a total volume of magma transferred to the upper crust of 1.5×10^5 km^3. This distribution is consistent with an average of ~10 vol% melt drained from a source of a similar horizontal area or footprint that was ~10 km thick; such an estimate ignores any mass input due to melting of asthenosphere in the mantle wedge. In another study from the Cretaceous central Sierra Nevada batholith in California—an accretionary orogenic belt that developed above an advancing trench at a continental margin—Cruden (2006) estimated magma volumes per unit area that are up to four times larger than those in the Lachlan fold belt. The difference may reflect a higher proportion of mass additions from the mantle and/or a higher degree of crustal melting in the formation of the Sierra Nevada batholith, which in turn may relate to plate kinematics and/or rates of subduction.

To a first approximation, the volume of magma emplaced in the middle to upper crust equals the volume of melt extracted from the middle to lower crust (Fig. 5). If the interval between melt-extraction events is on the order of 1000 yr, then for reasonable values of bulk viscosity and elastic shear modulus, the relaxation time of the crust is of the same order (Vigneresse, 2006; Ablay et al., 2008). Thus, extraction and emplacement are complementary actions between which there is a feedback relation modulated by processes in the ascent conduit, and space for emplacement is not a problem (Fig. 5; Brown, 2001a, 2001b, 2007, 2008, 2010a; Bons et al., 2008; Hobbs and Ord, 2010). Locally, various mechanisms act to accommodate pluton construction, as discussed earlier herein.

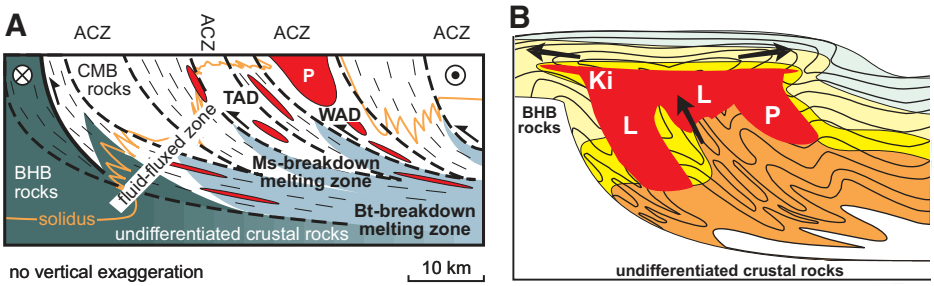

Figure 7. Schematic diagrams to illustrate the thermal structure and migmatite-pluton relations in a dextral transpressive system, based on the western Maine area in the Acadian orogen of the Northern Appalachians (Brown and Solar, 1998b, 1999; Solar and Brown, 2001a, 2001b; Tomascak et al., 2005). (A) Schematic structure section drawn perpendicular to foliation. The anatectic front is recorded in orogenic crust by the first appearance of migmatite traversing up-grade—corresponding to the shallowest crustal level reached by the solidus. Thus, the migmatite front, which tracks the solidus, was progressively extended into shallower parts of the orogenic system by advection of material during contractional thickening, including the sequential ascent of granite melt (Brown and Solar, 1999). The three-dimensional form of the final solidus surface projected onto the section illustrates the thermal structure at the peak of orogenesis (continuous line labeled "solidus"). An H_2O-rich volatile phase is exsolved at the solidus as granite crystallizes, which is postulated to be responsible for the widespread generation of retrograde muscovite in migmatites, and retrogression of staurolite and andalusite porphyroblasts in subsolidus rocks. Dashed lines are boundaries between structural domains (ACZ identifies zones of apparent constrictional strain inside zones of apparent flattening strain identified by the dashed ornament). BHB rocks—Bronson Hill belt rocks; CMB rocks—central Maine belt rocks; TAD and WAD—Tumbledown and Weld anatectic domains, respectively; P—the Phillips pluton; Ms—muscovite, Bt—biotite. This figure is modified from a similar version published in Solar and Brown (2001a) and is used in accordance with the publications rights policies of Oxford University Press. (B) Schematic WNW-ENE model section to show the immediately post-thermal peak stage of evolution in a transpressive system, based on the model for the structural evolution of the western Maine area by Solar and Brown (2001b); the form of the granites, which are projected ENE onto the plane of the section, is based on information in Brown and Solar (1998b, 1999). Notice that the granite plutons are rooted in the migmatites, and melt flow is interpreted to be upward along the fabrics (Brown and Solar, 1998a). The level of horizontal expansion and emplacement of the Lexington (L) and Kingsman (Ki) plutons, as exposed, is interpreted to correspond approximately to the contemporary ductile-to-brittle transition zone. Brown and Solar (1998b) speculated that the Lexington pluton was more laterally extensive within 1 km above this level and suggested that the upper part of the pluton may have been emplaced in a more extensive horizontal fracture that propagated laterally in an arc from the WSW to the ENE. At a deeper level, the Lexington pluton has a similar form to the Phillips (P) pluton (see part A), which is interpreted to be the root to a formerly more extensive pluton that has been eroded.

What is the Field Evidence for Ascent Mechanisms?

Dikes

Diking produces discordant bodies of granite that have very high aspect ratios, thicknesses that may vary from millimeters to decameters, and lateral dimensions that may extend over kilometers. Kisters et al. (2009) described an example of the relationship between anatectic leucosomes, interpreted to record local melt segregation into shallowly dipping dilatant fractures, and steeply dipping disc-shaped granite bodies, inferred to record upward transport of melt in isolated fractures (interpreted as hydrofractures). In this case, the volume of melt in the propagating hydrofracture was inferred to have increased by ingress of melt draining from the shallowly dipping dilatant fractures in response to the hydraulic potential gradient associated with the developing hydrofracture.

In the Ryoke migmatite belt of Shikoku in Japan, millimeter- to centimeter-scale dikelets of granite with centimetric to decimetric spacing are seen at outcrop (Fig. 8A). This discordant granite connects in petrographic continuity to millimetric stromatic leucosomes (Fig. 8B). Close to the tips, these dikelets have an open zigzag form (Fig. 8B, below the coin) and bifurcate or splay (Fig. 8A).

Similarly, in the southern Brittany migmatite belt of western France, centimeter- to meter-scale granite dikes are abundant at outcrop (Fig. 8C). Although the volumetric importance of the dikes varies in space, they may represent up to 20% of the area of an outcrop. At outcrop scale, small dikes have blunt fracture tips, zigzag geometry close to the fracture tips, and petrographic continuity between leucosome in host and granite in dikes (Figs. 8D and 8E; Brown, 2004, 2005, 2006, 2010a, 2010b). At map scale in the wider region, the dikes may be as large as several hundreds of meters in width, and further west, they form feeders to the Carnac granite, which formed during orogen-parallel extension (Turrillot et al., 2011). Around Port Navalo, dikes with thicknesses >10 cm show a power-law distribution with an exponent of 1.11 (Brown, 2005), suggesting that they may be scale invariant, although the data set is small (87 dikes), and the range of observations is only two orders of magnitude. The largest dikes measured were 3 m and 5.5 m wide, within the range of critical dike widths for flowing melt to advect heat faster than conduction through the walls and avoid freezing close to the source (Clemens, 1998).

The dikes in southern Brittany appear to crosscut structures in the migmatites (Fig. 8C), but the modal mineralogy, grain size and microstructure of the granite in the dikes are indistinguishable from those of leucosome (Figs. 8D and 8E). Marchildon and Brown (2003) interpreted these features to mean that both leucosomes and dikes hosted a continuous melt-bearing network, and to indicate that material in leucosomes and in dikes underwent final crystallization at the same time. This inference does not mean that leucosomes (or necessarily granite in dikes) have liquid compositions.

Intersections among leucosomes or dikes that are parallel to the extension direction form pipe-like "backbone" structures that enable faster extraction of melt (Figs. 9A and 9B). Interconnected dike and sill networks (Fig. 9D; Brown et al., 2011) represent melt intrusion along conjugate ductile fractures.

In Mesoproterozoic aluminous pelites from Broken Hill, Australia, White et al. (2004) described spatially focused melt formation where the resulting pathways for melt escape, as recorded by leucosome, are parallel to the foliation defined by highly depleted melanosomes. In contrast, in the Mount Hay area of the eastern Arunta Inlier, central Australia, melt is inferred to have migrated through Paleoproterozoic

lower crust via a network of narrow, structurally controlled pathways parallel to the moderately to steeply plunging regional elongation direction, as evidenced by leucosomes associated with coaxial folds and a strong mineral-elongation lineation (Fig. 10B; Collins and Sawyer, 1996).

Concordant Tabular and Cylindrical Granites

Structurally concordant tabular or cylindrical granites, which are also referred to as "sheets" and "pipes" of granite in the literature, with high aspect ratios, thicknesses up to decameters, and lateral dimensions that may extend over kilometers, occur in the high-grade parts of many orogenic belts. They are commonly, but not always, associated with host migmatite (Figs. 9C and 10).

In the transpressive Acadian belt in the Northern Appalachians, the form of the inferred magma-ascent conduits mimics the apparent strain ellipsoid recorded by the host-rock fabrics (Brown and Solar, 1999; Solar and Brown, 2001a). Concordant tabular granites occur in zones of apparent flattening strain (Fig. 10A), whereas concordant cylindrical granites occur in zones of apparent constrictional strain. Overall, the orogen-parallel orientation of the tabular granites demonstrates that magma was transferred in structures oriented at a high angle to the far-field maximum principal stress (Brown and Solar, 1998b, their fig. 7; Solar and Brown, 2001b).

A similar relationship between granite in ascent conduits and the regional stress field is observed in a variety of tectonic settings. For example, in the Karakoram shear zone of northwest India, tabular granites that link deeper migmatites to shallower plutons have orientations that lie between the strike of fold axial surfaces and the strike of the shear zone. This feature suggests that a large portion of the fugitive magma was transported in structures oriented at a high angle to the maximum principal stress (Reichardt and Weinberg, 2012b). Also, in the Cascade Mountains of the northwest United States, there are sheet-like bodies of granite emplaced into the middle crust that have length/width ratios that increase by an order of magnitude as the radii at the tips decrease from 850 to 100 m and the tip diameter/sheet width ratio decreases by half (Paterson and Miller, 1998). Paterson and Miller (1998) argued that these sheet geometries fall between those characteristic of dikes and elliptical diapirs. These sheets were emplaced at a high angle to the far-field maximum principal stress and are always associated with narrow structural aureoles that preserve evidence of ductile downward flow of the host rocks along sheet margins.

Role of Compaction

Efficient fluid expulsion from poorly drained rocks requires a dynamic mechanism in which the dilational deformation responsible for increasing permeability is balanced by a compaction mechanism at depth responsible for maintaining high fluid pressure. An essential feature of such a mechanism is that, irrespective of the mean stress gradient, hydraulic connectivity must be maintained over a vertical interval that is large enough to generate the effective pressures necessary to drive the deformation (Connolly and Podladchikov, 2007). Melt distribution in connected porosity in suprasolidus crust may be affected by small-scale variations in mineralogy (Watson, 1999), grain size (Wark and Watson, 2000), or grain orientation (Waff and Faul, 1992), and suprasolidus crust is likely to be characterized by nonuniform melt distribution as a result. In these circumstances, porosity waves may nucleate from such small perturbations in the distribution of melt due to a rheological asymmetry between compaction and decompaction in two-phase viscous materials (Connolly, 2010; Connolly and Podladchikov, 2007, 2012). The instabilities grow by drawing melt in from the permeable matrix, compacting that part of the source, causing dilation, increasing melt volume, and disaggregating the matrix to form a magmatic suspension (Fig. 11). Since flow is enhanced where melt fraction is higher, more melt drains to the instabilities from the background porosity, further enhancing the flow, which induces additional influx of melt to grow a developing porosity wave via this feedback relation. Coupling between flow and melt fraction leads to melt accumulation and transport in the form of upward-migrating melt-rich domains (Connolly, 2010; Connolly and Podladchikov, 1998, 2007, 2012).

Assumptions made in modeling compaction are that: melt pressure is near lithostatic, flow is governed by Darcy's law, permeability is continuous and a strong function of connected porosity, and deformation occurs by a viscous mechanism in response to effective pressure (Connolly and Podladchikov, 2012). If these assumptions are accepted, the consequence is that melt flow must be episodic and accompanied by oscillations in fluid pressure, even in idealized homogeneous crust perturbed by an idealized melting reaction. Porosity waves simply provide a mechanism to generate dilational stress, and, as a result, they bridge the extremes of porous and channelized flow. The way in which the dilational stress manifests itself in failure mode will depend on the local stress field, the orientation of fabrics, and the rheology, but in principle, porosity waves provide a mechanism to link melt in pores to magma in ascent conduits.

Mechanisms of Magma Ascent

Magma ascent is driven by buoyancy, but the style of ascent through subsolidus crust depends on wall-rock rheology. Diking sensu

Figure 8 (*on following page*). Features associated with the transition from melt in fabric-parallel sites (recorded by stromatic leucosomes) to dikes (recorded by discordant dikelets and dikes of granite) in granulite-facies metatexite migmatites. (A) Granite in transverse dikelets in petrographic continuity (with similar microstructure, mineralogy, and mode) with thin fabric-parallel leucosomes, consistent with melt flow down gradients in pressure from the host stromatic metatexite migmatite; the dikelets are interpreted to initiate by ductile fracture. From the Ryoke belt, Japan; diameter of coin is ~20 mm. (B) Close-up of A to show details of the linkage between leucosome in the stromata and leucosome in the dikelet, and the open zigzag form of the dikelet, which is consistent with ductile fracture; diameter of coin is ~20 mm. (C) View NW across a subhorizontal wave-cut platform to show several dikes (the two larger dikes are ~0.5 m wide). These dikes are apparently discordant viewed in some sections, but they exhibit petrographic continuity (with similar microstructure, mineralogy and mode) with leucosome in the foliation-parallel stomata in other sections (see D). From Le Petit Mont, Morbihan, France. For more details about this outcrop, see Brown (2004, 2006). (D) A small dike (center) splays from a larger dike (itself a splay from the main dike at the top of the image) and, after bifurcating (left of center), terminates with petrographic continuity (similar microstructure, mineralogy, and mode) in a transverse leucosome. From Le Petit Mont, Morbihan, France; diameter of coin is ~20 mm. For more details about this outcrop, see Brown (2004, 2006). (E) Leucosome in stromatic metatexite migmatite is in petrographic continuity with granite (with similar microstructure, mineralogy, and mode) in the highly discordant, apparently crosscutting dike, which bifurcates downward (in the image) into two dikelets with zigzag form close to the tips, which is consistent with ductile fracture. From Le Petit Mont, Morbihan, France; diameter of coin is ~20 mm. For more details about this outcrop, see Brown (2004, 2006).

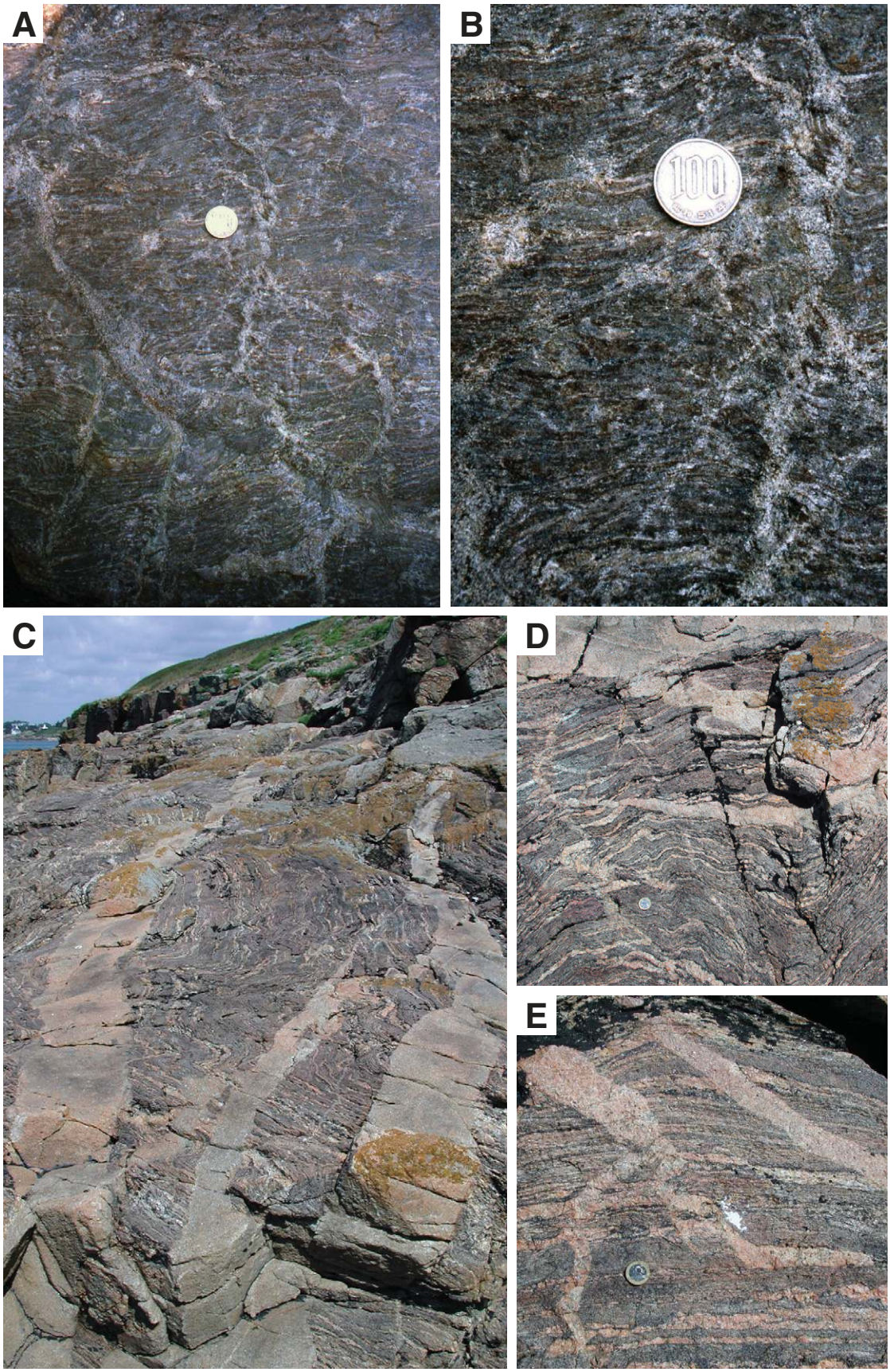

Figure 8.

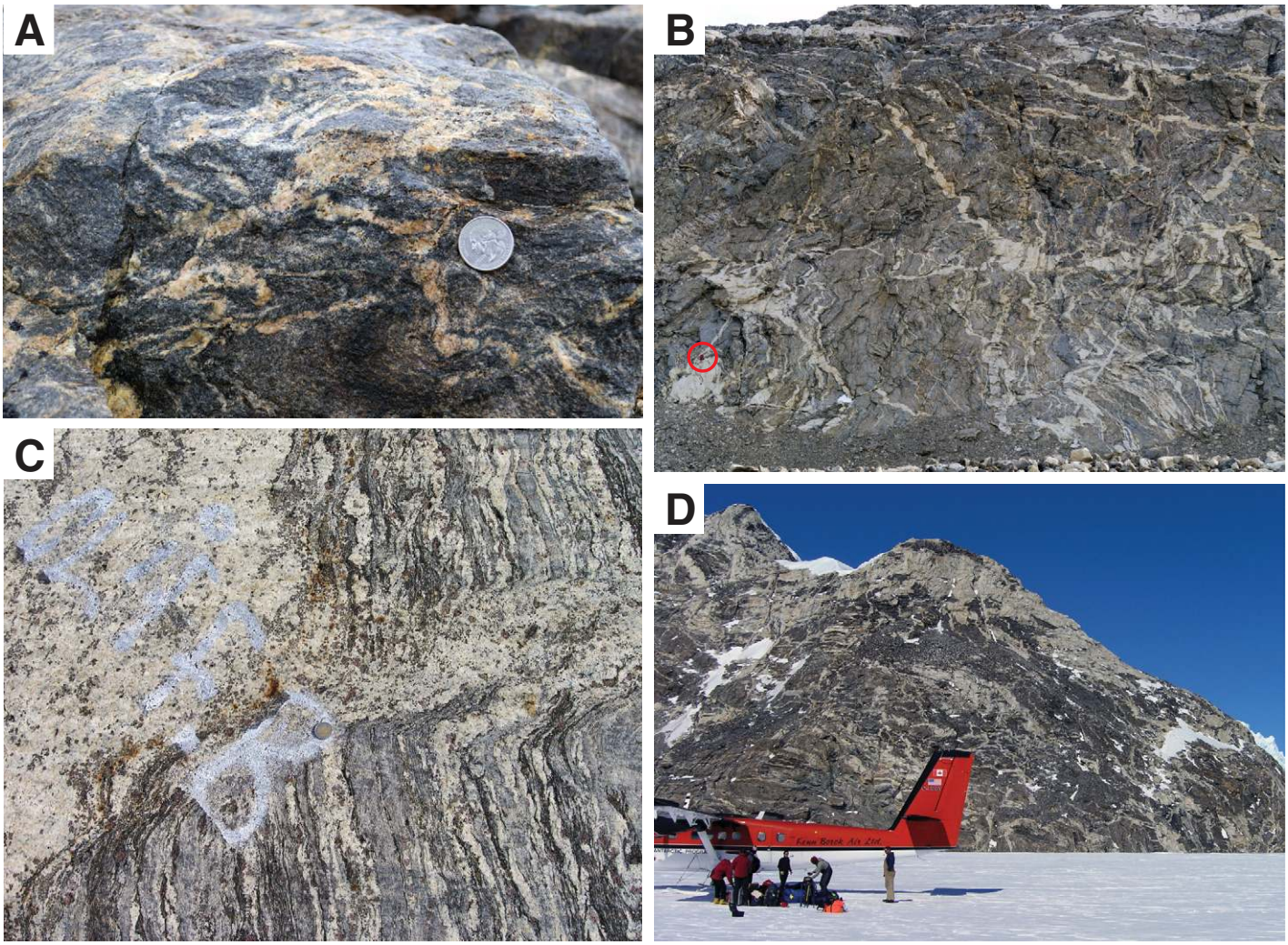

Figure 9. Examples of former melt flow pathways and extraction structures. (A) Steep surface approximately perpendicular to the mineral elongation lineation to show migmatite with thin irregular leucosomes intersecting in roughly cylindrical leucosome-filled structures parallel to the lineation. These structures are inferred to represent evidence of pervasive melt flow through the crust parallel to lineation. From the north end of Thompson Ridge, in the western part of the Fosdick migmatite-granite complex, Marie Byrd Land, West Antarctica; diameter of coin is ~20 mm. (B) Steep cliff to show stromatic metatexite migmatite hosting variably oriented, slightly irregular, high-aspect-ratio, meter-scale tabular granites that intersect at decametric, roughly cylindrical, granite-filled structures ("spider" structure of Marchildon and Brown, 2003). These structures are interpreted to represent evidence of channelized melt transport through the suprasolidus crust. From Mount Avers in the central part of the Fosdick migmatite-granite complex, Marie Byrd Land, West Antarctica; the red circle locates a person for scale. (C) View of a horizontal outcrop surface approximately perpendicular to the steep foliation to show part of a roughly foliation-parallel dike of granite on the left that exhibits petrographic continuity (with similar microstructure, mineralogy, and mode) with leucosome in the shear band (center right) and leucosome in foliation-parallel stomata. From near Turku, Finland; coin for scale (2 cm diameter). (D) Sill and dike network in stromatic metatexite migmatite at Maigetter Peak (height 480 m) in the western part of the Fosdick migmatite-granite complex, Marie Byrd Land, West Antarctica. Intersecting dikes do not appear to truncate or displace each other; the sills and dikes of granite crosscut foliation but may be continuous with or discordant to leucosomes in the migmatite. The migmatite leucosomes contain pristine peritectic garnet and minor cordierite consistent with melt loss (see Brown et al., 2011, their Fig. 1).

stricto refers to brittle fracture at the crack tip and elastic deformation of the host rock. The elastic response is rapid, whereas the viscous flow of magma into the narrow crack tip is slow, and consequently magma viscosity controls the velocity of magma ascent. In contrast, diapiric rise of magma occurs by ductile (viscous) deformation of the host rock. Since the viscosity of the host rock is much larger than that of the magma, the host-rock viscosity, rather than the magma viscosity, controls the ascent velocity; ascent may be limited by the ductile-to-brittle transition zone (Sumita and Ota, 2011). Mesoscale pervasive migration limited to the suprasolidus and the high-temperature subsolidus crust immediately above the anatectic front is an alternative mechanism documented from many migmatite terrains.

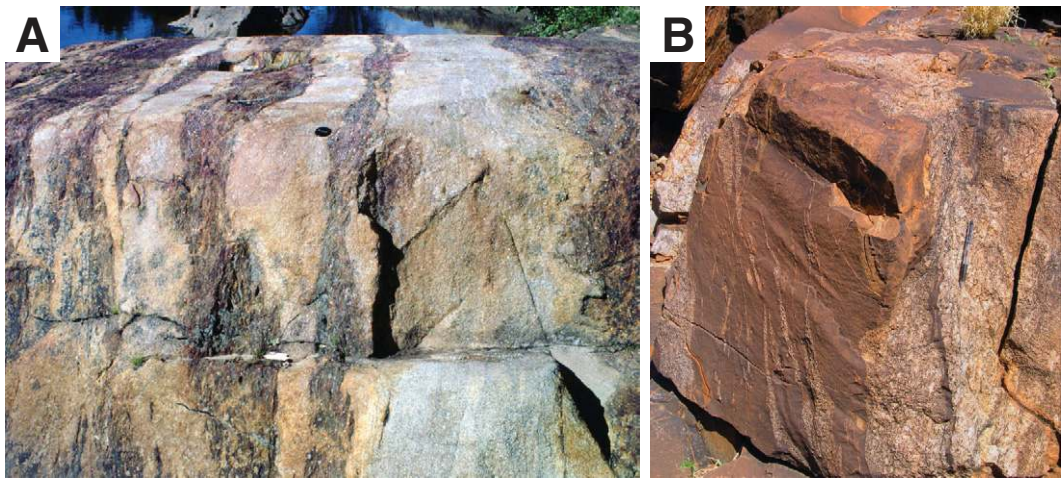

Figure 10. (A) Subhorizontal and subvertical outcrop surfaces exposing concordant irregular tabular granite layers in residual stromatic metatexite migmatite; the granite represents melt trapped during ascent within a regional-scale zone of apparent flattening strain, western Maine, United States (for more details, see Brown and Solar 1999). Lens cap in upper center of image for scale. (B) Lineation-parallel, irregularly shaped granite layer that is inferred to record melt migration through Paleoproterozoic lower crust via structurally controlled pathways parallel to the moderately to steeply plunging regional elongation direction (for more details, see Collins and Sawyer 1996). Pen (parallel to lineation) shows scale.

Diking

Here, the term diking is used in a simple morphological sense to refer to discordant bodies of granite that have very high aspect ratios. In the suprasolidus crust, dikes have been interpreted to form by hydrofracture (Bons et al., 2001, 2004) or by ductile fracture (Brown, 2004, 2010a; Weinberg and Regenauer-Lieb, 2010), and to propagate through the subsolidus crust by brittle-elastic fracture until the decrease in transport rate causes freezing of the melt (Hobbs and Ord, 2010). To extract melt from suprasolidus crust by diking requires sustained transient near-lithostatic to supralithostatic melt pore pressure in the melt flow network for the duration of a melt-extraction event to prevent immediate drawdown, a decrease in the transport rate, and the possible collapse of the melt flow network.

Diking by hydrofracture represents a response to internal melt pressure rather than to externally applied stress. Propagation of a hydrofracture is based on linear elastic fracture mechanics, where inelastic deformation associated with breaking bonds by intergranular and transgranular fracture occurs in a small process zone ahead of the fracture tip, with or without chemical weakening (subcritical brittle fracture or brittle fracture, respectively), driven by the magnified stresses at the tip (Lister and Kerr, 1991). Hydrofracture assumes an isotropic protolith, pervasive interconnected melt-filled porosity, initial failure due to melt-enhanced embrittlement, and gradients in fluid pressure sufficient to drive melt flow from interconnected pores to the fractures (Bons et al., 2001). In these circumstances, steeply oriented fluid-filled fractures may become unstable if they exceed a critical crack length and move together with their fluid content. Smaller-volume melt-filled mobile hydrofractures in suprasolidus crust are argued to propagate, coalesce, and drain via stepwise and discontinuous aggregation to form larger-volume potentially crustal-scale hydrofractures for melt ascent. In this way, the crustal-scale hydrofractures are thought to drain the anatectic zone of melt and transport it through the subsolidus crust in a small number of dikes. The effect is modeled as a highly dynamic self-organized system in which intermittent, local events of fracture propagation cause avalanches of instabilities and merging of hydrofractures (Bons et al., 2004).

Exactly how melt stored in pores in very weak suprasolidus crust links to segregated melt transport in propagating hydrofractures is not clear. First, the critical crack length for propagation is too long to permit the cracks to initiate spontaneously from a matrix with pervasively distributed melt (Rubin, 1998). Second, even if able to propagate, the ability of hydrofractures to drain melt from suprasolidus crust depends critically on the horizontal permeability and the viscosity of the melt. Granite melt is more viscous than basalt melt, and the compaction length in suprasolidus crust is on the order of meters to decameters (Petford, 1995; Weinberg, 1999). Both of these factors limit the rate of porous flow of melt to a potential hydrofracture, which requires that any melt to be extracted during diking most likely was already segregated into networks of melt-filled veins. These problems potentially may be overcome if diking occurs by ductile fracture.

In ductile fracturing, thermally activated flow processes lead to extensive inelastic deformation and blunting of crack tips, together with processes similar to those in creep failure of ceramics at high homologous temperature under low rates of loading, such as nucleation, growth, and coalescence of pores by predominantly diffusive deformation mechanisms (Eichhubl, 2004). Thus, fracture propagation in suprasolidus crust most likely takes place by the development and coalescence of melt-filled pores ahead of a fracture tip, with fracture opening involving extensive inelastic deformation and diffusive mass transfer. Melt is inferred to flow through self-generated melt-induced deformation band networks (the reservoir for melt storage) down hydraulic potential gradients to crack-like, ductile opening-mode fractures propagating from dilation or shear bands (Figs. 8A and 8B; Brown, 2004, 2005).

If diking is a general mechanism for the ascent of crustal melts, it is likely that ductile fracture is the mechanism by which the dikes initiate in the suprasolidus crust. However, during ascent, as viscosity of the subsolidus crust increases, propagation may change from a ductile fracture process to a brittle-elastic fracture process (Fig. 12; Brown, 2008, 2010a; Weinberg and Regenauer-Lieb, 2010; Brown et al., 2011; Sumita and Ota, 2011). The experimental work of Sumita and Ota (2011) is particularly interesting since it suggests that the style of magma ascent through the crust might change as the wall-rock rheology evolves from ductile to brittle, so that a buoyancy-driven liquid-filled crack might migrate as a diapir-dike hybrid (Fig. 13). This style of migration may be explained in terms of the force balance between the buoyancy of the magma and the yield stress of the wall rock.

The propagation of small volumes of magma into subsolidus crust will be limited by freezing (Clemens, 1998), so an important consideration is the way in which the magma plumbing system coarsens to facilitate ascent to the shallow crust.

Ito and Martel (2002) investigated how dikes might potentially coalesce due to interactions with the local stress field to increase the volume of melt, enabling the larger dike to migrate further. These authors discovered that neighboring dikes create distortions in the local stress field that can be attractive or repulsive according to the vertical and horizontal spacing. Dikes that are sufficiently close to each other and that are offset appropriately in depth may coalesce to focus melt ascent into a smaller number of larger-volume and more widely spaced dikes.

Alternatively, the progressive coarsening of the magma plumbing system with decreasing depth has been attributed to changes in the viscosity and constitutive behavior of the magma from elastic-viscous to elastic-plastic as it cools (Hobbs and Ord, 2010). In the lower part of the ascent zone, the transport network is expected to be closely spaced and in local thermal equilibrium with the host rock, so that, regionally, the isotherms continue to be elevated. As a result, the temperature is suprasolidus for the melt but subsolidus for the host rocks. With decreasing depth, the transport network becomes more widely spaced, and the magma loses heat to its surroundings, such that elevated isotherms occur only near the dikes.

Diapirism

Diapiric ascent has been proposed as the mechanism for the emplacement of granites in the deep crust in continental arcs (Paterson and Miller, 1998; Miller and Paterson, 1999, 2001). A structural analogy is sometimes argued between granites and salt diapirs, but it is clear that regional extension is the trigger for salt diapirism (Jackson and Vendeville, 1994), whereas the diapirs described by these authors were emplaced during regional contractional deformation. In many respects, these deep continental arc plutons have many features in common with the sheeted tabular granites that pass downward into regional migmatite-granite complexes, as discussed in the following.

Mesoscale Pervasive Migration of Melt

As discussed earlier herein, outcrop observations from many migmatite-granite complexes demonstrate that melt extraction from suprasolidus crust commonly occurs via a network of veins, as marked by leucosome, and structurally concordant channels of various shapes and sizes, as recorded by bodies of granite (Brown and Solar, 1998a, 1999; Solar and Brown, 2001a, 2001b). Similar observations have been made from injection complexes where granite was emplaced pervasively into hot subsolidus country rock (Weinberg and Searle, 1998). Based on these observations, Weinberg (1999)

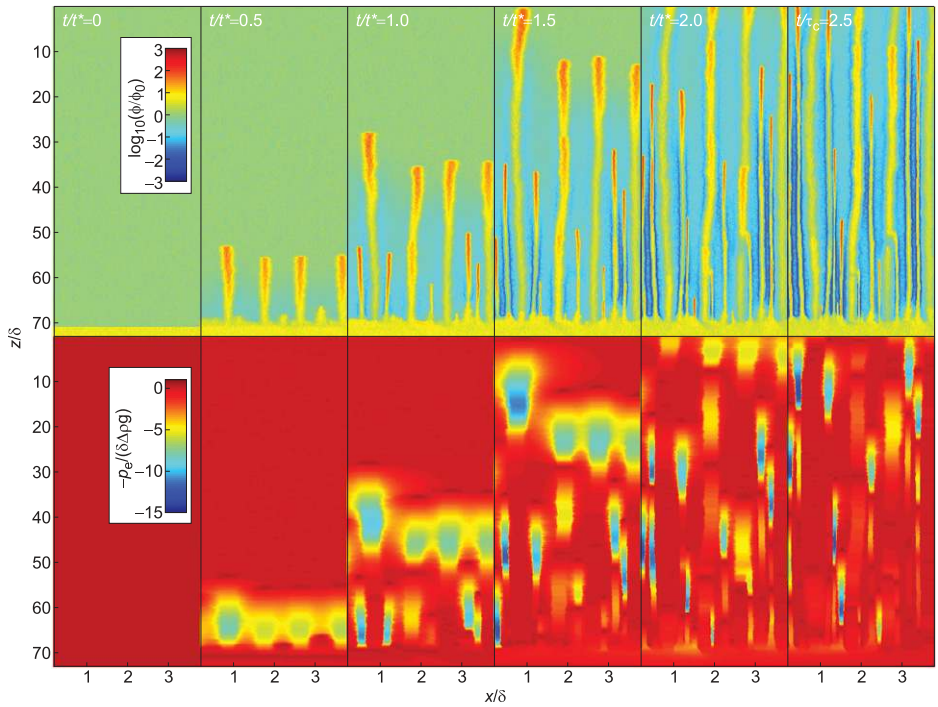

Figure 11. Two-dimensional numerical simulation of fluid flow through a matrix with decompaction weakening as it evolves from a layer with elevated porosity that is bounded from above and below by regions with an order of magnitude lower porosity. Upper panels show porosity in the uppermost portion of the layer at the base and in the overlying region. Lower panels show the corresponding distribution of fluid overpressure. Initial waves form with characteristic spacing identical to the viscous compaction length and leave a trail of slightly elevated porosity, flanked by a fluid-depleted matrix. Depletion of the matrix reduces the local compaction length scale for the initiation of subsequent waves. Later waves collect within the trails of the initial waves. Figure is from Connolly and Podladchikov (2007), used with permission under Copyright Clearance Center's RightsLink License Number: 3115980422769.

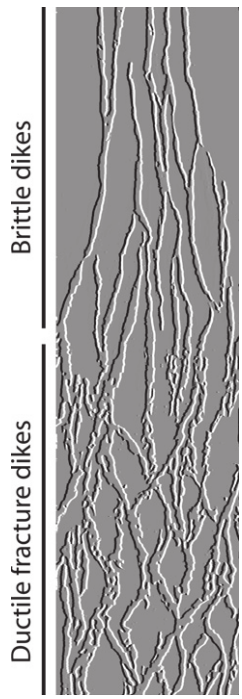

Figure 12. Sketch showing ductile fracture dikes feeding brittle-elastic dikes (from Weinberg and Regenauer-Lieb, 2010; published with permission from the Geological Society of America).

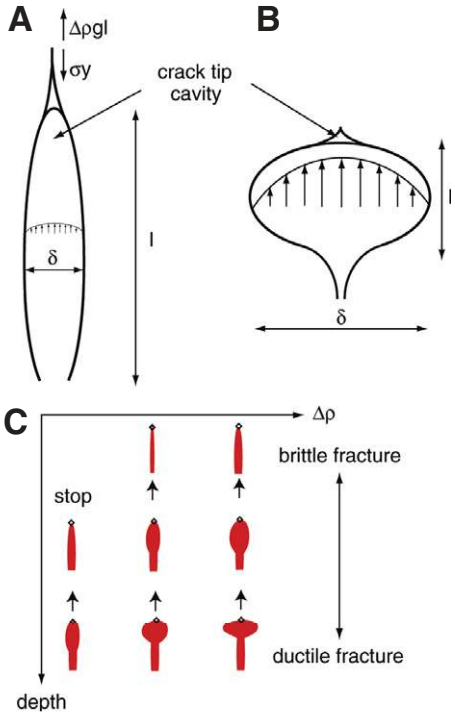

Figure 13. (A) Schematic diagram of a blade-like crack viewed in the direction parallel to the crack plane, showing the channel flow and the balance between the yield stress σy and buoyancy Δρgl at the crack tip; l and δ are the height and thickness scales, respectively, of the fluid-filled crack head. (B) Same as A but for the case when the medium is softer or density difference is larger, thus forming a diaper-dike hybrid. Here the volumes of A and B are assumed to be the same. As the crack head bulges, the crack becomes thicker (large δ), and its length becomes shorter (small l). (C) Schematic diagram to show how a buoyancy-driven liquid-filled crack may change its shape as it ascends through the ductile-to-brittle transition zone. Here, three cases for the same volume but different density difference are shown. Diamonds indicate fracturing at the crack tip. Figure is from Sumita and Ota (2011), used with permission under Copyright Clearance Center's RightsLink License Number: 3087080276836.

argued for processes involving pervasive migration to form melt sheets preferentially emplaced parallel to high-permeability zones such as fabrics. The melt is able to exploit suitably oriented fabrics as planes of weakness, if the melt pressure is high and the differential stress is low, that is, if the differential stress is less than the difference between the tensile strength of the crust normal to and parallel to the fabric (Brown and Solar, 1998b). The resulting granites will be similar to the strain-controlled tabular and cylindrical granites found in zones of apparent flattening and apparent constrictional strain, respectively, such as in melt-depleted migmatites from Maine (Brown and Solar, 1998a, 1999; Solar and Brown, 2001a, 2001b).

The evolution of these systems is controlled by processes that operate at the anatectic front, a rising isotherm that defines melt initiation, particularly the generation of a melt flux that controls the permeability distribution in the system, the height of the transport/emplacement region, and the size of the resulting plutons (Hobbs and Ord, 2010). To produce the melt volumes necessary to form plutons within 10^4–10^7 yr demands that the isotherm velocity is regulated by melt advection in deformation-induced channel ways. This velocity is one constraint on the melt flux generated down temperature of the anatectic front, which is the control valve for the behavior of the system as a whole. Heat advected with migrating melt and latent heat of crystallization expand the suprasolidus domain upward to allow ascent of melt to shallower depths (Brown and Solar, 1999; Weinberg, 1999; Leitch and Weinberg, 2002; Jackson et al., 2003, 2005). This feedback relation between migration of melt and heating allows younger batches of melt to reach increasingly shallower levels.

Once the accumulated melt has sufficient buoyancy to escape the anatectic front, a conduit width-selection process must operate, driven by changes in melt viscosity and constitutive behavior to facilitate ascent to the level of pluton emplacement. At this level, magma emplacement is controlled by the transition in constitutive behavior of the melt/magma from elastic-viscous at high temperatures to elastic-plastic-viscous approaching the solidus of the melt, enabling finite-thickness plutons to develop (Hobbs and Ord, 2010). These authors calculated that a melt flux at the anatectic front of the order of 10^{-10} m s^{-1} is close to the maximum possible given the physical parameters of anatectic systems. This corresponds to a maximum thickness for the anatectic zone of 21 km and is sufficient to produce plutons >3 km thick in a single intrusive event over a period of 10^6 yr.

Relationship between Mechanisms of Ascent and Porosity Waves

Discordant dikes and concordant high-aspect-ratio tabular granites in migmatites (Figs. 8, 9, and 10) may simply record different failure modes related to the local stress field and fabric orientation in weak suprasolidus crust (Cosgrove, 1997; Brown and Solar, 1998b), and, accordingly, they may represent different physical expressions of porosity waves moving melt up through the crust. Examples of each mode may be represented by the dikes of granite in the southern Brittany migmatite belt of western France (Marchildon and Brown, 2003; Brown, 2004, 2005, 2010a) and the midcrustal magmatic sheets (diapirs) of Paterson and Miller (1998) and Miller and Paterson (1999, 2001). Connolly and Podladchikov (2007, 2012) made an analogy with the three-dimensional viscous case studied by Wiggins and Spiegelman (1995) to infer that the three-dimensional expression of porosity wave channels might be pipe-like, perhaps as represented by cylindrical granites in the zones of apparent constrictional strain in the Acadian belt in the Northern Appalachians (Brown and Solar, 1999). Notwithstanding, in the presence of far-field stress, Connolly and Podladchikov (2007, 2012) argued that kinematic effects might be expected to flatten these structures in the direction of the minimum principal horizontal stress, perhaps as represented by tabular granites in the zones of apparent flattening strain in the Acadian belt in the Northern Appalachians (Brown and Solar, 1999).

Large-scale tectonic perturbations to the lithostatic mean stress gradient are likely to have relatively minor influence on the rate and direction of compaction-driven fluid flow. In extension, the mean stress gradient in the crust is increased, which accelerates compaction-driven fluid flow, favoring the formation of porosity waves for which the physical expression is likely to be as dikes, such as those in the southern Brittany migmatite belt of western France (Marchildon and Brown, 2003; Brown, 2004, 2005, 2010a). In contraction, an inversion in the mean stress gradient approaching the ductile-to-brittle transition zone creates a barrier to magma ascent, which may cause the magma to stall, leading to back freezing in the ascent conduit, as occurred in the Acadian belt in the Northern Appalachians (Brown and Solar, 1999). Gravity modeling of plutons shows that they tend to form at the depth of the contemporary ductile-to-brittle transition zone (e.g., Vigneresse, 1995), suggesting that magma ascent commonly ends at this transition.

The temperature dependence of the viscous rheology leads to an upward strengthening of the deep crust and a consequent increase in viscous compaction length with decreasing depth that may cause channelized flows to anastomose upward through the anatectic zone (Connolly and Podladchikov, 2007, 2012). The mechanism of melt transfer into subsolidus crust might involve melt-enhanced embrittlement, since the solidus represents the boundary to the anatectic zone with its interconnected melt-filled porosity. Compaction within the anatectic

zone may generate strong variations in pressure near the solidus, which may enable deformation at the solidus to be essentially brittle-elastic in character. Under this condition, melt may be transported across the solidus into the subsolidus (zero-porosity) crust by an elastic shock (Chauveau and Kaminski, 2008). However, the anatectic front is also an unstable interface, so that amplification of flow instabilities across the solidus by ductile processes might be an alternative mechanism to continue melt ascent in some circumstances (Connolly and Podladchikov, 1998). Experiments by Whitehead and Helfrich (1991) showed that flow instabilities develop increasing resistance as they advance into cooler regions across an interface, and the number of advancing fingers rapidly decreases with time to one as the flow becomes focused. In both cases, the physical expression of the transfer of melt across the anatectic front might the tabular and cylindrical granites described earlier that link down into the anatectic zone.

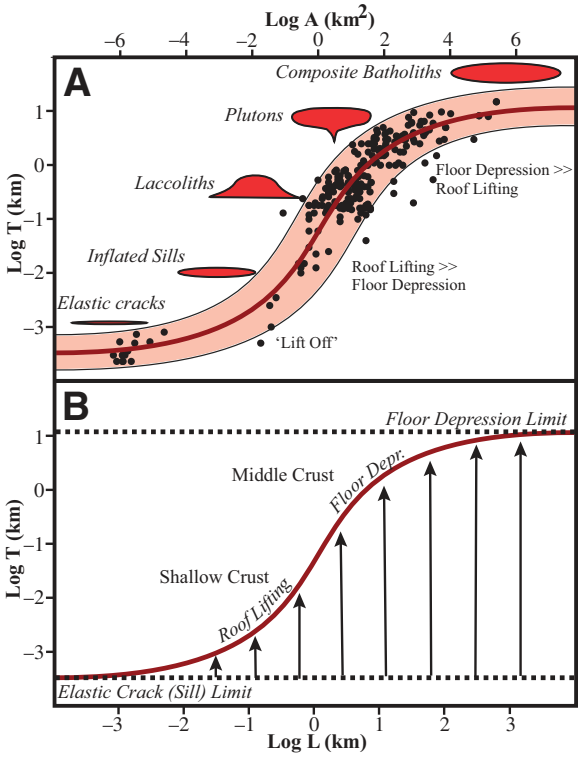

Figure 14. (A) Compilation of intrusion thickness (*T*), width (*L*), and horizontal area (*A*) data (McCaffrey and Cruden, 2002). The solid S-curve is drawn though the data by eye, and the shaded area represents the approximate limits of the data about the curve. Representative intrusion styles are shown adjacent to appropriate parts of the curve. (B) An interpretation of the S-curve in terms of minimum and maximum growth limit, dominant emplacement mechanism, and depth of emplacement in the crust (Cruden and McCaffrey, 2002). Arrows show vertical growth trajectories along a possible end-member growth curve with a slope $a = \infty$. This diagram is reproduced with permission of the Geological Society Publishing House (from Brown, 2007).

A General Model for Granite Emplacement

In this section, a general model for the emplacement of laccoliths and plutons is proposed. This model accommodates the systematic variation in three-dimensional shape of intrusions with depth, from shallower laccoliths and wedge-shaped (lopoliths) plutons in the brittle regime to deeper vertical tabular and blobby plutons (e.g., Brown and Solar, 1998b; Brown, 2007, 2010b; Cruden, 1998, 2006).

Brittle Regime

In the brittle regime, emplacement occurs when mainly vertical flow switches to predominantly horizontal flow and vertical inflation. Depression of the floor and/or lifting of the roof allow inflation (Cruden, 1998, 2006), sometimes with a component of ductile strain in the aureole (e.g., Wagner et al., 2006) or associated with faulting (Benn et al., 1997; Clemens and Benn, 2010). Structural and geophysical data indicate two main types of pluton morphology. Laccoliths are thin (3–4 km) and tend to be equidimensional (e.g., Clemens and Benn, 2010); they may have multiple root zones (Vigneresse et al., 1999). These contrast with thick (>10 km) wedge-shaped plutons, which tend to be elongated along one direction and tend to have single or only a few root zones (e.g., Brown and Solar, 1998b; Vigneresse et al., 1999). The South Mountain batholith in Nova Scotia, Canada, is large, covering more than 7000 km^2, and it has been interpreted as a laccolith based on its internal sheeted structure (Benn et al., 1997). However, the South Mountain batholith is large for a laccolith, and gravity modeling (Benn et al., 1999) suggests that the constituent plutons have flat or gently dipping floors at ~7.0 km depth underlain by deeper (>10 km) elongate root zones. Thus, it might be better classified with the large wedge-shaped plutons.

Dimensional data for sills, laccoliths, plutons, and composite batholiths have been compiled from various sources by McCaffrey and Petford (1997) and McCaffrey and Cruden (2002). Thickness (*T*) versus width (*L*) and horizontal area (*A*) data define an S-shaped distribution when plotted in log *T* versus log *A* or *L* space (Fig. 14), which implies vertical limits for intrusions of $T < 1$ m when $L < 10$ m and $T > 10$ km when $L > 500$ km (Fig. 14B). Between the limits, *T* increases with increasing *L* and *A*, with a maximum slope of $a \sim 1.5$ at $L \sim 1$ km, and *L*/*T* decreases because vertical thickening dominates over horizontal lengthening (McCaffrey and Cruden, 2002). However, as *T* approaches 10 km, horizontal lengthening begins to dominate over vertical thickening and vertical thickening appears to be limited to ~15 km. Earlier empirical power-law scaling relationships for laccoliths showing $a = 0.8$ and plutons showing $a = 0.6$ (McCaffrey and Petford, 1997; Cruden and McCaffrey, 2001) likely define tangents to the S-curve in Figure 14, rather than representing unique scaling relationships for different classes of intrusions.

Limiting factors on vertical growth of plutons include the host-rock mechanical properties and the depth of emplacement. To lift the roof, P_{melt} must overcome the lithostatic load and any tectonic overpressure. At shallow levels, intrusions that grow by vertical inflation from a larger horizontal area are better able to lift the roof, but with increasing depth, vertical growth of plutons occurs dominantly by floor depression, which is limited by the thickness of the source and the degree of melting in that zone (Cruden, 1998, 2006; Cruden and McCaffrey, 2001, 2002).

Mechanical theories for the initiation and growth of sills and laccoliths are reasonably well established (e.g., Cruden and McCaffrey, 2002; Bunger and Cruden, 2011). Sills initiate due to a change in the local stress regime associated with magma ascent whereby the minimum principal stress switches from horizontal to vertical, transforming vertical ascent to horizontal emplacement (Vigneresse et al., 1999). One key parameter in the analysis of such intrusions is the geometric ratio of the intrusion width to its emplacement depth, *L*/*h*. Given sufficient melt pressure, the sill-to-laccolith transition occurs where $L/h > 2$–3, depending on the geometry of the sill and the rheology of the melt. This reflects shallow emplacement ($h = 0.5$–5 km) for intrusions where $L = 1$–10 km, corresponding to the lower half of the S-curve (Fig. 14), with the change of slope at $L = 0.1$–1 km recording the increasing ability of shallow intrusions to lift their roofs as their horizontal area increases. The steepest slope likely represents a limiting curve

for laccoliths to expand vertically from an initial sill by roof lifting along a growth line with $a >> 1$ (Fig. 14; McCaffrey and Cruden, 2002). After this point, vertical growth of moderate to large plutons occurs dominantly by floor depression (Cruden, 1998, 2006; Brown and Solar, 1998b; Cruden and McCaffrey, 2001, 2002).

Floor depression may occur by elastic downbending of the pluton floor if L/h is small (deep emplacement) and if the strength of the material beneath the pluton is significantly less than that above it, as might be expected close to the ductile-to-brittle transition zone. A number of different structural arrangements of phases of granite within plutons are predicted depending upon the growth mode (tabular vs. wedge) and the type of melt delivery (continuous vs. pulsed; top-down vs. base-up). Kinematic models of floor depression involving piston and cantilever mechanisms suggest that emplacement and growth are geologically rapid processes, with typical plutons able to form over thousands to hundreds of thousands of years, at geologically reasonable strain rates (Cruden, 2006). An alternative mechanism for floor depression may be subsidence accommodated by the compacting source as melt is extracted, although the relationship is unlikely to be simple, since the magma volume in the pluton is from a much larger source volume. In this case, the vertical growth limit is imposed by the thickness of the source, degree of melting, and the efficiency of melt extraction. Composite batholiths with $L > 100$ km lie on the uppermost part of the S-curve, where $a << 1$ (Fig. 14). Cruden and McCaffrey (2002) proposed that this is likely an upper limit for multiple stacking of intrusions in the middle crust, resulting from the maximum amount of floor subsidence that is possible.

Ductile Regime

In the ductile regime, emplacement may occur simply by a decrease in the rate of magma ascent approaching the ductile-to-brittle transition zone and back freezing downward. Multiple uses of such ascent conduits may lead to construction of sheeted plutons (e.g., Brown and Solar, 1998a; Miller and Paterson, 2001; Mahan et al., 2003; Bartley et al., 2008). In addition, the magma sheets or diapiric plutons of Paterson and Miller (1998) and Miller and Paterson (1999) may have been emplaced by simple back freezing, with the diapiric form being a result of wall-rock ductility (cf. the experiments of Sumita and Ota, 2011).

Magma ascent may be slowed by lateral expansion of the ascent conduit localized by amplification of instabilities in the magma–wall-rock system (Brown, 2001a, 2001b). Instabilities may be external to the ascent column, such as variations in the strength of the wall rock or the stress field around the ascent column. Magma exploits the weaker/lower-stress sectors, locally expanding the ascent column to form blob-like plutons, perhaps similar to the model proposed by Lagarde et al. (1990). The nested diapirs of Paterson and Vernon (1995) may have been emplaced by such a mechanism, involving sequential arrival of successive batches of magma. Alternatively, instabilities may be internal to the ascent column, such as fluctuations in the flow rate and/or changes in cross-sectional shape, as might occur, for example, immediately above the anatectic zone. Here, such differences in flow rate or cross-sectional shape may lead to fluctuations around the critical width for flow without freezing. If freezing occurs in the slower/wider parts of the conduit, flow will focus in the faster/narrower parts. Advective heating of the host rock at these locations may cause weakening of the wall rock, allowing swelling of the conduit, leading to a slowing rate of magma ascent, and, perhaps, freezing.

Emplacement at the Top of the Anatectic Zone

As discussed already, melt may not be able to cross the solidus surface at the top of the anatectic zone, but instead it may be trapped under this surface, as anticipated by Bowen (1947, p. 277). The Carnac granite in the southern Brittany migmatite belt of western France appears to be an example where this has occurred, since the pluton is fed from beneath by multiple dikes and thins laterally, eventually giving way to a series of granite dikes cutting migmatite (Turrillot et al., 2011). Furthermore, a significant portion of the melt generated under granulite-facies conditions may be retained in the source as diatexite migmatite and granite. For example, Morfin et al. (2013) have described an injection complex in granulite facies migmatites of the Opinaca belt of the Superior Province in Canada that formed as melt became trapped by the granite solidus during transport through the deep crust.

TIME SCALES

Melting occurs along grain boundaries in a fertile source (less than a cubic millimeter) during a metamorphic cycle that may take several millions to several tens of millions of years (10^6–10^7 yr; e.g., Hermann and Rubatto, 2003; Reno et al., 2009, 2012; Korhonen et al., 2012). In contrast, a pluton represents a large volume of magma (10^3–10^4 km^3 or more) aggregated from many batches of melt (each perhaps 10^{-1}–10^2 km^3) that crystallized during tens of thousands to several millions of years (10^4–10^7 yr; Brown, 2001b, 2010a; Coleman et al., 2004; Matzel et al., 2006; Miller, 2008). Thus, melt extraction from segregation to emplacement is a process with a length scale that spans more than seven orders of magnitude, or a volume concentration factor that exceeds 10^{21} (Brown, 2004, 2010a).

Anatectic melts are commonly undersaturated in light rare earth elements and zirconium, consistent with fast rates of deformation-assisted segregation, perhaps on the order of 10–10^4 yr for a single batch of melt (Sawyer, 1991; Harris et al., 2000), but see following. In addition, unusually high zircon inheritance due to limited dissolution of zircon during high-temperature crustal melting indicates rapid production of melt, probably in $<10^4$ yr (Bea et al., 2007). Ascent times for melt in a dike, likely $<<1$ yr for an ascent rate of 10^{-2}–10^{-1} m s^{-1} (Petford et al., 1993; Clemens, 1998), suggest that a small dike 1 km in length and 3 m wide could transfer 10^3 km^3 of melt from source to sink in ~10^3 yr. Thus, melt extraction from segregation to emplacement is a process with a time scale that spans at least seven orders of magnitude, and probably more (Brown, 2004, 2010a).

The time scale for crustal melting and the rate of melt production are determined by the rate of heat flow into the crust, which is a function of the mechanism of heating and the thermal diffusivities of the protoliths. Numerical modeling of prograde heating of the deep crust suggests that the time scale required to achieve ultrahigh temperatures of >900 °C might be tens of millions of years (Thompson and Connolly, 1995; Clark et al., 2011), with much of this evolution being suprasolidus. This is broadly consistent with some determinations of the residence times for melt in anatectic crust (e.g., Rubatto et al., 2001; Montero et al., 2004; Gordon et al., 2010; Korhonen et al., 2013; Weinberg et al., 2013), but not with others (e.g., Solar et al., 1998; Matzel et al., 2004; Hinchey and Carr, 2006; Gordon et al., 2008; Rubatto et al., 2009, 2013; Jeon et al., 2012).

The assignment of unique crystallization ages to granites based on U-Pb zircon dating is complicated by the propensity of zircon to survive emplacement of multiple pulses of magma that eventually crystallize to a large pluton (Miller et al., 2007). As a result, distinctions must be made between zircons entrained from the source, xenocrystic zircons derived locally from host rocks during magma ascent and/or emplacement, and growth and recycling of new zircon during the emplacement and crystallization of multiple pulses of magma to form a pluton.

There is no denying that the process from deposition of the protolith to crystallization of the magma may be rapid. Matzel et al. (2004) documented rapid burial of the Swakane Gneiss in the North Cascades, United States, by thrusting to a depth of ~30 km, followed by partial

melting within a period of 5 m.y. Similarly, Jeon et al. (2012) have argued for a short time scale from the beginning of melting to final crystallization in the generation of a Permian granite in the New England orogen of eastern Australia. These authors reported a 15 m.y. difference between the age of the youngest inherited zircon population entrained from the source and the oldest melt-precipitated zircon cores, and another 5 m.y. difference between the age of these new cores and melt-precipitated zircon rims. They argue that the 5 m.y. age difference was the mean time interval between the initiation of melting and post-emplacement melt crystallization.

The early stage of melt segregation involving diffusive mass transfer is a slow process, perhaps operating on time scales that approach a million years, given the many variables that affect diffusion rates and efficiencies (Costa et al., 2003; Dohmen and Chakraborty, 2003). However, as the melt fraction approaches the melt percolation threshold, advective mass transfer will dominate (Rabinowicz and Vigneresse, 2004; Rosenberg and Handy, 2005). Calculated times for melt extraction by shear-enhanced compaction and dilatant shear failure based on deformation experiments on suprasolidus granite are on the order of tens of thousands of years (e.g., Rutter and Mecklenburgh, 2006), whereas numerical modeling yields extraction times of a few hundreds of thousands of years (e.g., Rabinowicz and Vigneresse, 2004).

Faster still are rates of melt extraction, ascent, and emplacement based on inverse modeling of the geochemistry of Himalayan granites by Harris et al. (2000). Undersaturation of the light rare earth elements in granites suggests that melt could have been extracted in less than 10,000 yr (Ayres and Harris, 1997), whereas experimental studies indicate that some melts were undersaturated in zirconium (Patiño Douce and Harris, 1998), implying extraction could have occurred in as little as 100 yr. Such short time scales require deformation-driven mechanisms to segregate and focus the melt for extraction from the source. As discussed already, dissolution rates of accessory minerals depend strongly on the temperature and water content of the melt, and shielding of accessory mineral inclusions by their host may prohibit dissolution; maybe such fast rates are an artifact of the methodology? Crystallization of the melt could have taken from 500 to 30,000 yr, depending on whether the granite laccoliths were constructed from multiple batches of melt or not (Harris et al., 2000).

For disequilibrium to be preserved, crustal melts must segregate on time scales shorter than required for diffusive equilibration (Sawyer, 1991; Watt et al., 1996). Segregation of melt on time scales of hundreds to thousands of years would be significantly faster than the time scale required for diffusion to erase, for example, strontium compositional gradients, which takes a few million to tens of millions of years (Tommasini and Davies, 1997). This in turn implies that the production of disequilibrium compositions during nonmodal melting may be a fundamental process in determining the composition of the crustal melts, even at high melt fractions (Barbero et al., 1995; Zeng et al., 2005a, 2005b, 2005c), and that inversion of the geochemistry of granites to determine rate of extraction should be viable. For example, Barbero et al. (1995) invoked nonmodal melting of a mineral assemblage including biotite and plagioclase combined with restricted Sr diffusion to account for the observed disequilibrium in anatectic granites from central Spain. The coalescence of numerous batches of melt from compositionally distinct protoliths, each of which is out of equilibrium with its source, has the potential to produce geochemically complex crustal granites, provided the rate of emplacement is fast (Acosta-Vigil et al., 2010, 2012a, 2012b).

Annen et al. (2006a) used thermal modeling to investigate the time scale for the emplacement of the Manaslu granite in the Himalayas, assuming that is was the successive emplacement of numerous thin sills that contributed to the final intrusion. They concluded that the thermal aureole temperature and thickness and the isotopic heterogeneities within the granite can be explained by the accretion of 20–60-m-thick sills of melt emplaced every 20,000–60,000 yr for 5 m.y. Five million years is two to four orders of magnitude longer than the range of time scales implied by the inverse geochemical modeling of Harris et al. (2000).

QUO VADIMUS?

Resolution of some of the issues discussed in this review requires advances in a number of different specialties, wider application of newly developed techniques, and, in some cases, more data to test hypotheses. Examples where progress may be made in the next decade include the following topics.

Forward Modeling of Suprasolidus Phase Equilibria

To fully explain the process of crustal differentiation by intracrustal melting, it is important to be able to apply quantitative phase equilibria modeling across a wider range of protolith compositions than is presently possible, particularly to mafic rocks. In addition, this is a prerequisite to better interpret the petrogenesis of the tonalite-trondhjemite-granodiorite series, which is fundamental in relation to the generation of continental crust in the Archean.

The importance of such an advance in the application of quantitative phase equilibria modeling may be assessed by considering the recent work by Nagel et al. (2012) to model fluid-absent hydrate-breakdown partial melting of two hydrated mafic compositions, a modern mid-oceanic-ridge basalt and a typical Eoarchean arc tholeiite. Although these authors acknowledge that the data set "is actually designed for haplogranitic compositions up to 10–12 kbar," they justify using it "because it predicts the formation of tonalitic melt in hydrated basaltic host rocks for reasonable temperatures and melt fractions." However, this argument is a fallacy, because the consequent is a non sequitur, and the melt compositions derived from the phase equilibria modeling may or may not be reasonable! Furthermore, the conclusion that tonalite-trondhjemite-granodiorite series magmas are derived from Eoarchean arc tholeiites relies on the melt compositions derived from the phase equilibria modeling. Thus, this conclusion cannot be accepted unless replicated by modeling using appropriate thermodynamic models.

In addition, it is essential to be able to model melting at higher pressures than is possible at present if we are to recognize fully the possible contribution of melting to the exhumation of high-temperature, ultrahigh-pressure metamorphic terranes. These demands require the development of a new thermodynamic model for melt that is appropriate to a wider range of compositions and intensive variables, particularly pressure, and improvements to activity-composition models for minerals such as amphibole and pyroxene. This work is in progress. Thus, we should expect to see further advances in our understanding of crustal melting across a wider range of protolith compositions and under high-temperature, ultrahigh-pressure metamorphic conditions in the near future.

Fluid-Present Melting

Fluid-present melting has not been studied as extensively as fluid-absent hydrate-breakdown melting. In particular, fluid-present melting may be invoked where the mechanism by which the fluid gained access to the source is not clear. A better understanding of the physics of pervasive fluid infiltration during high-grade metamorphism is necessary to further our interpretation of fluid-present melting in crustal evolution. This is central to developing a better comprehension of crustal reworking in the Archean, where fluid-present melting of tonalite-trondhjemite-granodiorite series rocks was widespread.

Peritectic Assemblage Entrainment

The hypothesis that the chemistry of granite suites is controlled by peritectic assemblage entrainment should be tested more widely. In addition, the conflicting views about whether granites image heterogeneous crustal sources or represent some combination of crustal and mantle inputs must be resolved. For example, how widespread is the transfer of source heterogeneity to individual batches of magma during melting and melt extraction? This question may be resolved by the wider application of combined hafnium and oxygen isotope studies of zircons to suites of granite from different tectonic settings. At present, the proportion of crustal reworking to crustal growth in the generation of granites is disputed, but this is a fundamental issue to resolve, since the outcome is pivotal to models for crustal evolution.

Quantitative Inverse Modeling of Chemical Data

The rates of the various processes involved in granite petrogenesis discussed herein vary by more than an order of magnitude. Is this wide range realistic or an artifact of the different methods by which the rates have been determined? Assessing the extent of trace-element and isotope disequilibrium during nonmodal melting of crustal rocks by wider application of quantitative modeling of chemical data from granites might lead to a resolution. With a better knowledge of the nature and impact of disequilibrium processes on the trace-element and isotope compositions of granites, it should be possible to develop methods to better estimate the time scales of melt segregation by inversion of trace-element and isotope data. If the rates derived from modeling disequilibrium features of granite chemistry are correct, what might be the reasons for the disparity between these rates and those determined from U-Pb geochronology on accessory minerals? It is critical to resolve this issue, since knowledge of these rates is a prerequisite to assessing the effects of crustal melting on the rates of orogenic processes.

Melt Segregation and Extraction at Low Melt Fraction

Our understanding of melt segregation and extraction at low melt fractions in crustal rocks is based on models assuming textural equilibrium, which predict that melt resides in channels along grain edges. We know that the porosity in residual granulites as determined from pseudomorphs of relict melt is less than the melt connectivity transition of 7 vol%, implying that melt segregation and extraction are efficient. Since deep crustal rocks have melted extensively, this observation implies that the porosity of the suprasolidus crust was controlled by the balance between the pace of melt generation as controlled by heat flow and the rate of melt extraction by processes such as shear-enhanced compaction and localized dilatant shear failure. However, the crust is anisotropic at a variety of scales, which imparts an anisotropy to the permeability at low porosities in particular horizons. Furthermore, at suprasolidus conditions, the rheology of the crust varies according to composition and, therefore, degree of melting, as well as varying throughout the melt-extraction cycle—weakening up to the melt connectivity transition but strengthening as melt drains from the system. Thus, an explanation of melt segregation and extraction at low melt fractions requires better knowledge of the transport properties of deforming anisotropic crustal rocks under suprasolidus conditions with variable degrees of melt-related weakening. This is a key factor because a better understanding of the effects of anisotropy on melt segregation and extraction at low melt fractions and on rheology will improve our insight into the processes by which orogens are built and destroyed.

Porosity Waves in Suprasolidus Crust

The hypothesis that melt extraction and ascent in orogenic crust occur via porosity waves should be tested against the geological record. An assessment of the imprint of porosity waves in the crust will require the generation of new quantitative field data, such as the spacing and size of fossil melt flow structures at all scales from leucosome veins in migmatites to granites crystallized in ascent conduits. It is recognized that these fossil structures are likely to have necked-down as the rate of melt/magma flow declined and the remaining fill crystallized. Nonetheless, with due consideration for the changes during solidification, these natural data may be inverted for comparison with the scales of porosity waves predicted in numerical simulations to ensure that the rheological and hydraulic properties required by the model are consistent with what is known about rock mechanics. Relating the model to nature is paramount; although compaction is the means by which high fluid pressure is generated in suprasolidus crust, which is a necessary condition for melt extraction, failure mode depends on local stresses and rheology. Thus, it is essential to develop a better understanding of the way in which the necessary high fluid pressure manifests itself in nature; such an advance should be possible during the next few years.

Melting, Melt Drainage, and Crustal Rheology during Orogenesis

There has been no systematic investigation of melting and melt drainage along either clockwise or counterclockwise *P-T* paths, and the implications of episodic drainage of melt from orogenic crust during the prograde evolution have not been fully explored. We know that the amount of H_2O required to saturate the solidus at low crustal pressures is much less than that required at high crustal pressures. As a result, there will be differences in the details of melting reactions, the rate of melt production, the *P-T* conditions and number of melt drainage events, the chemistry of the melts, and the evolution of crustal rheology along different *P-T* paths. The ways in which these differences might affect the amount of melt produced, the style of deformation during prograde heating, melting, and melt drainage, and the geometry and evolution of the melt flow networks are unknown. Furthermore, we require better quantitative descriptions of leucosome networks and their linkages to ascent conduits in different tectonic settings to discriminate among the various processes postulated for linking melt extraction to magma ascent, and whether these might be different according to the *P-T* evolution. This is a key to interpreting the temporal evolution of the melt drainage system, and particularly the issues of timing of melt interconnectivity versus extraction, cyclicity in melt extraction, and the evolving rheology as melt drainage dries the residual crust.

Counterclockwise *P-T* paths exhibit thickening during heating, but thickening seems to occur only after the prograde evolution exceeds the solidus. What is the relationship among heat flow, melting, and melt loss, and the evolving rheology on the amount of thickening and the peak temperature for these *P-T* paths? Does the type of *P-T* path, that is, heating and thickening versus heating and decompression, affect the mechanism of magma ascent to the upper crust and its emplacement in plutons? These questions could be addressed by the wider application of thermo-mechanical numerical modeling to a systematic investigation of anatectic systems and *P-T* paths.

Decompression melting has been invoked as a process by which to increase buoyancy during exhumation of high-temperature, ultrahigh-pressure metamorphic terranes, and as a weakening mechanism to facilitate orogenic collapse and crustal extension. However, the way in which episodic melt loss along the prograde *P-T* path affects the volume of melt that could be produced during decompression has not been evaluated. Furthermore, the *P-T* path is critical. Decompression could be accompanied

by heating, for example, caused by superheated melt ascending fast enough through the decompressing crust to advect heat at a faster rate than the rate of decompression. Nonetheless, in adiabatic-isentropic systems, decompression melting must lead to cooling, because temperature is a dependent variable and melting consumes heat of fusion. Thus, the simple view of decompression melting as an isothermal process cannot be correct, and the assumption that melting occurs during decompression may sometimes be false.

A quantitative evaluation of melting and melt drainage along clockwise and counterclockwise *P-T* paths is in progress. Thus, we should soon expect to have a better comprehension of the implications of episodic drainage of melt from orogenic crust for melt production, crustal rheology, and the development of clockwise (thickening before heating to peak temperature) and counterclockwise (heating before thickening to peak pressure) orogens.

High-Precision Geochronology

There is a clear and demonstrated need to have better information about the rates of crustal melting, the time scales of melt segregation and extraction, the rates of magma ascent and emplacement, and the time scales of pluton construction from individual pulses of magma. The wider application of high-precision U-Pb dating of accessory minerals is necessary at each stage of the process. However, there is a fundamental question about the separate processes that are being dated with zircon, melting or crystallization, and there is a need for better physical models to explain the mix of zircon populations found in plutons.

Do ranges of concordant U-Pb ages retrieved from accessory minerals record the duration of a process such as crustal melting or simply register the time taken for the magma to crystallize? Can the beginning of melting or the time when the melt volume reaches the melt connectivity transition be dated using accessory minerals? Does new growth depend on the size of the melt reservoir? Do small melt reservoirs, for example, where the degree of melting was low, limit the dissolution of preexisting grains and new growth? Do variations in the size of melt reservoirs explain differences in the morphology, chemistry, and inheritance that are evident between accessory minerals in migmatites and coeval granites? What differences are there in the behavior of accessory minerals during lower-temperature, fluid-present melting and higher-temperature, fluid absent melting and between closed and open system partial melting? Answers to these questions will significantly improve our knowledge of the rates of the different process involved in crustal differentiation by intracrustal melting.

FINAL REMARKS

We have come a long way since the debate between Bowen and Read more than 60 yr ago, and even since the GSA centennial paper by Whitney 25 yr ago (Whitney, 1988). Although we have a good understanding of melting in some common metaclastic sedimentary and meta-igneous rocks, our thermodynamic models will always be open to improvement, and the range of compositions to which quantitative phase equilibria modeling may be applied will expand during the next few years. Differences of opinion over the interpretation of petrogenetic isotope data in relation to granite petrogenesis need to be resolved as soon as practicable. We have a basic knowledge of fluid flow and the rheology of two-phase materials, but there is scope for improvement in physical models for fluid infiltration and in characterization of critical thresholds in melt-bearing systems. Our interpretation of melt segregation in the crust at low melt fractions and of magma emplacement in plutons has improved significantly since 1988, but we lack a good explanation of the way in which segregation of melt into veins links to the ascent of magma in conduits or the way in which porosity waves might relate to structures in the field. A better knowledge of the rates of the processes that contribute to the genesis and emplacement of granite is important if we are to better understand the process of orogenesis. At present, the information we have about time scales is inadequate and contradictory, and more work is required from both geochronology and inverse geochemical modeling to resolve these differences.

ACKNOWLEDGMENTS

I thank Brendan Murphy for the invitation to write this review and his helpful editorial advice. I acknowledge and thank Tim Johnson (Mainz), Ron Vernon (Macquarie), and especially Roberto Weinberg (Monash) for providing many helpful corrections and insightful suggestions in their reviews, but the responsibility for misrepresentation or errors that may persist is mine alone. In reviewing a topic this broad, work that should have been included may have been overlooked; for this I apologize. My understanding of the topics covered by this review owes as much to the many discussions indoors and in the field that I have had with colleagues and students as to my own investigations and contributions—you know who you are, and I thank you all for your generosity and tolerance. I acknowledge Chris Yakymchuk for help with the figures, and the University of Maryland for supporting my research into high-grade metamorphism and crustal melting. Some of this material is based upon work supported by the National Science Foundation under grant ANT-0944615.

REFERENCES CITED

Ablay, G.J., Clemens, J.D., and Petford, N., 2008, Large-scale mechanics of fracture-mediated felsic magma intrusion driven by hydraulic inflation and buoyancy pumping, *in* Thompson, K., and Petford, N., eds., Structure and Emplacement of High-Level Magmatic Systems: Geological Society of London Special Publication 302, p. 3–29.

Acosta-Vigil, A., Buick, I., Hermann, J., Cesare, B., Rubatto, D., London, D., and Morgan, G.B.V.I., 2010, Mechanisms of crustal anatexis: A geochemical study of partially melted metapelitic enclaves and host dacite, SE Spain: Journal of Petrology, v. 51, p. 785–821, doi:10.1093/petrology/egp095.

Acosta-Vigil, A., Buick, I., Cesare, B., London, D., and Morgan VI, G.B., 2012a, The extent of equilibration between melt and residuum during regional anatexis and its implications for differentiation of the continental crust: A study of partially melted metapelitic enclaves: Journal of Petrology, v. 53, p. 1319–1356, doi:10.1093/petrology/egs018.

Acosta-Vigil, A., London, D., and Morgan VI, G.B., 2012b, Chemical diffusion of major components in granitic liquids: Implications for the rates of homogenization of crustal melts: Lithos, v. 153, p. 308–323, doi:10.1016/j.lithos.2012.06.017.

Allibone, A.H., and Norris, R.J., 1992, Segregation of leucogranite microplutons during syn-anatectic deformation—An example from the Taylor Valley, Antarctica: Journal of Metamorphic Geology, v. 10, p. 589–600, doi:10.1111/j.1525-1314.1992.tb00107.x.

Annen, C., Scaillet, B., and Sparks, R.S.J., 2006a, Thermal constraints on the emplacement rate of a large intrusive complex: The Manaslu leucogranite, Nepal Himalaya: Journal of Petrology, v. 47, p. 71–95, doi:10.1093/petrology/egi068.

Annen, C., Blundy, J.D., and Sparks, R.S.J., 2006b, The genesis of intermediate and silicic magmas in deep crustal hot zones: Journal of Petrology, v. 47, p. 505–539, doi:10.1093/petrology/egi084.

Arzi, A.A., 1978, Critical phenomena in the rheology of partially melted rocks: Tectonophysics, v. 44, p. 173–184, doi:10.1016/0040-1951(78)90069-0.

Atherton, M.P., 1993, Granite magmatism: Journal of the Geological Society of London, v. 150, p. 1009–1023, doi:10.1144/gsjgs.150.6.1009.

Ayres, M., and Harris, N., 1997, REE fractionation and Nd-isotope disequilibrium during crustal anatexis: Constraints from Himalayan leucogranites: Lithos, v. 139, p. 249–269.

Barbero, L., Villaseca, C., Rogers, G., and Brown, P.E., 1995, Geochemical and isotopic disequilibrium in crustal melting: An insight from the anatectic granitoids from Toledo, Spain: Journal of Geophysical Research, v. 100, p. 15,745–15,765, doi:10.1029/95JB00036.

Bartley, J.M., Coleman, D.S., and Glazner, A.F., 2008, Incremental pluton emplacement by magmatic crack-seal: Transactions of the Royal Society of Edinburgh–Earth Sciences, v. 97, p. 383–396.

Bartoli, O., Cesare, B., Poli, S., Bodnar, R.J., Acosta-Vigil, A., Frezzotti, M.L., and Meli, S., 2013, Recovering the composition of melt and the fluid regime at the onset of crustal anatexis and S-type granite formation: Geology, v. 41, p. 115–118, doi:10.1130/G33455.1.

Bea, F., 1996, Residence of REE, Y, Th and U in granites and crustal protoliths: Implications for the chemistry of crustal melts: Journal of Petrology, v. 37, p. 521–552, doi:10.1093/petrology/37.3.521.

Bea, F., 2012, The sources of energy for crustal melting and the geochemistry of heat-producing elements: Lithos, v. 153, p. 278–291, doi:10.1016/j.lithos.2012.01.017.

Bea, F., and Montero, P., 1999, Behavior of accessory phases and redistribution of Zr, REE, Y, Th, and U during metamorphism and partial melting of metapelites in the lower crust: An example from the Kinzigite Formation of Ivrea-Verbano, NW Italy: Geochimica et Cosmochimica Acta, v. 63, p. 1133–1153, doi:10.1016/S0016-7037(98)00292-0.

Bea, F., Montero, P., and Ortega, M., 2006, A LA-ICP-MS evaluation of Zr reservoirs in common crustal rocks: Implications for Zr and Hf geochemistry, and zircon-

forming processes: Canadian Mineralogist, v. 44, p. 693–714, doi:10.2113/gscanmin.44.3.693.

Bea, F., Montero, P., González-Lodeiro, F., and Talavera, C., 2007, Zircon inheritance reveals exceptionally fast crustal magma generation processes in central Iberia during the Cambro-Ordovician: Journal of Petrology, v. 48, p. 2327–2339, doi:10.1093/petrology/egm061.

Benn, K., Horne, R.J., Kontak, D.J., Pignotta, G.S., and Evans, N.G., 1997, Syn-Acadian emplacement model for the South Mountain batholith, Meguma terrane, Nova Scotia: Magnetic fabric and structural analyses: Geological Society of America Bulletin, v. 109, p. 1279–1293, doi:10.1130/0016-7606(1997)109<1279:SAEMFT>2.3.CO;2.

Benn, K., Roest, W.R., Rochette, P., Evans, N.G., and Pignotta, G.S., 1999, Geophysical and structural signatures of syntectonic batholith construction: The South Mountain batholith, Meguma terrane, Nova Scotia: Geophysical Journal International, v. 136, p. 144–158, doi:10.1046/j.1365-246X.1999.00700.x.

Bergantz, G.W., 1989, Underplating and partial melting implications for melt generation and extraction: Science, v. 254, p. 1039–1095.

Berger, A., Burri, T., Alt-Epping, P., and Engi, M., 2008, Tectonically controlled fluid flow and water assisted melting in the middle crust: An example from the central Alps: Lithos, v. 102, p. 598–615, doi:10.1016/j.lithos.2007.07.027.

Bons, P.D., and Elburg, M.A., 2001, Fractal size distribution of plutons: An example from the Lachlan fold belt, Australia, *in* Chappell, B.W., and Fleming, P.D., eds., S-Type Granites and Related Rocks: Australian Geological Survey Organisation Record 2001/2, p. 21–22.

Bons, P.D., and van Milligen, B.P., 2001, New experiment to model self-organized critical transport and accumulation of melt and hydrocarbons from their source rocks: Geology, v. 29, p. 919–922, doi:10.1130/0091-7613(2001)029<0919:NETMSO>2.0.CO;2.

Bons, P.D., Dougherty-Page, J., and Elburg, M.A., 2001, Stepwise accumulation and ascent of magmas: Journal of Metamorphic Geology, v. 19, p. 627–633, doi:10.1046/j.0263-4929.2001.00334.x.

Bons, P.D., Arnold, J., Elburg, M.A., Kalda, J., Soesoo, A., and van Milligen, B.P., 2004, Melt extraction and accumulation from partially molten rocks: Lithos, v. 78, p. 25–42, doi:10.1016/j.lithos.2004.04.041.

Bons, P.D., Druguet, E., Castaño, L.-M., and Elburg, M.A., 2008, Finding what is now not there anymore: Recognizing missing fluid and magma volumes: Geology, v. 36, p. 851–854, doi:10.1130/G24984A.1.

Bowen, N.L., 1947, Magmas: Geological Society of America Bulletin, v. 58, p. 263–280, doi:10.1130/0016-7606(1947)58[263:M]2.0.CO;2.

Bowen, N.L., 1948, The granite problem and the method of multiple prejudices, *in* Gilluly, J., ed., Origin of Granite: Geological Society of America Memoir 28, p. 79–90.

Brown, E.H., and McClelland, W.C., 2000, Pluton emplacement by sheeting and vertical ballooning in part of the southeast Coast plutonic complex, British Columbia: Geological Society of America Bulletin, v. 112, p. 708–719, doi:10.1130/0016-7606(2000)112<708:PEBSAV>2.0.CO;2.

Brown, M., 1994, The generation, segregation, ascent and emplacement of granite magma: The migmatite-to-crustally-derived granite connection in thickened orogens: Earth-Science Reviews, v. 36, p. 83–130, doi:10.1016/0012-8252(94)90009-4.

Brown, M., 2001a, Crustal melting and granite magmatism: Key issues: Physics and Chemistry of the Earth, v. 26, p. 201–212, doi:10.1016/S1464-1895(01)00047-3.

Brown, M., 2001b, Orogeny, migmatites and leucogranites: A review: Proceedings of the Indiana Academy of Sciences, v. 110, p. 313–336.

Brown, M., 2002, Prograde and retrograde processes in migmatites revisited: Journal of Metamorphic Geology, v. 20, p. 25–40, doi:10.1046/j.0263-4929.2001.00362.x.

Brown, M., 2004, Melt extraction from lower continental crust: Transactions of the Royal Society of Edinburgh–Earth Sciences, v. 95, p. 35–48, doi:10.1017/S0263593300000900.

Brown, M., 2005, Synergistic effects of melting and deformation: An example from the Variscan belt, western France, *in* Gapais, D., Brun, J.-P., and Cobbold, P.R., eds., Deformation Mechanism, Rheology and Tectonics: From Minerals to the Lithosphere: Geological Society of London Special Publication 243, p. 205–226.

Brown, M., 2006, Melt extraction from the lower continental crust of orogens: The field evidence, *in* Brown, M., and Rushmer, T., eds., Evolution and Differentiation of the Continental Crust: Cambridge, UK, Cambridge University Press, p. 332–384.

Brown, M., 2007, Crustal melting and melt extraction, ascent and emplacement in orogens: Mechanisms and consequences: Journal of the Geological Society of London, v. 164, p. 709–730, doi:10.1144/0016-76492006-171.

Brown, M., 2008, Chapter 6: Granites, migmatites and residual granulites: Relationships and processes, *in* Sawyer, E.W., and Brown, M., eds., Working with Migmatites: Mineralogical Association of Canada, Short Course Series 38, p. 97–144.

Brown, M., 2010a, The spatial and temporal patterning of the deep crust and implications for the process of melt extraction: Philosophical Transactions of the Royal Society, ser. A, v. 368, p. 11–51, doi:10.1098/rsta.2009.0200.

Brown, M., 2010b, Melting of the continental crust during orogenesis: The thermal, rheological and compositional consequences of melt transport from lower to upper continental crust: Canadian Journal of Earth Sciences, v. 47, p. 655–694, doi:10.1139/E09-057.

Brown, M., 2012, Introduction to a virtual special issue on crustal melting: Journal of Metamorphic Geology, v. 30, p. 453–456, doi:10.1111/j.1525-1314.2012.00976.x.

Brown, M., and Dallmeyer, R.D., 1996, Rapid Variscan exhumation and role of magma in core complex formation: Southern Brittany metamorphic belt, France: Journal of Metamorphic Geology, v. 14, p. 361–379, doi:10.1111/j.1525-1314.1996.00361.x.

Brown, M., and D'Lemos, R.S., 1991, The Cadomian granites of Mancellia, north-east Armorican Massif of France: Relationship to the St. Malo migmatite belt, petrogenesis and tectonic setting: Precambrian Research, v. 51, p. 393–427, doi:10.1016/0301-9268(91)90110-V.

Brown, M., and Korhonen, F.J., 2009, Some remarks on melting and extreme metamorphism of crustal rocks, *in* Dasgupta, S., ed., Physics and Chemistry of the Earth: New York, Published for the Indian National Science Academy by Springer, p. 67–87.

Brown, M., and Pressley, R.A., 1999, Crustal melting in nature: Prosecuting source processes: Physics and Chemistry of the Earth, v. 24, p. 305–316, doi:10.1016/S1464-1895(99)00034-4.

Brown, M., and Rushmer, T., 1997, The role of deformation in the movement of granite melt: Views from the laboratory and the field, *in* Holness, M.B., eds., Deformation-Enhanced Fluid Transport in the Earth's Crust and Mantle: The Mineralogical Society Series 8: London, Chapman and Hall, p. 111–144.

Brown, M., and Rushmer, T., 2006, Evolution and Differentiation of the Continental Crust: Cambridge, UK, Cambridge University Press, 562 p.

Brown, M., and Solar, G.S., 1998a, Shear zone systems and melts: Feedback relations and self-organization in orogenic belts: Journal of Structural Geology, v. 20, p. 211–227, doi:10.1016/S0191-8141(97)00068-0.

Brown, M., and Solar, G.S., 1998b, Granite ascent and emplacement during contractional deformation in convergent orogens: Journal of Structural Geology, v. 20, p. 1365–1393.

Brown, M., and Solar, G.S., 1999, The mechanism of ascent and emplacement of granite magma during transpression: A syntectonic granite paradigm: Tectonophysics, v. 312, p. 1–33, doi:10.1016/S0040-1951(99)00169-9.

Brown, M., Friend, C.R.L., McGregor, V.R., and Perkins, W.T., 1981, The Late Archaean Qôrqut granite complex of southern West Greenland: Journal of Geophysical Research, v. 86, p. 10,617–10,632, doi:10.1029/JB086iB11p10617.

Brown, M., Averkin, Y.A., McLellan, E.L., and Sawyer, E.W., 1995, Melt segregation in migmatites: Journal of Geophysical Research, v. 100, p. 15,655–15,679, doi:10.1029/95JB00517.

Brown, M., Korhonen, F.J., and Siddoway, C.S., 2011, Organizing melt flow through the crust: Elements, v. 7, p. 261–266, doi:10.2113/gselements.7.4.261.

Brown, M.A., Brown, M., Carlson, W.D., and Denison, C., 1999, Topology of syntectonic melt flow networks in the deep crust: Inferences from three-dimensional images of leucosome geometry in migmatites: The American Mineralogist, v. 84, p. 1793–1818.

Buddington, A.F., 1959, Granite emplacement with special reference to North America: Geological Society of America Bulletin, v. 70, p. 671–747, doi:10.1130/0016-7606(1959)70[671:GEWSRT]2.0.CO;2.

Bunger, A.P., and Cruden, A.R., 2011, Modeling the growth of laccoliths and large mafic sills: Role of magma body forces: Journal of Geophysical Research–Solid Earth, v. 116, article no. b02203; and correction: Journal of Geophysical Research–Solid Earth, v. 116, B08211, doi:10.1029/2011JB008618.

Burov, E., Jaupart, C., and Guillou-Frottier, L., 2003, Ascent and emplacement of buoyant magma bodies in brittle-ductile upper crust: Journal of Geophysical Research, v. 108, p. 2177, doi:10.1029/2002JB001904.

Campbell, I.H., and Taylor, S.R., 1983, No water, no granites—No oceans, no continents: Geophysical Research Letters, v. 10, p. 1061–1064.

Carrington, D.P., and Harley, S.L., 1995, Partial melting and phase-relations in high-grade metapelites—An experimental petrogenetic grid in the KFMASH system: Contributions to Mineralogy and Petrology, v. 120, p. 270–291, doi:10.1007/BF00306508.

Cesare, B., Acosta-Vigil, A., Ferrero, S., and Bartoli, O., 2011, Melt inclusions in migmatites and granulites, *in* Forster, M.A., and Fitz Gerald, J.D., eds., The Science of Microstructure—Part II: Journal of the Virtual Explorer, Electronic Edition, v. 38, paper 2. doi:10.3809/jvirtex.2011.00268.

Chappell, B.W., and White, A.J.R., 1974, Two contrasting granite types: Pacific Geology, v. 8, p. 173–174.

Chappell, B.W., and White, A.J.R., 1974, I- and S-type granites in the Lachlan Fold Belt, southeastern Australia, *in* Keqin X., and Guangchi T., eds., Geology of Granites and Their Metallogenic Relations, Science Press, Beijing, p. 87–101.

Chappell, B.W., White, A.J.R., and Wyborn, D., 1987, The importance of residual source material (restite) in granite petrogenesis: Journal of Petrology, v. 28, p. 1111–1138.

Chappell, B.W., White, A.J.R., Williams, I.S., and Wyborn, D., 2004, Low- and high-temperature granites: Transactions of the Royal Society of Edinburgh–Earth Sciences, v. 95, p. 125–140, doi:10.1017/S0263593300000973.

Chauveau, B., and Kaminski, E., 2008, Porous compaction in transient creep regime and implications for melt, petroleum, and CO_2 circulation: Journal of Geophysical Research, v. 113, B09406, doi:10.1029/2007JB005088.

Clark, C., Fitzsimons, I.C.W., Healy, D., and Harley, S.L., 2011, How does the continental crust get really hot?: Elements, v. 7, p. 235–240, doi:10.2113/gselements.7.4.235.

Clarke, D.B., and Erdmann, S., 2008, Is stoping a volumetrically significant pluton emplacement process?: Geological Society of America Bulletin, v. 120, p. 1072–1074, doi:10.1130/B26147.1.

Clarke, G.L., White, R.W., Lui, S., Fitzherbert, J.A., and Pearson, N.J., 2007, Contrasting behaviour of rare earth and major elements during partial melting in granulite facies migmatites, Wuluma Hills, Arunta block, central Australia: Journal of Metamorphic Geology, v. 25, p. 1–18, doi:10.1111/j.1525-1314.2006.00673.x.

Clemens, J.D., 1998, Observations on the origins and ascent mechanisms of granitic magmas: Journal of the Geological Society of London, v. 155, p. 843–851, doi:10.1144/gsjgs.155.5.0843.

Clemens, J.D., 2003, S-type granitic magmas—Petrogenetic issues, models and evidence: Earth-Science Reviews, v. 61, p. 1–18, doi:10.1016/S0012-8252(02)00107-1.

Clemens, J.D., 2006, Melting of the continental crust: Fluid regimes, melting reactions, and source-rock fertility, *in* Brown, M., and Rushmer, T., eds., Evolution and Differentiation of the Continental Crust: Cambridge, UK, Cambridge University Press, p. 297–331.

Clemens, J.D., and Benn, K., 2010, Anatomy, emplacement and evolution of a shallow-level, post-tectonic laccolith: The Mt. Disappointment pluton, SE Australia: Journal of the Geological Society of London, v. 167, p. 915–941, doi:10.1144/0016-76492009-120.

Clemens, J.D., and Mawer, C.K., 1992, Granitic magma transport by fracture propagation: Tectonophysics, v. 204, p. 339–360, doi:10.1016/0040-1951(92)90316-X.

Clemens, J.D., and Stevens, G., 2012, What controls chemical variation in granitic magmas?: Lithos, v. 134–135, p. 317–329, doi:10.1016/j.lithos.2012.01.001.

Clemens, J.D., and Vielzeuf, D., 1987, Constraints on melting and magma production in the crust: Earth and Planetary Science Letters, v. 86, p. 287–306, doi:10.1016/0012-821X(87)90227-5.

Clemens, J.D., Holloway, J.R., and White, A.J.R., 1986, Origin of an A-type granite: Experimental constraints: The American Mineralogist, v. 71, p. 317–324.

Clemens, J.D., Stevens, G., and Farina, F., 2011, The enigmatic sources of I-type granites: The peritectic connexion: Lithos, v. 126, p. 174–181, doi:10.1016/j.lithos.2011.07.004.

Coleman, D.S., Gray, W., and Glazner, A.F., 2004, Rethinking the emplacement and evolution of zoned plutons: Geochronologic evidence for incremental assembly of the Tuolumne Intrusive Suite, California: Geology, v. 32, p. 433–436, doi:10.1130/G20220.1.

Collins, W.J., 1996, Lachlan fold belt granitoids: Products of three-component mixing: Transactions of the Royal Society of Edinburgh–Earth Sciences, v. 87, p. 171–181, doi:10.1017/S0263593300006581.

Collins, W.J., and Sawyer, E.W., 1996, Pervasive magma transfer through the lower-middle crust during noncoaxial compressional deformation: An alternative to diking: Journal of Metamorphic Geology, v. 14, p. 565–579, doi:10.1046/j.1525-1314.1996.00442.x.

Collins, W.J., Beams, S.D., White, A.J.R., and Chappell, B.W., 1982, Nature and origin of A-type granites with particular reference to southeastern Australia: Contributions to Mineralogy and Petrology, v. 80, p. 189–200, doi:10.1007/BF00374895.

Connolly, J.A.D., 2010, The mechanics of metamorphic fluid expulsion: Elements, v. 6, p. 165–172, doi:10.2113/gselements.6.3.165.

Connolly, J.A.D., and Podladchikov, Y.Y., 1998, Compaction-driven fluid flow in viscoelastic rock: Geodinamica Acta, v. 11, p. 55–84, doi:10.1016/S0985-3111(98)80006-5.

Connolly, J.A.D., and Podladchikov, Y.Y., 2004, Fluid flow in compressive tectonic settings: Implications for mid-crustal seismic reflectors and downward fluid migration: Journal of Geophysical Research, v. 109, B04201, doi:10.1029/2003JB002822.

Connolly, J.A.D., and Podladchikov, Y.Y., 2007, Decompaction weakening and channeling instability in ductile porous media: Implications for asthenospheric melt segregation: Journal of Geophysical Research, v. 112, B10205, doi:10.1029/2005JB004213.

Connolly, J.A.D., and Podladchikov, Y.Y., 2012, A hydromechanical model for lower crustal fluid flow, *in* Harlov, D.E., and Austrheim, H., eds., Metasomatism and the Chemical Transformation of Rock, Lecture Notes in Earth System Sciences: Berlin, Heidelberg, Springer-Verlag, p. 599–658, doi:10.1007/978-3-642-28394-9.

Connolly, J.A.D., and Thompson, A.B., 1989, Fluid and enthalpy production during regional metamorphism: Contributions to Mineralogy and Petrology, v. 102, p. 347–366, doi:10.1007/BF00373728.

Conrad, W.K., Nicholls, I.A., and Wall, V.J., 1988, Water-saturated and -undersaturated melting of metaluminous and peraluminous crustal compositions at 10 kb: Evidence for the origin of silicic magmas in the Taupo volcanic zone, New Zealand, and other occurrences: Journal of Petrology, v. 29, p. 765–803, doi:10.1093/petrology/29.4.765.

Cosgrove, J.W., 1997, The influence of mechanical anisotropy on the behaviour of the lower crust: Tectonophysics, v. 280, p. 1–14, doi:10.1016/S0040-1951(97)00145-5.

Costa, F., Chakraborty, S., and Dohmen, R., 2003, Diffusion coupling between trace and major elements and a model for calculation of magma residence times using plagioclase: Geochimica et Cosmochimica Acta, v. 67, p. 2189–2200.

Creaser, R.A., Price, R.C., and Wormald, R.J., 1991, A-type granites revisited: Assessment of a residual-source model: Geology, v. 19, p. 163–166, doi:10.1130/0091-7613(1991)019<0163:ATGRAO>2.3.CO;2.

Cruden, A.R., 1998, On the emplacement of tabular granites: Journal of the Geological Society of London, v. 155, p. 853–862, doi:10.1144/gsjgs.155.5.0853.

Cruden, A.R., 2006, Emplacement and growth of plutons: Implications for rates of melting and mass transfer in continental crust, *in* Brown, M., and Rushmer, T., eds., Evolution and Differentiation of the Continental Crust: Cambridge, UK, Cambridge University Press, p. 455–519.

Cruden, A.R., and McCaffrey, K.J.W., 2001, Growth of plutons by floor subsidence: Implications for rates of emplacement, intrusion spacing and melt-extraction mechanisms: Physics and Chemistry of the Earth, Part A: Solid Earth and Geodesy, v. 26, p. 303–315, doi:10.1016/S1464-1895(01)00060-6.

Cruden, A.R., and McCaffrey, K.J.W., 2002, Different scaling laws for sills, laccoliths and plutons: Mechanical thresholds on roof lifting and floor depression, *in* Breitkreuz, C., Mock, A., and Petford, N., eds., First International Workshop: Physical Geology of Subvolcanic Systems—Laccoliths, Sills and Dikes (LASI): Freiberg, Germany, Wissenschaftliche Mitteilung Instute für Geologie Technische Universität Bergakademie Freiberg, 20/2002, p. 15–17.

Daczko, N.R., Clarke, G.L., and Klepeis, K.A., 2001, Transformation of two-pyroxene hornblende granulite to garnet granulite involving simultaneous melting and fracturing of the lower crust, Fiordland, New Zealand: Journal of Metamorphic Geology, v. 19, p. 549–562, doi:10.1046/j.0263-4929.2001.00328.x.

Davidson, J.P., Hora, J.M., Garrison, J.M., and Dungan, M.A., 2005, Crustal forensics in arc magmas: Journal of Volcanology and Geothermal Research, v. 140, p. 157–170, doi:10.1016/j.jvolgeores.2004.07.019.

Degeling, H., Eggins, S., and Ellis, D.J., 2001, Zr budgets for metamorphic reactions, and the formation of zircon from garnet breakdown: Mineralogical Magazine, v. 65, p. 749–758, doi:10.1180/0026461016560006.

Dell'Angelo, L.N., and Tullis, J., 1988, Experimental deformation of partially melted granitic aggregates: Journal of Metamorphic Geology, v. 6, p. 495–515, doi:10.1111/j.1525-1314.1988.tb00436.x.

DePaoli, M.C., Clarke, G.L., and Daczko, N.R., 2012, Mineral equilibria modeling of the granulite-eclogite transition: Effects of whole-rock composition on metamorphic facies-type assemblages: Journal of Petrology, v. 53, p. 949–970, doi:10.1093/petrology/egs004.

Deniel, C., Vidal, P., Fernandez, A., LeFort, P., and Peucat, J.J., 1987, Isotopic study of the Manaslu granite (Himalaya, Nepal)—Inferences on the age and source of Himalayan leucogranites: Contributions to Mineralogy and Petrology, v. 96, p. 78–92, doi:10.1007/BF00375529.

D'Lemos, R.S., Brown, M., and Strachan, R.A., 1992, Granite magma generation, ascent and emplacement within a transpressional orogeny: Journal of the Geological Society of London, v. 149, p. 487–490, doi:10.1144/gsjgs.149.4.0487.

Dohmen, R., and Chakraborty, S., 2003, Mechanism and kinetics of element and isotopic exchange mediated by a fluid phase: American Mineralogist, v. 88, p. 1251–1270.

Dorais, M.J., and Tubrett, M., 2012, Detecting peritectic garnet in the peraluminous Cardigan pluton, New Hampshire: Journal of Petrology, v. 53, p. 299–324, doi:10.1093/petrology/egr063.

Dorais, M.J., Pett, T.K., and Tubrett, M., 2009, Garnetites of the Cardigan pluton, New Hampshire: Evidence for peritectic garnet entrainment and implications for source rock compositions: Journal of Petrology, v. 50, p. 1993–2016, doi:10.1093/petrology/egp058.

Droop, G.T.R., and Brodie, K.H., 2012, Anatectic melt volumes in the thermal aureole of the Etive Complex, Scotland: The roles of fluid-present and fluid-absent melting: Journal of Metamorphic Geology, v. 30, p. 843–864, doi:10.1111/j.1525-1314.2012.01001.x.

Dufek, J., and Bergantz, G.W., 2005, Lower crustal magma genesis and preservation: A stochastic framework for the evaluation of basalt-crust interaction: Journal of Petrology, v. 46, p. 2167–2195.

Eichhubl, P., 2004, Growth of ductile opening-mode fractures in geomaterials, *in* Cosgrove, J.W., and Engelder, T., eds., The Initiation, Propagation, and Arrest of Joints and Other Fractures: Geological Society of London Special Publication 231, p. 11–24.

Ellis, D.J., and Thompson, A.B., 1986, Subsolidus and partial melting reactions in the quartz-excess CaO + MgO + Al_2O_3 + SiO_2 + H_2O system under water-excess and water-deficient conditions to 10 kb: Some implications for the origin of peraluminous melts from mafic rocks: Journal of Petrology, v. 27, p. 91–121, doi:10.1093/petrology/27.1.91.

Farina, F., and Stevens, G., 2011, Source controlled Sr^{87}/Sr^{86} isotope variability in granitic magmas: The inevitable consequence of mineral-scale isotopic disequilibrium in the protolith: Lithos, v. 122, p. 189–200, doi:10.1016/j.lithos.2011.01.001.

Fountain, J.C., Hodge, D.S., and Shaw, R.P., 1989, Melt segregation in anatectic granites: A thermo-mechanical model: Journal of Volcanology and Geothermal Research, v. 39, p. 279–296, doi:10.1016/0377-0273(89)90093-0.

Fraser, G., Ellis, D., and Eggins, S., 1997, Zirconium abundance in granulite-facies minerals, with implications for zircon geochronology in high-grade rocks: Geology, v. 25, p. 607–610, doi:10.1130/0091-7613(1997)025<0607:ZAIGFM>2.3.CO;2.

Gardien, V., Thompson, A.B., Grujic, D., and Ulmer, P., 1995, Experimental melting of biotite + plagioclase + quartz ± muscovite assemblages and implications for crustal melting: Journal of Geophysical Research, v. 100, p. 15,581–15,591, doi:10.1029/95JB00916.

Genier, F., Bussy, F., Epard, J.-L., and Baumgartner, L., 2008, Water-assisted migmatization of metagreywackes in a Variscan shear zone, Aiguilles-Rouges massif, western Alps: Lithos, v. 102, p. 575–597, doi:10.1016/j.lithos.2007.07.024.

Getsinger, A., Rushmer, T., Jackson, M.D., and Baker, D., 2009, Generating high Mg-numbers and chemical diversity in tonalite-trondhjemite-granodiorite (TTG) magmas during melting and melt segregation in the continental crust: Journal of Petrology, v. 50, p. 1935–1954.

Gilluly, J., ed., 1948, Origin of Granite: Geological Society of America Memoir 28, 139 p.

Glazner, A.F., and Bartley, J.M., 2006, Is stoping a volumetrically significant pluton emplacement process?: Geological Society of America Bulletin, v. 118, p. 1185–1195.

Glazner, A.F., and Bartley, J.M., 2008, Reply to comments on "Is stoping a volumetrically significant pluton emplacement process?": Geological Society of America Bulletin, v. 120, p. 1082–1087, doi:10.1130/B26312.1.

Gordon, S.M., Whitney, D.L., Teyssier, C., Grove, M., and Dunlap, W.J., 2008, Timescales of migmatization, melt crystallization, and cooling in a Cordilleran gneiss dome: Valhalla complex, southeastern British Columbia: Tectonics, v. 27, TC4010, doi:10.1029/2007TC002103.

Gordon, S.M., Bowring, S.A., Whitney, D.L., Miller, R.B., and McLean, N., 2010, Time scales of metamorphism, deformation, and crustal melting in a continental arc, North Cascades USA: Geological Society of America Bulletin, v. 122, p. 1308–1330, doi:10.1130/B30060.1.

Grant, J.A., 2009, THERMOCALC and experimental modelling of melting of pelite, Morton Pass, Wyoming: Journal of Metamorphic Geology, v. 27, p. 571–578, doi:10.1111/j.1525-1314.2009.00846.x.

Gray, C.M., and Kemp, A.I.S., 2009, The two-component model for the genesis of granitic rocks in southeastern Australia—Nature of the metasedimentary-derived and basaltic end members: Lithos, v. 111, p. 113–124, doi:10.1016/j.lithos.2009.04.010.

Gregg, P.M., Hebert, L.B., Montési, L.G.J., and Katz, R.F., 2012, Geodynamic models of melt generation and extraction at mid-ocean ridges: Oceanography, v. 25, p. 79–89.

Grocott, J., Brown, M., Dallmeyer, R.D., Taylor, G.K., and Treloar, P.J., 1994, Mechanisms of continental growth in extensional arcs: An example from the Andean plate boundary zone: Geology, v. 22, p. 391–394, doi:10.1130/0091-7613(1994)022<0391:MOCGIE>2..CO;2.

Guernina, S., and Sawyer, E.W., 2003, Large-scale melt-depletion in granulite terranes: An example from the Archean Ashuanipi subprovince of Quebec: Journal of Metamorphic Geology, v. 21, p. 181–201, doi:10.1046/j.1525-1314.2003.00436.x.

Guineberteau, B., Bouchez, J.L., and Vigneresse, J.L., 1987, The Mortagne granite pluton (France) emplaced by pull-apart along a shear zone: Structural and gravimetric

arguments and regional implication: Geological Society of America Bulletin, v. 99, p. 763–770, doi:10.1130/0016-7606(1987)99<763:TMGPFE>2.0.CO;2.

Hall, D., and Kisters, A., 2012, The stabilization of self-organised leucogranite networks—Implications for melt segregation and far-field melt transfer in the continental crust: Earth and Planetary Science Letters, v. 355–356, p. 1–12, doi:10.1016/j.epsl.2012.08.033.

Hammouda, T., Pichavant, M., and Chaussidon, M., 1996, Isotopic equilibration during partial melting: An experimental test of the behavior of Sr: Earth and Planetary Science Letters, v. 144, p. 109–121, doi:10.1016/0012-821X(96)00144-6.

Handy, M.R., Mulch, A., Rosenau, N., and Rosenberg, C.L., 2001, The role of fault zones and melts as agents of weakening, hardening and differentiation of the continental crust: A synthesis, *in* Holdsworth, R.E., Magloughlin, J., Knipe, R.J., Strachan, R.A., and Searle, R.C., eds., The Nature and Tectonic Significance of Fault Zone Weakening: Geological Society of London Special Publication 186, p. 305–332.

Harris, N.B.W., and Inger, S., 1992, Trace-element modelling of pelite-derived granites: Contributions to Mineralogy and Petrology, v. 110, p. 46–56, doi:10.1007/BF00310881.

Harris, N.B.W., Vance, D., and Ayers, M., 2000, From sediment to granite: Time scales of anatexis in the upper crust: Chemical Geology, v. 162, p. 155–167, doi:10.1016/S0009-2541(99)00121-7.

Harrison, T.M., and Watson, E.B., 1983, Kinetics of zircon dissolution and zirconium diffusion in granitic melts of variable water-content: Contributions to Mineralogy and Petrology, v. 84, p. 66–72, doi:10.1007/BF01132331.

Harrison, T.M., and Watson, E.B., 1984. The behavior of apatite during crustal anatexis—Equilibrium and kinetic considerations: Geochimica et Cosmochimica Acta, v. 48, p. 1467–1477.

Hasalová, P., Weinberg, R.F., and Macrae, C., 2011, Microstructural evidence for magma confluence and reusage of magma pathways: Implications for magma hybridization, Karakoram shear zone in NW India: Journal of Metamorphic Geology, v. 29, p. 875–900, doi:10.1111/j.1525-1314.2011.00945.x.

Hawkesworth, C.J., and Kemp, A.I.S., 2006, Evolution of the continental crust: Nature, v. 443, p. 811–817, doi:10.1038/nature05191.

Healy, B., Collins, W.J., and Richards, S.W., 2004, A hybrid origin for Lachlan S-type granites: The Murrumbidgee batholith example: Lithos, v. 78, p. 197–216, doi:10.1016/j.lithos.2004.04.047.

Hermann, J., and Rubatto, D., 2003, Relating zircon and monazite domains to garnet growth zones: Age and duration of granulite facies metamorphism in the Val Malenco lower crust: Journal of Metamorphic Geology, v. 21, p. 833–852, doi:10.1046/j.1525-1314.2003.00484.x.

Hinchey, A.M., and Carr, S.D., 2006, The S-type Ladybird leucogranite suite of southeastern British Columbia: Geochemical and isotopic evidence for a genetic link with migmatite formation in the North American basement gneisses of the Monashee complex: Lithos, v. 90, p. 223–248, doi:10.1016/j.lithos.2006.03.003.

Hobbs, B.E., and Ord, A., 2010, The mechanics of granitoid systems and maximum entropy production rates: Philosophical Transactions of The Royal Society, ser. A, v. 368, p. 53–93, doi:10.1098/rsta.2009.0202.

Hogan, J.P., and Sinha, A.K., 1991, The effect of accessory minerals on the redistribution of lead isotopes during crustal anatexis: A model: Geochimica et Cosmochimica Acta, v. 55, p. 335–348, doi:10.1016/0016-7037(91)90422-2.

Holk, G.J., and Taylor, H.P., 2000, Water as a petrologic catalyst driving $^{18}O/^{16}O$ homogenization and anatexis of the middle crust in the metamorphic core complexes of British Columbia: International Geology Review, v. 42, p. 97–130, doi:10.1080/00206810009465072.

Holland, T.J.B., and Powell, R., 1998, An internally consistent thermodynamic data set for phases of petrological interest: Journal of Metamorphic Geology, v. 16, p. 309–343, doi:10.1111/j.1525-1314.1998.00140.x.

Holness, M.B., and Sawyer, E.W., 2008, On the pseudomorphing of melt-filled pores during the crystallization of migmatites: Journal of Petrology, v. 49, p. 1343–1363.

Huppert, H.E., and Sparks, R.S.J., 1988, The generation of granitic magmas by intrusion of basalt into continental crust: Journal of Petrology, v. 29, p. 599–624, doi:10.1093/petrology/29.3.599.

Hutton, D.H.W., 1982, A tectonic model for the emplacement of the Main Donegal Granite, NW Ireland: Journal of the Geological Society of London, v. 139, p. 615–631, doi:10.1144/gsjgs.139.5.0615.

Hutton, D.H.W., 1988a, Granite emplacement mechanisms and tectonic controls: Inferences from deformation studies: Transactions of the Royal Society of Edinburgh–Earth Sciences, v. 79, p. 245–255, doi:10.1017/S0263593300014255.

Hutton, D.H.W., 1988b, Igneous emplacement in a shear zone termination: The biotite granite at Strontian, Scotland: Geological Society of America Bulletin, v. 100, p. 1392–1399.

Hutton, D.H.W., and Reavy, R.J., 1992, Strike-slip tectonics and granite petrogenesis: Tectonics, v. 11, p. 960–967, doi:10.1029/92TC00336.

Hutton, D.H.W., Dempster, T.J., Brown, P.E., and Becker, S.D., 1990, A new mechanism of granite emplacement: Intrusion in active extensional shear zones: Nature, v. 343, p. 452–455, doi:10.1038/343452a0.

Ingram, G.M., and Hutton, D.H.W., 1994, The Great Tonalite sill: Emplacement into a contractional shear zone and implications for Late Cretaceous to early Eocene tectonics in southeastern Alaska and British Columbia: Geological Society of America Bulletin, v. 106, p. 715–728, doi:10.1130/0016-7606(1994)106<0715:TGTSEI>2.3.CO;2.

Ito, G., and Martel, S.J., 2002, Focusing of magma in the upper mantle through dike interaction: Journal of Geophysical Research–Solid Earth, v. 107, 2223, doi:10.1029/2001JB000251.

Jackson, M.D., Cheadle, M.J., and Atherton, M.P., 2003, Quantitative modeling of granitic melt generation and segregation in the continental crust: Journal of Geophysical Research–Solid Earth, v. 108, 2332, doi:10.1029/2001JB001050.

Jackson, M.D., Gallagher, K., Petford, N., and Cheadle, M.J., 2005, Towards a coupled physical and chemical model for tonalite-trondhjemite-granodiorite magma formation: Lithos, v. 79, p. 43–60, doi:10.1016/j.lithos.2004.05.004.

Jackson, M.P.A., and Vendeville, B.C., 1994, Regional extension as a geologic trigger for diapirism: Geological Society of America Bulletin, v. 106, p. 57–73, doi:10.1130/0016-7606(1994)106<0057:REAAGT>2.3.CO;2.

Jahn, B.-M., Wu, F., and Chen, B., 2000, Granitoids of the Central Asian orogenic belt and continental growth in the Phanerozoic: Transactions of the Royal Society of Edinburgh–Earth Sciences, v. 91, p. 181–193, doi:10.1017/S0263593300007367.

Jeon, H., Williams, I.S., and Chappell, B.W., 2012, Magma to mud to magma: Rapid crustal recycling by Permian granite magmatism near the eastern Gondwana margin: Earth and Planetary Science Letters, v. 319–320, p. 104–117, doi:10.1016/j.epsl.2011.12.010.

Johannes, W., 1984, Beginning of melting in the granite system Qz-Ab-Or-An-H_2O: Contributions to Mineralogy and Petrology, v. 86, p. 264–273, doi:10.1007/BF00373672.

Johnson, T.E., and Brown, M., 2004, Quantitative constraints on metamorphism in the Variscides of southern Brittany—A complementary pseudosection approach: Journal of Petrology, v. 45, p. 1237–1259, doi:10.1093/petrology/egh012.

Johnson, T.E., Hudson, N.F.C., and Droop, G.T.R., 2001, Melt segregation structures within the Inzie Head gneisses of the northeastern Dalradian: Scottish Journal of Geology, v. 37, p. 59–72, doi:10.1144/sjg37020059.

Johnson, T.E., Brown, M., and Solar, G.S., 2003a, Low-pressure subsolidus and suprasolidus phase equilibria in the MnNCKFMASH system: Constraints on conditions of regional metamorphism in western Maine, Northern Appalachians: The American Mineralogist, v. 88, p. 624–638.

Johnson, T.E., Gibson, R.L., Brown, M., Buick, I., and Cartwright, I., 2003b, Partial melting of metapelitic rocks beneath the Bushveld Complex, South Africa: Journal of Petrology, v. 44, p. 789–813, doi:10.1093/petrology/44.5.789.

Johnson, T.E., Hudson, N.F.C., and Droop, G.T.R., 2003c, Evidence for a genetic granite-migmatite link in the Dalradian of NE Scotland: Journal of the Geological Society of London, v. 160, p. 447–457, doi:10.1144/0016-764902-069.

Johnson, T.E., Brown, M., Gibson, R., and Wing, B., 2004, Spinel-cordierite symplectites replacing andalusite: Evidence for melt-assisted diapirism in the Bushveld Complex, South Africa: Journal of Metamorphic Geology, v. 22, p. 529–545, doi:10.1111/j.1525-1314.2004.00531.x.

Johnson, T.E., White, R.W., and Powell, R., 2008, Partial melting of metagreywacke: A calculated mineral equilibria study: Journal of Metamorphic Geology, v. 26, p. 837–853, doi:10.1111/j.1525-1314.2008.00790.x.

Johnson, T.E., Brown, M., and White, R.W., 2010, Petrogenetic modelling of strongly residual metapelitic xenoliths within the southern Platreef, Bushveld Complex, South Africa: Journal of Metamorphic Geology, v. 28, p. 269–291, doi:10.1111/j.1525-1314.2010.00868.x.

Johnson, T.E., White, R.W., and Brown, M., 2011, A year in the life of an aluminous metapelite xenolith—The role of heating rates, reaction overstep, H_2O retention and melt loss: Lithos, v. 124, p. 132–143, doi:10.1016/j.lithos.2010.08.009.

Johnson, T.E., Fischer, S., White, R., Brown, M., and Rollinson, H., 2012, Intracrustal differentiation from partial melting of metagabbro—Field and geochemical evidence from the central region of the Neoarchaean Lewisian Complex, NW Scotland: Journal of Petrology, v. 53, p. 2115–2138, doi:10.1093/petrology/egs046.

Jones, K.A., and Brown, M., 1990, High temperature 'clockwise' *P-T* paths and melting in the development of regional migmatites: An example from southern Brittany, France: Journal of Metamorphic Geology, v. 8, p. 551–578, doi:10.1111/j.1525-1314.1990.tb00486.x.

Jung, S., 2005, Isotopic equilibrium/disequilibrium in granites, metasedimentary rocks and migmatites (Damara orogen, Namibia)—A consequence of polymetamorphism and melting: Lithos, v. 84, p. 168–184, doi:10.1016/j.lithos.2005.03.013.

Keay, S., Collins, W.J., and McCulloch, M.T., 1997, A three-component Sr-Nd isotopic mixing model for granitoid genesis, Lachlan fold belt, eastern Australia: Geology, v. 25, p. 307–310, doi:10.1130/0091-7613(1997)025<0307:ATCSNI>2.3.CO;2.

Kelly, N.M., Clarke, G.L., and Harley, S.L., 2005, Monazite behaviour and age significance in poly-metamorphic high-grade terrains: A case study from the western Musgrave block, central Australia: Lithos, v. 88, p. 100–134, doi:10.1016/j.lithos.2005.08.007.

Kelsey, D.E., and Powell, R., 2011, Progress in linking accessory mineral growth and breakdown to major mineral evolution in metamorphic rocks: A thermodynamic approach in the Na_2O-CaO-K_2O-FeO-MgO-Al_2O_3-SiO_2-H_2O-TiO_2-ZrO_2 system: Journal of Metamorphic Geology, v. 29, p. 151–166, doi:10.1111/j.1525-1314.2010.00910.x.

Kelsey, D.E., Clark, C., and Hand, M., 2008, Thermobarometric modelling of zircon and monazite growth in melt-bearing systems: Examples using model metapelitic and metapsammitic granulites: Journal of Metamorphic Geology, v. 26, p. 199–212, doi:10.1111/j.1525-1314.2007.00757.x.

Kemp, A.I.S., Wormald, R.J., Whitehouse, M.J., and Price, R.C., 2005, Hf isotopes in zircon reveal contrasting sources and crystallization histories for alkaline to peralkaline granites of Temora, southeastern Australia: Geology, v. 33, p. 797–800, doi:10.1130/G21706.1.

Kemp, A.I.S., Hawkesworth, C.J., Foster, G.L., Paterson, B.A., Woodhead, J.D., Hergt, J.M., Gray, C.M., and Whitehouse, M.J., 2007, Magmatic and crustal differentiation history of granitic rocks from Hf-O isotopes in zircon: Science, v. 315, p. 980–983, doi:10.1126/science.1136154.

Kemp, A.I.S., Hawkesworth, C.J., Collins, W.J., Gray, C.M., and Blevin, P.L., 2009, Isotopic evidence for rapid continental growth in an extensional accretionary orogen: The Tasmanides, eastern Australia: Earth and Planetary Science Letters, v. 284, p. 455–466, doi:10.1016/j.epsl.2009.05.011.

Kilpatrick, J.A., and Ellis, D.J., 1992, C-type magmas: Igneous charnockites and their extrusive equivalents: Transactions of the Royal Society of Edinburgh–Earth Sciences, v. 83, p. 155–164, doi:10.1017/S0263593300007847.

Kisters, A.F.M., Ward, R.A., Anthonissen, C.J., and Vietze, M.E., 2009, Melt segregation and far-field melt transfer in the mid-crust: Journal of the Geological Society of London, v. 166, p. 905–918, doi:10.1144/0016-76492009-012.

Koester, E., Pawley, A.R., Fernandes, L.A.D., Porcher, C.C., and Soliani, E., Jr., 2002, Experimental melting of cordierite gneiss and the petrogenesis of syntranscurrent peraluminous granites in southern Brazil: Journal of Petrology, v. 43, p. 1595–1616, doi:10.1093/petrology/43.8.1595.

Korhonen, F.J., Saito, S., Brown, M., and Siddoway, C.S., 2010a, Modeling multiple melt loss events in the evolution of an active continental margin: Lithos, v. 116, p. 230–248, doi:10.1016/j.lithos.2009.09.004.

Korhonen, F.J., Saito, S., Brown, M., and Siddoway, C.S., 2010b, Multiple generations of granite in the Fosdick Mountains, Marie Byrd Land, West Antarctica: Implications for polyphase intracrustal differentiation in a continental margin setting: Journal of Petrology, v. 51, p. 627–670, doi:10.1093/petrology/egp093.

Korhonen, F.J., Brown, M., Grove, M., Siddoway, C.S., Baxter, E.F., and Inglis, J.D., 2012, Placing constraints on the timing of melting and melt loss events during polymetamorphism in the Fosdick migmatite-granite complex, West Antarctica: Journal of Metamorphic Geology, v. 30, p. 165–192, doi:10.1111/j.1525-1314.2011.00961.x.

Korhonen, F.J., Clark, C., Brown, M., Bhattacharya, S. and Taylor, R., 2013, Long-lived ultrahigh temperature (UHT) metamorphism in the Eastern Ghats orogenic belt, India: Constraints from zircon and monazite geochronology: Precambrian Research, doi:10.1016/j.precamres.2012.12.001 (in press).

Koukouvelas, I.K., Pe-Piper, G., and Piper, D.J.W., 2006, The relationship between length and width of plutons within the crustal-scale Cobequid shear zone, Northern Appalachians, Canada: International Journal of Earth Sciences, v. 95, p. 963–976, doi:10.1007/s00531-006-0077-7.

Lackey, J.S., Valley, J.W., Chen, J.H., and Stockli, D.F., 2008, Dynamic magma systems, crustal recycling, and alteration in the central Sierra Nevada batholith: The oxygen isotope record: Journal of Petrology, v. 49, p. 1397–1426.

Lagarde, J.L., Brun, J.P., and Gapais, D., 1990, Formation of epizonal granitic plutons by in situ assemblage of laterally expanding magma: Comptes Rendus de l'Academies des Sciences, Serie II, v. 310, p. 109–114.

Laporte, D., Rapaille, C., and Provost, A., 1997, Wetting angles, equilibrium melt geometry, and the permeability threshold of partially molten crustal protoliths, *in* Bouchez, J.L., Hutton, D.H.W., and Stephens, W.E. eds., Granite: From Segregation of Melt to Emplacement Fabrics: Dordrecht, The Netherlands, Kluwer Academic Publishers, p. 31–54.

Lavaure, S., and Sawyer, E.W., 2011, Source of biotite in the Wuluma pluton: Replacement of ferromagnesian phases and disaggregation of enclaves and schlieren: Lithos, v. 125, p. 757–780, doi:10.1016/j.lithos.2011.04.005.

Le Breton, N., and Thompson, A.B., 1988, Fluid-absent (dehydration) melting of biotite in metapelites in the early stages of crustal anatexis: Contributions to Mineralogy and Petrology, v. 99, p. 226–237, doi:10.1007/BF00371463.

Leitch, A.M., and Weinberg, R.F., 2002, Modelling granite migration by mesoscale pervasive flow: Earth and Planetary Science Letters, v. 200, p. 131–146, doi:10.1016/S0012-821X(02)00596-4.

Lister, J.R., and Kerr, R.C., 1991, Fluid-mechanical models of crack propagation and their application to magma transport in dykes: Journal of Geophysical Research, v. 96, p. 10,049–10,077, doi:10.1029/91JB00600.

Loiselle, M.C., and Wones, D.S., 1979, Characteristics and origin of anorogenic granites: Geological Society of America Abstracts with Programs, v. 11, no. 7, p. 468.

Lucas, S.B., and St. Onge, M.R., 1995, Syn-tectonic magmatism and the development of compositional layering, Ungava orogen (northern Quebec, Canada): Journal of Structural Geology, v. 17, p. 475–491, doi:10.1016/0191-8141(94)00076-C.

Luth, W.C., Jahns, F.H., and Tuttle, O.F., 1964, The granite system at pressures of 4 to 10 kilobars: Journal of Geophysical Research, v. 69, p. 759–773, doi:10.1029/JZ069i004p00759.

Maaløe, S., 1992, Melting and diffusion processes in closed-system migmatization: Journal of Metamorphic Geology, v. 10, p. 503–516, doi:10.1111/j.1525-1314.1992.tb00101.x.

Maaløe, S., and Wyllie, P.J., 1975, Water content of a granite magma deduced from the sequence of crystallization determined experimentally with water-undersaturated conditions: Contributions to Mineralogy and Petrology, v. 52, p. 175–191, doi:10.1007/BF00457293.

Mahan, K.H., Bartley, J.M., Coleman, D.S., Glazner, A.F., and Carl, B.S., 2003, Sheeted intrusion of the synkinematic McDoogle pluton, Sierra Nevada, California: Geological Society of America Bulletin, v. 115, p. 1570–1582, doi:10.1130/B22083.1.

Marchildon, N., and Brown, M., 2001, Melt segregation in late syn-tectonic anatectic migmatites: An example from the Onawa contact aureole, Maine, U.S.A.: Physics and Chemistry of the Earth, v. 26, p. 225–229, doi:10.1016/S1464-1895(01)00049-7.

Marchildon, N., and Brown, M., 2002, Grain-scale melt distribution in two contact aureole rocks: Implication for controls on melt localization and deformation: Journal of Metamorphic Geology, v. 20, p. 381–396, doi:10.1046/j.1525-1314.2002.00376.x.

Marchildon, N., and Brown, M., 2003, Spatial distribution of melt-bearing structures in anatectic rocks from southern Brittany: Implications for melt-transfer at grain- to orogen-scale: Tectonophysics, v. 364, p. 215–235, doi:10.1016/S0040-1951(03)00061-1.

Marcotte, S.B., Klepeis, K.A., Clarke, G.L., Gehrels, G., and Hollis, J.A., 2005, Intra-arc transpression in the lower crust and its relationship to magmatism in a Mesozoic magmatic arc: Tectonophysics, v. 407, p. 135–163, doi:10.1016/j.tecto.2005.07.007.

Matzel, J.E.P., Bowring, S.A., and Miller, R.B., 2004, Protolith age of the Swakane Gneiss, North Cascades, Washington: Evidence of rapid underthrusting of sediments beneath an arc: Tectonics, v. 23, TC6009, doi:10.1029/2003TC001577.

Matzel, J.E.P., Mundil, R., Paterson, S., Renne, P., and Nomade, S., 2005, Evaluating pluton growth models using high resolution geochronology: Tuolumne intrusive suite, Sierra Nevada, CA: Geological Society of America Abstracts with Programs, v. 37, no. 6, p. 131.

Matzel, J.E.P., Bowring, S.A., and Miller, R.B., 2006, Time scales of pluton construction at differing crustal levels: Examples from the Mount Stuart and Tenpeak intrusions, North Cascades, Washington: Geological Society of America Bulletin, v. 118, p. 1412–1430.

McCaffrey, K.J.W., and Cruden, A.R., 2002, Dimensional data and growth models for intrusions, *in* Breitkreuz, C., Mock, A., and Petford, N., eds., First International Workshop: Physical Geology of Subvolcanic Systems—Laccoliths, Sills and Dikes (LASI): Freiberg, Germany, Wissenschaftliche Mitteilung Instute für Geologie Technische Universität Bergakademie Freiberg, 20/2002, p. 37–39.

McCaffrey, K.J.W., and Petford, N., 1997, Are granitic intrusions scale invariant?: Journal of the Geological Society of London, v. 154, p. 1–4, doi:10.1144/gsjgs.154.1.0001.

McCulloch, M.T., and Chappell, B.W., 1982, Nd isotopic characteristics of S- and I-type granites: Earth and Planetary Science Letters, v. 58, p. 51–64, doi:10.1016/0012-821X(82)90102-9.

McLeod, C.L., Davidson, J.P., Nowell, G.M., and de Silva, S.L., 2012, Disequilibrium melting during crustal anatexis and implications for modeling open magmatic systems: Geology, v. 40, p. 435–438, doi:10.1130/G33000.1.

Miller, C.F., McDowell, S.M., and Mapes, R.W., 2003, Hot and cold granites? Implications of zircon saturation temperatures and preservation of inheritance: Geology, v. 31, p. 529–532, doi:10.1130/0091-7613(2003)031<0529:HACGIO>2.0.CO;2.

Miller, J.S., 2008, Assembling a pluton…one increment at a time: Geology, v. 36, p. 511–512, doi:10.1130/focus062008.1.

Miller, J.S., Matzel, J.E.P., Miller, C.F., Burgess, S.D., and Miller, R.B., 2007, Zircon growth and recycling during the assembly of large, composite arc plutons: Journal of Volcanology and Geothermal Research, v. 167, p. 282–299, doi:10.1016/j.jvolgeores.2007.04.019.

Miller, R.B., and Paterson, S.R., 1999, In defense of magmatic diapirs: Journal of Structural Geology, v. 21, p. 1161–1173.

Miller, R.B., and Paterson, S.R., 2001, Construction of mid-crustal sheeted plutons: Examples from the North Cascades, Washington: Geological Society of America Bulletin, v. 113, p. 1423–1442.

Milord, I., Sawyer, E.W., and Brown, M., 2001, Formation of diatexite migmatite and granite magma during anatexis of semipelitic metasedimentary rocks: An example from St. Malo, France: Journal of Petrology, v. 42, p. 487–505, doi:10.1093/petrology/42.3.487.

Montel, J.M., 1993, A model for monazite/melt equilibrium and application to the generation of granitic magmas: Chemical Geology, v. 110, p. 127–146, doi:10.1016/0009-2541(93)90250-M.

Montel, J.M., and Vielzeuf, D., 1997, Partial melting of metagreywackes: 2. Compositions of minerals and melts: Contributions to Mineralogy and Petrology, v. 128, p. 176–196, doi:10.1007/s004100050302.

Montero, P., Bea, F., Zinger, T.F., Scarrow, J.H., Molina, J.F., and Whitehouse, M., 2004, 55 million years of continuous anatexis in Central Iberia: Single-zircon dating of the Pena Negra Complex: Journal of the Geological Society of London, v. 161, p. 255–263, doi:10.1144/0016-764903-024.

Morfin, S., Sawyer, E., and Bandyayera, D., 2013, Large volumes of anatectic melt retained in granulite facies migmatites: An injection complex in northern Quebec: Lithos, v. 168–169, p. 200–218.

Nagel, T.J., Hoffmann, J.E., and Münker, C., 2012, Generation of Eoarchean tonalite-trondhjemite-granodiorite series from thickened mafic arc crust: Geology, v. 40, p. 375–378, doi:10.1130/G32729.1.

Nemchin, A., and Bodorkos, S., 2000, Zr and LREE concentrations in anatectic melt as a function of crystal size distributions of zircon and monazite in the source region: Geological Society of America Abstracts and Programs, abstract no. 52286.

Oliver, N.H.S., and Barr, T.D., 1997, The geometry and evolution of magma pathways through migmatites of the Halls Creek orogen, Western Australia: Mineralogical Magazine, v. 61, p. 3–14, doi:10.1180/minmag.1997.061.404.02.

Olsen, S.N., Marsh, B.D., and Baumgartner, L.P., 2004, Modelling mid-crustal migmatite terrains as feeder zones for granite plutons: The competing dynamics of melt transfer by bulk versus porous flow: Transactions of the Royal Society of Edinburgh–Earth Sciences, v. 95, p. 49–58, doi:10.1017/S0263593300000912.

Paterson, S.R., and Fowler, T.K., Jr., 1993, Re-examining pluton emplacement processes: Journal of Structural Geology, v. 15, p. 191–206, doi:10.1016/0191-8141(93)90095-R.

Paterson, S.R., and Miller, R.B., 1998, Mid-crustal magmatic sheets in the Cascades Mountains, Washington: Implications for magma ascent: Journal of Structural Geology, v. 20, p. 1345–1363, doi:10.1016/S0191-8141(98)00072-8.

Paterson, S.R., and Vernon, R.H., 1995, Bursting the bubble of ballooning plutons: A return to nested diapirs emplaced by multiple processes: Geological Society of America Bulletin, v. 107, p. 1356–1380.

Paterson, S.R., Pignotta, G.S., Farris, D., Memeti, V., Miller, R.B., Vernon, R.H., and Žák, J., 2008, Is stoping a volumetrically significant pluton emplacement process?: Geological Society of America Bulletin, v. 120, p. 1075–1079, doi:10.1130/B26148.1.

Patiño Douce, A.E., 1997, Generation of metaluminous A-type granites by low-pressure melting of calc-alkaline granitoids: Geology, v. 25, p. 743–746, doi:10.1130/0091-7613(1997)025<0743:GOMATG>2.3.CO;2.

Patiño Douce, A.E., 1999, What do experiments tell us about the relative contributions of crust and mantle to the

origin of granitic magmas?, *in* Castro, A., Fernandez, C., and Vigneresse, J.L., eds., Understanding Granites: Integrating New and Classical Techniques: Geological Society of London Special Publication 168, p. 77–94.

Patiño Douce, A.E., and Beard, J.S., 1995, Dehydration-melting of biotite gneiss and quartz amphibolite from 3 to 15 kbar: Journal of Petrology, v. 36, p. 707–738, doi:10.1093/petrology/36.3.707.

Patiño Douce, A.E., and Harris, N., 1998, Experimental constraints on Himalayan anatexis: Journal of Petrology, v. 39, p. 689–710, doi:10.1093/petroj/39.4.689.

Patiño Douce, A.E., and Johnston, A.D., 1991, Phase equilibria and melt productivity in the pelitic system: Implications for the origin of peraluminous granitoids and aluminous granulites: Contributions to Mineralogy and Petrology, v. 107, p. 202–218, doi:10.1007/BF00310707.

Pattison, D.R.M., and Harte, B., 1988, Evolution of structurally contrasting anatectic migmatites in the 3-kbar Ballachulish aureole, Scotland: Journal of Metamorphic Geology, v. 6, p. 475–494, doi:10.1111/j.1525-1314.1988.tb00435.x.

Perini, G., Cesare, B., Gómez-Pugnaire, M.T., Ghezzi, L., and Tommasini, S., 2009, Armouring effect on Sr-Nd isotope during disequilibrium crustal melting: The case study of frozen migmatites from El Hoyazo and Mazarrón, SE Spain: European Journal of Mineralogy, v. 21, p. 117–131, doi:10.1127/0935-1221/2009/0021-1882.

Petford, N., 1995, Segregation of tonalitic-trondhjemitic melts in the continental crust: The mantle connection: Journal of Geophysical Research, v. 100, p. 15,735–15,743, doi:10.1029/94JB03259.

Petford, N., 1996, Dykes or diapirs?: Transactions of the Royal Society of Edinburgh–Earth Sciences, v. 87, p. 105–114, doi:10.1017/S0263593300006520.

Petford, N., and Gallagher, K., 2001, Partial melting of mafic (amphibolitic) lower crust by periodic influx of basaltic magma: Earth and Planetary Science Letters, v. 193, p. 483–499, doi:10.1016/S0012-821X(01)00481-2.

Petford, N., and Koenders, M.A., 1998, Self-organization and fracture connectivity in rapidly heated continental crust: Journal of Structural Geology, v. 20, p. 1425–1434, doi:10.1016/S0191-8141(98)00081-9.

Petford, N., Kerr, R.C., and Lister, J.R., 1993, Dike transport of granitoid magmas: Geology, v. 21, p. 845–848, doi:10.1130/0091-7613(1993)021<0845:DTOGM>2.3.CO;2.

Petford, N., Cruden, A.R., McCaffrey, K.J.W., and Vigneresse, J.L., 2000, Granite magma formation, transport and emplacement in the Earth's crust: Nature, v. 408, p. 669–673, doi:10.1038/35047000.

Petrini, K., and Podladchikov, Y.Y., 2000, Lithospheric pressure-depth relationship in compressive regions of thickened crust: Journal of Metamorphic Geology, v. 18, p. 67–77, doi:10.1046/j.1525-1314.2000.00240.x.

Powell, R., and Downes, J., 1990, Garnet porphyroblast-bearing leucosomes in metapelites: Mechanisms, phase diagrams and an example from Broken Hill, *in* Ashworth, J.R., and Brown, M., eds., High Temperature Metamorphism and Crustal Anatexis: London, Unwin Hyman, p. 105–123.

Presnall, D.C., and Bateman, P.C., 1973, Fusion relations in the system $NaAlSi_3O_8$–$CaAl_2Si_2O_8$–$KAlSi_3O_8$–SiO_2–H_2O and generation of granitic magmas in the Sierra Nevada batholith: Geological Society of America Bulletin, v. 84, p. 3181–3202, doi:10.1130/0016-7606(1973)84<3181:FRITSN>2.0.CO;2.

Pressley, R.A., and Brown, M., 1999, The Phillips pluton, Maine, USA: Evidence of heterogeneous crustal sources, and implications for granite ascent and emplacement mechanisms in convergent orogens: Lithos, v. 46, p. 335–366, doi:10.1016/S0024-4937(98)00073-5.

Pyle, J.M., Spear, F.S., Rudnick, R.L., and McDonough, W.F., 2001, Monazite-xenotime-garnet equilibrium in metapelites and the new monazite-garnet thermometer: Journal of Petrology, v. 42, p. 2083–2107.

Rabinowicz, M., and Vigneresse, J.L., 2004, Melt segregation under compaction and shear channeling: Application to granitic magma segregation in a continental crust: Journal of Geophysical Research, v. 109, p. B04407, doi:10.1029/2002JB002372.

Ramsay, J.G., 1989, Emplacement kinematics of a granite diapir: The Chindamora batholith, Zimbabwe: Journal of Structural Geology, v. 11, p. 191–209, doi:10.1016/0191-8141(89)90043-6.

Rapp, R., and Watson, E.B., 1986, Monazite solubility and dissolution kinetics—Implications for the thorium and light rare-earth chemistry of felsic magmas: Contributions to Mineralogy and Petrology, v. 94, p. 304–316, doi:10.1007/BF00371439.

Rapp, R., Watson, E.B., and Miller, C.F., 1991, Partial melting of amphibolite/eclogite and the origin of Archean trondhjemites and tonalities: Precambrian Research, v. 51, p. 1–25, doi:10.1016/0301-9268(91)90092-O.

Read, H.H., 1948a, Granites and granites, *in* Gilluly, J., ed., Origin of Granite: Geological Society of America Memoir 28, p. 1–19.

Read, H.H., 1948b, A commentary on place in plutonism: Quarterly Journal of the Geological Society of London, v. 104, p. 155–205, doi:10.1144/GSL.JGS.1948.104.01-04.08.

Read, H.H., 1949, A commentary of time in plutonism: Quarterly Journal of the Geological Society of London, v. 105, p. 101–156, doi:10.1144/GSL.JGS.1949.105.01-04.06.

Reichardt, H., and Weinberg, R.F., 2012a, The dike swarm of the Karakoram shear zone, Ladakh, NW India: Linking granite source to batholith: Geological Society of America Bulletin, v. 124, p. 89–103, doi:10.1130/B30394.1.

Reichardt, H., and Weinberg, R.F., 2012b, Hornblende chemistry in meta- and diatexites and its retention in the source of leucogranites: An example from the Karakoram shear zone, NW India: Journal of Petrology, v. 53, p. 1287–1318, doi:10.1093/petrology/egs017.

Reichardt, H., Weinberg, R.F., Andersson, U.B., and Fanning, C.M., 2010, Hybridization of granitic magmas in the source: The origin of the Karakoram batholith, Ladakh, NW India: Lithos, v. 116, p. 249–272, doi:10.1016/j.lithos.2009.11.013.

Reid, M.R., 1990, Ion probe investigation of rare earth element distributions and partial melting of metasedimentary granulite, *in* Vielzeuf, D., and Vidal, P., eds., Granulites and Crustal Evolution: NATO ASI Series C: Mathematical and Physical Sciences, Volume 311: Dordrecht, Netherlands, Kluwer Academic Publishers, p. 507–522.

Reno, B.L., Brown, M., Kobayashi, O.T., Nakamura, E., Piccoli, P.M., and Trouw, R.A.J., 2009, Eclogite–high-pressure granulite metamorphism records early collision in West Gondwana: New data from the southern Brasília belt, Brazil: Journal of the Geological Society of London, v. 166, p. 1013–1032, doi:10.1144/0016-76492008-140.

Reno, B.L., Piccoli, P.M., Brown, M., and Trouw, R., 2012, In situ chemical dating of monazite from the southern Brazília belt, Brazil: Journal of Metamorphic Geology, v. 30, p. 81–112, doi:10.1111/j.1525-1314.2011.00957.x.

Roberts, M.P., and Finger, F., 1997, Do U-Pb zircon ages from granulites reflect peak metamorphic conditions?: Geology, v. 25, p. 319–322, doi:10.1130/0091-7613(1997)025<0319:DUPZAF>2.3.CO;2.

Rosenberg, C.L., 2004, Shear zones and magma ascent: A model based on a review of the Tertiary magmatism in the Alps: Tectonics, v. 23, TC3002, doi:10.1029/2003TC001526.

Rosenberg, C.L., and Handy, M.R., 2005, Experimental deformation of partially melted granite revisited: Implications for the continental crust: Journal of Metamorphic Geology, v. 23, p. 19–28, doi:10.1111/j.1525-1314.2005.00555.x.

Rubatto, D., Williams, I.S., and Buick, I.S., 2001, Zircon and monazite response to prograde metamorphism in the Reynolds Range, central Australia: Contributions to Mineralogy and Petrology, v. 140, p. 458–468, doi:10.1007/PL00007673.

Rubatto, D., Herman, J., Berger, A., and Engi, M., 2009, Protracted fluid-induced melting during Barrovian metamorphism in the central Alps: Contributions to Mineralogy and Petrology, v. 158, p. 703–722, doi:10.1007/s00410-009-0406-5.

Rubatto, D., Chakraborty, S., and Dasgupta, S., 2013, Timescales of crustal melting in the Higher Himalayan Crystallines (Sikkim, Eastern Himalaya) inferred from trace element–constrained monazite and zircon chronology: Contributions to Mineralogy and Petrology, v. 165, p. 349–372, doi:10.1007/s00410-012-0812-y.

Rubin, A.M., 1998, Dike ascent in partially molten rock: Journal of Geophysical Research–Solid Earth, v. 103, p. 20,901–20,919, doi:10.1029/98JB01349.

Rudnick, R.L., and Gao, S., 2003, The composition of the continental crust, *in* Rudnick, R.L., ed., The Crust Volume 3, Treatise on Geochemistry: Oxford, UK, Elsevier-Pergamon, p. 1–64.

Rushmer, T., 1991, Partial melting of two amphibolites: Contrasting experimental results under fluid-absent conditions: Contributions to Mineralogy and Petrology, v. 107, p. 41–59, doi:10.1007/BF00311184.

Rutter, E.H., 1997, The influence of deformation on the extraction of crustal melts: A consideration of the role of melt-assisted granular flow, *in* Holness, M.B., ed., Deformation-Enhanced Fluid Transport in the Earth's Crust and Mantle: London, Chapman and Hall, p. 82–110.

Rutter, E.H., and Mecklenburgh, J., 2006, The extraction of melt from crustal protoliths and the flow behavior of partially molten crustal rocks: An experimental perspective, *in* Brown, M., and Rushmer, T., eds., Evolution and Differentiation of the Continental Crust: Cambridge, UK, Cambridge University Press, p. 386–429.

Rutter, E.H., and Neumann, D.H.K., 1995, Experimental deformation of Westerly granite under fluid-absent conditions, with implications for the extraction of granitic magmas: Journal of Geophysical Research, v. 100, p. 15,697–15,715, doi:10.1029/94JB03388.

Saito, S., Arima, M., and Nakajima, T., 2007, Hybridization of a shallow 'I-type' granitoid pluton and its host migmatite by magma-chamber wall collapse: The Tokuwa pluton, central Japan: Journal of Petrology, v. 48, p. 79–111, doi:10.1093/petrology/egl055.

Sawyer, E.W., 1987, The role of partial melting and fractional crystallization in determining discordant migmatite leucosome compositions: Journal of Petrology, v. 28, p. 445–473, doi:10.1093/petrology/28.3.445.

Sawyer, E.W., 1991, Disequilibrium melting and the rate of melt residuum separation during migmatization of mafic rocks from the Grenville Front, Quebec: Journal of Petrology, v. 32, p. 701–738, doi:10.1093/petrology/32.4.701.

Sawyer, E.W., 1994, Melt segregation in the continental crust: Geology, v. 22, p. 1019–1022, doi:10.1130/0091-7613(1994)022<1019:MSITCC>2.3.CO;2.

Sawyer, E.W., 1998, Formation and evolution of granite magmas during crustal reworking: The significance of diatexites: Journal of Petrology, v. 39, p. 1147–1167.

Sawyer, E.W., 1999, Criteria for the recognition of partial melting: Physics and Chemistry of the Earth, ser. A, v. 24, p. 269–279.

Sawyer, E.W., 2001, Melt segregation in the continental crust: Distribution and movement of melt in anatectic rocks: Journal of Metamorphic Geology, v. 19, p. 291–309, doi:10.1046/j.0263-4929.2000.00312.x.

Sawyer, E.W., 2010, Migmatites formed by water-fluxed partial melting of a leucogranodiorite protolith: Microstructures in the residual rocks and source of the fluid: Lithos, v. 116, p. 273–286, doi:10.1016/j.lithos.2009.07.003.

Sawyer, E.W., Dombrowski, C., and Collins, W.J., 1999, Movement of melt during synchronous regional deformation and granulite-facies anatexis, an example from the Wuluma Hills, central Australia, *in* Castro, A., Fernandez, C., and Vigneresse, J.-C., eds., Understanding Granites: Integrating New and Classical Techniques: Geological Society of London Special Publication 168, p. 221–237.

Sawyer, E.W., Cesare, B., and Brown, M., 2011, When the continental crust melts: Elements, v. 7, p. 229–234, doi:10.2113/gselements.7.4.229.

Scaillet, B., Pichavant, M., and Roux, J., 1995, Experimental crystallization of leucogranite magmas: Journal of Petrology, v. 36, p. 663–705, doi:10.1093/petrology/36.3.663.

Schaltegger, U., Brack, P., Ovtcharova, M., Peytcheva, I., Schoene, B., Stracke, A., Marocchi, M., and Bargossi, G.M., 2009, Zircon and titanite recording 1.5 million years of magma accretion, crystallization and initial cooling in a composite pluton (southern Adamello batholith, northern Italy): Earth and Planetary Science Letters, v. 286, p. 208–218, doi:10.1016/j.epsl.2009.06.028.

Schulmann, K., Martelat, J., Ulrich, S., Lexa, O., Štípská, P., and Becker, J.K., 2008, Evolution of microstructure and melt topology in partially molten granitic mylonite: Implications for rheology of felsic middle crust: Journal of Geophysical Research, v. 113, B10406, doi:10.1029/2007JB005508.

Searle, M.P., Parrish, R.R., Hodges, K.V., Hurford, A.J., Ayres, M.W., and Whitehouse, M.J., 1997, Shisha Pangma leucogranite, south Tibetan Himalaya: Field relations, geochemistry, age, origin, and emplacement: The Journal of Geology, v. 105, p. 295–318, doi:10.1086/515924.

Sheldon, H.A., Barnicoat, A.C., and Ord, A., 2006, Numerical modelling of faulting and fluid flow in porous rocks: An approach based on critical state soil mechanics: Journal of Structural Geology, v. 28, p. 1468–1482, doi:10.1016/j.jsg.2006.03.039.

Skjerlie, K.P., and Johnston, A.D., 1992, Vapor-absent melting at 10 kbar of a biotite- and amphibole-bearing tonalitic gneiss: Implications for the generation of A-type granites: Geology, v. 20, p. 263–266, doi:10.1130/0091-7613(1992)020<0263:VAMAKO>2.3.CO;2.

Slagstad, T., Jamieson, R.A., and Culshaw, N.G., 2005, Formation, crystallization, and migration of melt in the mid-orogenic crust: Muskoka domain migmatites, Grenville Province, Ontario: Journal of Petrology, v. 46, p. 893–919, doi:10.1093/petrology/egi004.

Solar, G.S., and Brown, M., 2001a, Petrogenesis of migmatites in Maine, USA: Possible source of peraluminous leucogranite in plutons: Journal of Petrology, v. 42, p. 789–823, doi:10.1093/petrology/42.4.789.

Solar, G.S., and Brown, M., 2001b, Deformation partitioning during transpression in response to Early Devonian oblique convergence, Northern Appalachian orogen, USA: Journal of Structural Geology, v. 23, p. 1043–1065.

Solar, G.S., Pressley, R.A., Brown, M., and Tucker, R.D., 1998, Granite ascent in convergent orogenic belts: Testing a model: Geology, v. 26, p. 711–714, doi:10.1130/0091-7613(1998)026<0711:GAICOB>2.3.CO;2.

Sparks, D.W., and Parmentier, E.M., 1991, Melt extraction from the mantle beneath spreading centers: Earth and Planetary Science Letters, v. 105, p. 368–377, doi:10.1016/0012-821X(91)90178-K.

Spear, F.S., Kohn, M.J., and Cheney, J.T., 1999, *P-T* paths from anatectic pelites: Contributions to Mineralogy and Petrology, v. 134, p. 17–32, doi:10.1007/s004100050466.

Stevens, G., Clemens, J.D., and Droop, G.T.R., 1997, Melt production during granulite-facies anatexis: Experimental data from 'primitive' metasedimentary protoliths: Contributions to Mineralogy and Petrology, v. 128, p. 352–370, doi:10.1007/s004100050314.

Stevens, G., Villaros, A., and Moyen, J.-F., 2007, Selective peritectic garnet entrainment as the origin of geochemical diversity in S-type granites: Geology, v. 35, p. 9–12, doi:10.1130/G22959A.1.

Stevenson, C.T.E., Owens, W.H., and Hutton, D.H.W., 2007, Flow lobes in granite: The determination of magma flow directions in the Trawenagh Bay Granite, northwestern Ireland, using anisotropy of magnetic susceptibility: Geological Society of America Bulletin, v. 119, p. 1368–1386, doi:10.1130/B25970.1.

Strong, D.F., and Hanmer, S.K., 1981, Peraluminous granites: Canadian Mineralogist, v. 19, p. 163–176.

Stüwe, K., and Sandiford, M., 1994, Contribution of deviatoric stresses to metamorphic *P-T* paths—An example appropriate to low-*P*, high-*T* metamorphism: Journal of Metamorphic Geology, v. 12, p. 445–454, doi:10.1111/j.1525-1314.1994.tb00034.x.

Stüwe, K., Sandiford, M., and Powell, R., 1993, Episodic metamorphism and deformation in low-pressure, high-temperature terranes: Geology, v. 21, p. 829–832, doi:10.1130/0091-7613(1993)021<0829:EMADIL>2.3.CO;2.

Sumita, I., and Ota, Y., 2011, Experiments on buoyancy-driven crack around the brittle-ductile transition: Earth and Planetary Science Letters, v. 304, p. 337–346, doi:10.1016/j.epsl.2011.01.032.

Symmes, G.H., and Ferry, J.M., 1995, Metamorphism, fluid-flow and partial melting in pelitic rocks from the Onawa contact aureole, central Maine, USA: Journal of Petrology, v. 36, p. 587–612, doi:10.1093/petrology/36.2.587.

Tanner, D.C., 1999, The scale-invariant nature of migmatites from the Oberpfalz, NE Bavaria, and its significance for melt transport: Tectonophysics, v. 302, p. 297–305, doi:10.1016/S0040-1951(98)00286-8.

Taylor, J., and Stevens, G., 2010, Selective entrainment of peritectic garnet into S-type granitic magmas: Evidence from Archaean mid-crustal anatectites: Lithos, v. 120, p. 277–292, doi:10.1016/j.lithos.2010.08.015.

Thompson, A.B., 1982, Dehydration melting of pelitic rocks and the generation of H_2O–undersaturated granitic liquids: American Journal of Science, v. 282, p. 1567–1595.

Thompson, A.B., and Algor, J.R., 1977, Model systems for anatexis of pelitic rocks: I. Theory of melting reactions in the system $KAlO_2$-$NaAlO_2$-Al_2O_3-SiO_2-H_2O: Contributions to Mineralogy and Petrology, v. 63, p. 247–269, doi:10.1007/BF00375575.

Thompson, A.B., and Connolly, J., 1995, Melting of the continental crust: Some thermal and petrological constraints on anatexis in continental collision zones and other tectonic settings: Journal of Geophysical Research, v. 100, no. B8, p. 15,565–15,579, doi:10.1029/95JB00191.

Thompson, A.B., and Tracy, R.J., 1979, Model systems for anatexis of pelitic rocks: 2. Facies series melting and reactions in the system CaO-$KAlO_2$-$NaAlO_2$-Al_2O_3-SiO_2-H_2O: Contributions to Mineralogy and Petrology, v. 70, p. 429–438, doi:10.1007/BF00371049.

Tomascak, P.B., Brown, M., Solar, G.S., Becker, H.J., Centorbi, T.L., and Tian, J., 2005, Source contributions to Devonian granite magmatism near the Laurentian border, New Hampshire and western Maine, USA: Lithos, v. 80, p. 75–99, doi:10.1016/j.lithos.2004.04.059.

Tommasini, S., and Davies, G.R., 1997, Isotope disequilibrium during anatexis: A case study of contact melting, Sierra Nevada, California: Earth and Planetary Science Letters, v. 148, p. 273–285, doi:10.1016/S0012-821X(97)00031-9.

Turner, S.P., Foden, J.D., and Morrison, R.S., 1992, Derivation of some A-type magmas by fractionation of basaltic magma—An example from the Padthaway Ridge, South Australia: Lithos, v. 28, p. 151–179, doi:10.1016/0024-4937(92)90029-X.

Turrillot, P., Faure, M., Martelet, G., Chen, Y., and Augier, R., 2011, Pluton-dyke relationships in a Variscan granitic complex from AMS and gravity modelling. Inception of the extensional tectonics in the South Armorican Domain (France): Journal of Structural Geology, v. 33, p. 1681–1698, doi:10.1016/j.jsg.2011.08.004.

Tuttle, O.F., and Bowen, N.L., 1958, Origin of granite in the light of experimental studies in the system: $NaAlSi_3O_8$–$KAlSi_3O_8$–SiO_2–H_2O: Geological Society of America Memoir 74, 153 p.

van der Molen, I., 1985, Interlayer material transport during layer-normal shortening: II. Boudinage, pinch-and-swell and migmatite at Søndre Strømfjord Airport, West Greenland: Tectonophysics, v. 115, p. 275–295, doi:10.1016/0040-1951(85)90142-8.

van der Molen, I., and Paterson, M.S., 1979, Experimental deformation of partially-melted granite: Contributions to Mineralogy and Petrology, v. 70, p. 299–318, doi:10.1007/BF00375359.

Vernon, R.H., 1984, Microgranitoid enclaves in granites—Globules of hybrid magma quenched in a plutonic environment: Nature, v. 309, p. 438–439, doi:10.1038/309438a0.

Vernon, R.H., 1990, Crystallization and hybridism in microgranitoid enclave magmas—Microstructural evidence: Journal of Geophysical Research–Solid Earth and Planets, v. 95, p. 17,849–17,859.

Vernon, R.H., 2007, Problems in identifying restite in S-type granites of southeastern Australia, with speculations on sources of magma and enclaves: Canadian Mineralogist, v. 45, p. 147–178, doi:10.2113/gscanmin.45.1.147.

Vernon, R.H., 2010, Granites really are magmatic: Using microstructural evidence to refute some obstinate hypotheses: Journal of the Virtual Explorer, v. 35, paper 1, doi:10.3809/jvirtex.2011.00264.

Vernon, R.H., and Paterson, S.R., 2001, Axial-surface leucosomes in anatectic migmatites: Tectonophysics, v. 335, p. 183–192, doi:10.1016/S0040-1951(01)00049-X.

Vernon, R.H., Etheridge, M.A., and Wall, V.J., 1988, Shape and microstructure of microgranitoid enclaves—Indicators of magma mingling and flow: Lithos, v. 22, p. 1–11, doi:10.1016/0024-4937(88)90024-2.

Vielzeuf, D., and Holloway, J.R., 1988, Experimental determination of the fluid-absent melting relations in the pelitic system—Consequences for crustal differentiation: Contributions to Mineralogy and Petrology, v. 98, p. 257–276, doi:10.1007/BF00375178.

Vielzeuf, D., and Montel, J.M., 1994, Partial melting of metagreywackes: 1. Fluid-absent experiments and phase-relationships: Contributions to Mineralogy and Petrology, v. 117, p. 375–393, doi:10.1007/BF00307272.

Vielzeuf, D., and Schmidt, M.W., 2001, Melting relations in hydrous systems revisited: Application to metapelites, metagreywackes and metabasalts: Contributions to Mineralogy and Petrology, v. 141, p. 251–267, doi:10.1007/s004100100237.

Vigneresse, J.-L., 1988, Shape and volume of granitic intrusions: Bulletin de la Société Géologique de France, v. 4, p. 897–906.

Vigneresse, J.-L., 1995, Crustal regime of deformation and ascent of granitic magma: Tectonophysics, v. 249, p. 187–202, doi:10.1016/0040-1951(95)00005-8.

Vigneresse, J.-L., 2004, Rheology of a two-phase material with applications to partially molten rocks, plastic deformation and saturated soils, *in* Alsop, G.I., Holdsworth, R.E., McCaffrey, K.J.W., and Hand, M., eds., Flow Processes in Faults and Shear Zones: Geological Society of London Special Publication 224, p. 79–94.

Vigneresse, J.-L., 2006, Granitic batholiths: From pervasive and continuous melting in the lower crust to discontinuous and spaced plutonism in the upper crust: Transactions of the Royal Society of Edinburgh–Earth Sciences, v. 97, p. 311–324, doi:10.1017/S0263593300001474.

Vigneresse, J.-L., Barbey, P., and Cuney, M., 1996, Rheological transitions during partial melting and crystallization with application to felsic magma segregation and transfer: Journal of Petrology, v. 37, p. 1579–1600.

Vigneresse, J.-L., Tikoff, B., and Ameglio, L., 1999, Modification of the regional stress field by magma intrusion and formation of tabular granitic plutons: Tectonophysics, v. 302, p. 203–224, doi:10.1016/S0040-1951(98)00285-6.

Villaros, A., Stevens, G., and Buick, I.S., 2009a, Tracking S-type granite from source to emplacement: Clues from garnet in the Cape Granite Suite: Lithos, v. 112, p. 217–235, doi:10.1016/j.lithos.2009.02.011.

Villaros, A., Stevens, G., Moyen, J.-F., and Buick, I.S., 2009b, The trace element compositions of S-type granites: Evidence for disequilibrium melting and accessory phase entrainment in the source: Contributions to Mineralogy and Petrology, v. 158, p. 543–561, doi:10.1007/s00410-009-0396-3.

Villaros, A., Buick, I.S., and Stevens, G., 2012, Isotopic variations in S-type granites: An inheritance from a heterogeneous source?: Contributions to Mineralogy and Petrology, v. 163, p. 243–257, doi:10.1007/s00410-011-0673-9.

Villaseca, C., Martín Romera, C., De La Rosa, J., and Barberp, L., 2003, Residence and redistribution of REE, Y, Zr, Th and U during granulite-facies metamorphism: Behaviour of accessory and major phases in peraluminous granulites of central Spain: Chemical Geology, v. 200, p. 293–323, doi:10.1016/S0009-2541(03)00200-6.

Villaseca, C., Orejana, D., and Paterson, B.A., 2007, Zr–LREE rich minerals in residual peraluminous granulites, another factor in the origin of low Zr–LREE granitic melts?: Lithos, v. 96, p. 375–386, doi:10.1016/j.lithos.2006.11.002.

Waff, H.S., and Faul, U.H., 1992, Effects of crystalline anisotropy on fluid distribution in ultramafic partial melts: Journal of Geophysical Research, v. 97, p. 9003–9014, doi:10.1029/92JB00066.

Wagner, R., Rosenberg, C., Handy, M.R., Möbus, C., and Albertz, M., 2006, Fracture-driven intrusion and upwelling of a mid-crustal pluton fed from a transpressive shear zone—The Rieserferner pluton (Eastern Alps): Geological Society of America Bulletin, v. 118, p. 219–237, doi:10.1130/B25842.1.

Wall, V.J., Clemens, J.D., and Clarke, D.B., 1987, Models for granitoid evolution and source compositions: The Journal of Geology, v. 95, p. 731–749, doi:10.1086/629174.

Walte, N.P., Bons, P.D., and Passchier, C.W., 2005, Deformation of melt-bearing systems—Insight from in situ

grain-scale analogue experiments: Journal of Structural Geology, v. 27, p. 1666–1679.
Ward, R., Stevens, G., and Kisters, A., 2008, Fluid and deformation induced partial melting and melt volumes in low-temperature granulite-facies metasediments, Damara Belt, Namibia: Lithos, v. 105, p. 253–271, doi:10.1016/j.lithos.2008.04.001.
Wark, D.A., and Miller, C.F., 1993, Accessory mineral behavior during differentiation of a granite suite: Monazite, xenotime and zircon in the Sweetwater Wash pluton, southeastern California, USA: Chemical Geology, v. 110, p. 49–67, doi:10.1016/0009-2541(93)90247-G.
Wark, D.A., and Watson, E.B., 2000, Effect of grain size on fluid and melt distribution in mantle and deep crustal rocks: Geophysical Research Letters, v. 27, p. 2029–2032, doi:10.1029/2000GL011503.
Waters, D.J., 1988, Partial melting and the formation of granulite facies assemblages in Namaqualand, South Africa: Journal of Metamorphic Geology, v. 6, p. 387–404, doi:10.1111/j.1525-1314.1988.tb00430.x.
Watson, E.B., 1996, Dissolution, growth and survival of zircons during crustal fusion: Kinetic principles, geological models and implications for isotopic inheritance: Transactions of the Royal Society of Edinburgh–Earth Sciences, v. 87, p. 43–56, doi:10.1017/S0263593300006465.
Watson, E.B., 1999, Lithologic partitioning of fluids and melts: The American Mineralogist, v. 84, p. 1693–1710.
Watson, E.B., and Harrison, T.M., 1983, Zircon saturation revisited—Temperature and composition effects in a variety of crustal magma types: Earth and Planetary Science Letters, v. 64, p. 295–304, doi:10.1016/0012-821X(83)90211-X.
Watson, E.B., Vicenzi, E.P., and Rapp, R.P., 1989, Inclusion/host relations involving accessory minerals in high-grade metamorphic and anatectic rocks: Contributions to Mineralogy and Petrology, v. 101, p. 220–231, doi:10.1007/BF00375308.
Watt, G.R., and Harley, S.L., 1993, Accessory phase controls on the geochemistry of crustal melts and restites produced during water-undersaturated partial melting: Contributions to Mineralogy and Petrology, v. 114, p. 550–566, doi:10.1007/BF00321759.
Watt, G.R., Burns, I.M., and Graham, G.A., 1996, Chemical characteristics of migmatites: Accessory phase distribution and evidence for fast melt segregation rates: Contributions to Mineralogy and Petrology, v. 125, p. 100–111, doi:10.1007/s004100050209.
Weinberg, R.F., 1999, Mesoscale pervasive felsic magma migration: Alternatives to diking: Lithos, v. 46, p. 393–410, doi:10.1016/S0024-4937(98)00075-9.
Weinberg, R.F., and Mark, G., 2008, Magma migration, folding, and disaggregation of migmatites in the Karakoram shear zone, Ladakh, NW India: Geological Society of America Bulletin, v. 120, p. 994–1009, doi:10.1130/B26227.1.
Weinberg, R.F., and Podladchikov, Y., 1994, Diapiric ascent of magmas through power-law crust and mantle: Journal of Geophysical Research, v. 99, p. 9543–9559, doi:10.1029/93JB03461.
Weinberg, R.F., and Regenauer-Lieb, K., 2010, Ductile fractures and magma migration from source: Geology, v. 38, p. 363–366, doi:10.1130/G30482.1.
Weinberg, R.F., and Searle, M.P., 1998, The Pangong injection complex, Indian Karakoram: A case of pervasive granite flow through hot viscous crust: Journal of the Geological Society of London, v. 155, p. 883–891, doi:10.1144/gsjgs.155.5.0883.
Weinberg, R.F., Sial, A., and Mariano, G., 2004, Close spatial relationship between plutons and shear zones: Geology, v. 32, p. 377–380, doi:10.1130/G20290.1.
Weinberg, R.F., Mark, G., and Reichardt, H., 2009, Magma ponding in the Karakoram shear zone, Ladakh, NW India: Geological Society of America Bulletin, v. 121, p. 278–285.
Weinberg, R.F., Hasalová, P., Ward, L., and Fanning, C.M., 2013, Interaction between deformation and magma extraction in migmatites: Examples from Kangaroo Island, South Australia: Geological Society of America Bulletin, v. 124, p. 000–000, doi:10.1130/B30781.1.
Whalen, J.B., Currie, K.L., and Chappell, B.W., 1987, A-type granites: Geochemical characteristics, discrimination and petrogenesis: Contributions to Mineralogy and Petrology, v. 95, p. 407–419, doi:10.1007/BF00402202.
White, A.J.R., 1979, Sources of granite magmas: Geological Society of America Abstracts with Programs, v. 11, no. 7, p. 539.
White, A.J.R., and Chappell, B.W., 1977, Ultrametamorphism and granitoid genesis: Tectonophysics, v. 43, p. 7–22, doi:10.1016/0040-1951(77)90003-8.
White, R.W., and Powell, R., 2002, Melt loss and the preservation of granulite facies mineral assemblages: Journal of Metamorphic Geology, v. 20, p. 621–632.
White, R.W., and Powell, R., 2010, Retrograde melt-residue interaction and the formation of near-anhydrous leucosomes in migmatites: Journal of Metamorphic Geology, v. 28, p. 579–597, doi:10.1111/j.1525-1314.2010.00881.x.
White, R.W., Powell, R., and Holland, T.J.B., 2001, Calculation of partial melting equilibria in the system Na_2O-CaO-K_2O-FeO-MgO-Al_2O_3-SiO_2-H_2O (NCKFMASH): Journal of Metamorphic Geology, v. 19, p. 139–153, doi:10.1046/j.0263-4929.2000.00303.x.
White, R.W., Powell, R., and Halpin, J.A., 2004, Spatially-focused melt formation in aluminous metapelites from Broken Hill, Australia: Journal of Metamorphic Geology, v. 22, p. 825–845, doi:10.1111/j.1525-1314.2004.00553.x.
White, R.W., Pomroy, N.E., and Powell, R., 2005, An in situ metatexite-diatexite transition in upper amphibolite facies rocks from Broken Hill, Australia: Journal of Metamorphic Geology, v. 23, p. 579–602, doi:10.1111/j.1525-1314.2005.00597.x.
White, R.W., Powell, R., and Holland, T.J.B., 2007, Progress relating to calculation of partial melting equilibria for metapelites: Journal of Metamorphic Geology, v. 25, p. 511–527, doi:10.1111/j.1525-1314.2007.00711.x.
White, R.W., Stevens, G., and Johnson, T.E., 2011, Is the crucible reproducible? Reconciling melting experiments with thermodynamic calculations: Elements, v. 7, p. 241–246, doi:10.2113/gselements.7.4.241.
Whitehead, J., and Helfrich, K., 1991, Instability of flow with temperature-dependent viscosity: A model of magma dynamics: Journal of Geophysical Research, v. 96, p. 4145–4155.
Whitney, J.A., 1988, The origin of granite: The role and source of water in the evolution of granitic magmas: Geological Society of America Bulletin, v. 100, p. 1886–1897.
Wickham, S.M., 1987, The segregation and emplacement of granitic magma: Journal of the Geological Society of London, v. 144, p. 281–297, doi:10.1144/gsjgs.144.2.0281.
Wiggins, C., and Spiegelman, M., 1995, Magma migration and magmatic solitary waves in 3-D: Geophysical Research Letters, v. 22, p. 1289–1292, doi:10.1029/95GL00269.
Wolf, M.B., and Wyllie, P.J., 1994, Dehydration-melting of amphibolite at 10 kbar: The effects of temperature and time: Contributions to Mineralogy and Petrology, v. 115, p. 369–383, doi:10.1007/BF00320972.
Xia, Q.-K., Yang, X.-Z., Deloule, E., Sheng, Y.-M., and Hao, Y.-T., 2006, Water in the lower crustal granulite xenoliths from Nushan, eastern China: Journal of Geophysical Research, v. 111, B11202, doi:10.1029/2006JB004296.
Yakymchuk, C., Korhonen, F., and Brown, M., 2011, Decompression melting in tectonics: Where's the melt? Mineralogical Magazine, v. 75, no. 3, p. 2200.
Yakymchuk, C., Brown, M., Korhonen, F.J., and Siddoway, C.S., 2012, Is melt extraction from the anatectic zone fractal? Proceedings of the 34th International Geological Congress 2012, 5–10 August 2012, Brisbane, Australia, Australian Geosciences Council ISBN 978-0-646-57800-2.
Yakymchuk, C., Siddoway, C.S., Fanning, C.M., McFadden, R., Korhonen, F., and Brown, M., 2013b, Anatectic reworking and differentiation of continental crust along the active margin of Gondwana: A zircon Hf-O perspective from West Antarctica, *in* Harley, S.L., Fitzsimons, I.C.W., and Zhao, Y., eds, Antarctica and Supercontinent Evolution: Geological Society of London Special Publication 383, doi:10.1144/SP383.7.
Yardley, B.W.D., and Valley, J.W., 1997, The petrologic case for a dry lower crust: Journal of Geophysical Research, v. 102, p. 12,173–12,185, doi:10.1029/97JB00508.
Yoshinobu, A.S., and Barnes, C.G., 2008, Is stoping a volumetrically significant pluton emplacement process?: Geological Society of America Bulletin, v. 120, p. 1080–1081, doi:10.1130/B26141.1.
Závada, P., Schulmann, K., Konopásek, J., Ulrich, S., and Lexa, O., 2007, Extreme ductility of feldspar aggregates—Melt-enhanced grain boundary sliding and creep failure: Rheological implications for felsic lower crust: Journal of Geophysical Research, v. 112, B10210, doi:10.1029/2006JB004820.
Zeng, L., Asimow, P.D., and Saleeby, J.B., 2005a, Coupling of anatectic reactions and dissolution of accessory phases and the Sr and Nd isotope systematics of anatectic melts from a metasedimentary source: Geochimica et Cosmochimica Acta, v. 69, p. 3671–3682, doi:10.1016/j.gca.2005.02.035.
Zeng, L., Saleeby, J.B., and Asimow, P., 2005b, Nd isotope disequilibrium during crustal anatexis; a record from the Goat Ranch migmatite complex, southern Sierra Nevada batholith, California: Geology, v. 33, p. 53–56, doi:10.1130/G20831.1.
Zeng, L., Saleeby, J.B., and Ducea, M., 2005c, Geochemical characteristics of crustal anatexis during the formation of migmatite at the southern Sierra Nevada, California: Contributions to Mineralogy and Petrology, v. 150, p. 386–402, doi:10.1007/s00410-005-0010-2.

Science Editor: J. Brendan Murphy

Manuscript Received 28 February 2013
Manuscript Accepted 1 March 2013

Printed in the USA